NORTHWESTERN UNIVERSITY

Enabling Exploration of CAR T-Cell Design and Integration of Social Justice Context into Chemical Engineering Courses

A DISSERTATION

SUBMITTED TO THE GRADUATE SCHOOL

IN PARTIAL FULFILLMENT OF THE REQUIREMENTS

for the degree

DOCTOR OF PHILOSOPHY

Chemical and Biological Engineering

By

Alexis N. Prybutok

EVANSTON, ILLINOIS

June 2022

Abstract

Chimeric antigen receptor (CAR) T-cell therapies marry advances in cellular engineering with personalized medicine to provide patient-specific, targeted cancer treatments. Though current CAR T-cell therapies successfully target blood cell cancers, treating solid tumors has proven to be more challenging. Solid-tumor CAR designs must overcome several challenges, including tumor microenvironment barriers preventing CAR T-cell infiltration and lack of unique tumor antigens for selective targeting. Given the vast design space and influential tumor context, testing every possible design in vitro or in vivo is prohibitively time-consuming and resource intensive. Thus, there exists a need to efficiently and systematically test designs, understand underlying biological phenomena, and describe emergent behavior. To address this gap, we developed a *flight simulator* for CAR T-cell therapies: a multi-scale, multi-class agent-based model (ABM)—a "bottom-up" computational model that utilizes first-principles to dictate probabilistic rules that guide agent behaviors and interactions within the context of a local environment—designed to elucidate how inherent tumor features and tunable cell therapy properties affect treatment outcomes. This work builds upon a previously established modeling framework ARCADE (Agent-based Representation of Cells And Dynamic Environments) to include CAR T-cell agents (CAR T-cell ARCADE, or CARCADE). CARCADE integrates the subcellular level details (modules), cell-level decision making (rules), and population-level emergent outcomes (environment and cell interactions). The agents include both cancerous and healthy tissue cells and $CD4^+$ (helper) and $CD8^+$ (cytotoxic) CAR T-cells, where each cell uses modules to manage nutrient uptake and environment sensing. Cells navigate through defined states and rules derived from experimental studies. Using CARCADE, I elucidated how inherent tumor features and tunable therapeutic properties differentially and simultaneously affect treatment outcomes in simulated `dish` and `tissue` contexts. CARCADE facilitates deeper biological understanding of treatment design and could ultimately enable identification of promising treatment strategies to accelerate solid tumor CAR T-cell design-build-test cycles.

Additionally, I dedicated much of my Ph.D. to engineering education research. Chemical engineering examples and homework problems often lack societal context, specifically failing to connect engineering content, decisions, and designs to diverse groups. Thus, students are rarely given the opportunity to

consider the positive or negative impacts of engineering efforts on communities with identities differing from their own. Along with other members of the ChBE Anti-Racism, Diversity, Equity, and Inclusion (ARDEI) Committee, we worked toward integrating ARDEI and social justice contexts into undergraduate and graduate curriculum through homework and example problems. By adding context into our classrooms, we hope to increase inclusivity, awareness of oppressions, and reflection on the intersection of identity and chemical engineering, thereby encouraging critical thinking through an equity lens.

Acknowledgments

While Ph.D. dissertations are presented as a body of work with one name on them, much like anything else in science, they are hardly completed alone. Throughout the last six years, and really throughout my whole life, I have been fortunate to learn from and receive the support, love, kindness, and advocacy of so many mentors, colleagues, friends, and family. Without each and every one of the following people, I would not have been able to complete my degree, let alone with my sanity still intact.

First, I would like to thank my co-advisors, Dr. Joshua Leonard and Dr. Neda Bagheri, for all of the support and mentorship I have received from them throughout the last six years. You both taught me so much as I worked on a project that perfectly married your expertise and gave me the space and time to pursue my interests in both computational immunology and engineering education. Josh, thank you for your positivity, activism, and infinite (bad) jokes. Neda, thank you for challenging me to continue pushing myself and growing, and for your support and advice throughout. I wouldn't be here without you both, and I'm grateful to not only have worked with you, but to join you as colleagues in chemical engineering faculty. I hope we get to continue to work together in the future.

I would also like to thank Dr. Jennifer Cole, who while she was not my official advisor, took me on as a mentee in teaching, activism, and engineering education research. You showed me exactly what I wanted my future career to be and who I wanted to be in that role. You do so much not only for me, but for all of your students, the department, the Northwestern community, and the broader chemical engineering community, and I admire and respect you for who you are both in and beyond your job. I owe so much of what I have gained out of my time in graduate school to your vast knowledge of teaching, deep involvement in social justice, and what I hope is a lifelong friendship and chemical engineering education comrade.

Thank you to Dr. Linda Broadbelt for all her wisdom, mentorship, and advocacy. I knew when I first met you at recruitment that I wanted to work with you in some capacity during my time in graduate school, whether that be through teaching or research. And it was not until I began TAing for your Kinetics class as a 3rd year graduate student that I realized I had never seen a woman teach a class, despite having two bachelor's degrees, a minor, and having completed my graduate courses. It was only after seeing you teach that I

could *see* myself as a chemical engineering professor. I am so honored to have worked with you not only as a co-instructor for the Teaching Apprentice Program (and with Becca Harmon and Sam Varner as our amazing TAs!), but also as a colleague on the McCormick Graduate Teaching Committee, and as a mentee of your academic excellence.

I would like to thank my Committee, Dr. Julius Lucks, Dr. Luis Amaral, and Dr. Evan Scott for your guidance, feedback, and support. Thank you also for supporting my research both from the start and as it pivoted to include the engineering education research that I am most passionate about.

Thank you also to the National Research Foundation Graduate Research Fellowship Program and Northwestern's Terminal Year Fellowship for funding my work, and to Northwestern's Quest High Performance Computing Cluster for enabling my thousands of agent-based modeling simulations.

Thank you to my wonderful undergraduate mentees, Antonio Hazboun, Andrea Collins, and Isabelle Chen. It has been an absolute pleasure to not only get to work with, get to know, and become friends with all of y'all. Toni, thanks for your comradery in all thing's politics, dance, and for making me a dictionary of millennial speak. Andrea, I cherish getting to catch up with you when you're back in town, and I am so proud of you for following your passions and desire to help people. And Isabelle, I admire your persistence, vulnerability, openness; please never stop sending me pictures of cats and telling me about your pet fish.

I owe so much thanks to all of the members of the Leonard and Bagheri Labs that I have had the pleasure of overlapping with in my time as a Ph.D. student at Northwestern. For the Leonard Lab, thank you to Dr. Kelly Sarnese, Dr. Andrew Younger, Dr. Patrick Donahue, Dr. Joe Muldoon, Dr. Taylor Dolberg, Dr. Devin Stranford, Dr. Aaron Morris, Hailey Edelstein, Kate Dray, Simrita Deol, Jon Boucher, Will Corcoran, Taylor Gunnels, Roxi Mitruț, Katie Dreyer, Gauri Bora, Amparo Cosio, Yannick Schreiber, Beth DiBiase, Max Ezekiel, Amy Hong, and Coconut the Palm Tree. For the Bagheri Lab, thank you to Dr. Ty Yacoub, Dr. Albert Xue, Dr. Jia Wu, Dr. Justin Finkle, Dr. Sebastian Bernasek, Dr. Jessica Yu, Dr. Mugdha Sathe, Dr. Narasimhan Balakrishnan, Jason Cain, Slava Butkovich, Po-Hao Chiu, Jacob Evarts, Sophia Jannetty, and Kate Dray and Joe Muldoon again for being my comrades in co-advisement. In particular, thank you to Jessica for all of your mentorship, and for giving me somebody to not only look up to but to crochet with.

Your hard work and care for the lab is both admirable and palpable, and my research project would not have been possible without your support. Thank you to Kate, and Melvin, for your friendship, openness, kindness, shared love of trash TV, and cookie dough balls. Any time I was having a hard day, I knew I could count on you to cheer me up, advocate for me and my mental health even when I couldn't for myself, and to find a positive outlook on things. Thank you to Hailey for your friendship, endless hard work and support, and kindness. You're somebody I could always count on to understand my anxiety and help me get through it; thanks for all the times you listened to me kvetch without judgement. Thank you to Taylor Dolberg for your support, for challenging me to do things I was afraid of, and for enriching my life with friendship, Lilo, delicious baking, and a newfound addiction to the Bachelor. I knew from the moment we met at recruitment when you expressed your love of S.V.U. that we would be friends, and I'm grateful to have our friendship extend beyond our overlapping time at Northwestern. And thank you to Jason, my lab brother, for tolerating all of my antics, sharing my radical politics, collaborating with me on the review article, and being an all-around good friend. I admire how much you do to support the lab, myself included.

Next, I would like to thank the Department of Chemical and Biological Engineering (ChBE) Anti-Racism Diversity, Equity, and Inclusion (ARDEI) Committee. Thank you (again) to Julius and Jennifer for your involvement, support, and willingness to learn and take concrete actions. Thank you to Carolyn Ramirez, Kavi Chintam, and Jonathan Chan for your commitment, bravery, and for all that you've done and taught me. You are all wonderful humans, and I'm so grateful that I got to work with you on these efforts. Carolyn, thanks especially for your friendship, from UT to NU I knew I could count on you. Thank you to Dr. Jennifer Cole, Lauren Simitz, Ayin Abegunde, Kenzie Sanroman Gutierrez, and Chloé Archuleta for your hard work on the undergraduate subcommittee and all that we have accomplished both for the department and the engineering education community. I am so honored and lucky to be able to work and publish with all of you. Helping start and being a part of the ARDEI Committee was one of the highlights of my time at NU.

Thank you to the ChBE Teaching Committee for all the opportunities you've given me to discuss teaching strategies, support TAs, and contribute to lasting resources for the department. The work and time spent leading this committee was invaluable to helping me figure out what service I hope to provide others one day as an educator.

Thank you to the McCormick Graduate Teaching Committee and to Dr. Nancy Ruggeri, Dr. Linda Broadbelt, and Abhi Amrithanath for helping me get it started. Much like the ChBE Teaching Committee, working on this committee gave me the opportunity to serve and advocate for TAs across McCormick, and I hope the committee can do great things in the future.

Thank you to the Searle Center for Advancing Learning and Teaching—and to Dr. Nancy Ruggeri, Kate Flom Derrick, and Dr. Katie Pierson—for all of the amazing programming and opportunities you provided me to explore and learn various teaching pedagogies and practices. Every program I participated in—including serving as a Graduate Student Teaching Conference 2020 Workshop Leader, participating in the Teaching Certificate Program 2020-2021, and serving as a Graduate Teaching Mentor 2021-2022—and all of those who helped make those programs have given me the confidence and training necessary to pursue my dream job as a teaching faculty. I cannot thank you all enough. I don't know how I would do this without you. And these programs were some of the highlights of my time at NU.

Thank you to Nichols Middle School, all the amazing kids there, Carah Ingram and Amanda Theile, and to the Morning Mentors tutoring program for the opportunity to give back to a community and support a wonderful group of students and teachers. Thanks to Emma and Shannon for getting it started, and to Adam Silverman, Bethany Sump, Jane Edgington, Katie Dreyer, and all the mentors for keeping it going.

Thank you to my therapist, Dr. Agila Rangarajan, for helping me get through the last six years. You gave me somewhere to vent, kept me sane, and taught me how to manage my anxiety and depression. Finding a therapist who clicks with you is extremely difficult, and I was so lucky to find you on the first try. I, and my mental health, could not have done this without you.

Thank you to all the friends and community I have developed in fellow graduate students in the ChBE Department. Thanks to Emily Cheng, who while we are so different, became a close friend and provided a listening ear. Thank you to Becca Harmon, who shared the journey of the entire teaching faculty job search and dissertation writing process with me. Spending one hour together writing and working each day helped me chip away at these daunting tasks, and I am so proud of us for both coming out the other end with the

best possible option for each of us. I am so excited to have you as a colleague and friend in chemical engineering education.

Thank you to my roommates Andrew Hunt, Peter Tran, Daniel de Castro Assumpção, and unofficial roommate Angelia Wang, for all the fun, board games, shared times watching TV, and memories. Together we survived graduate school, through a pandemic, and stayed friends along the way. Andrew, you're a weirdo. Peter, you're infinitely clever. Angelia, you talented soul. Daniel, you are such a joy. Thank you to you all! I couldn't have asked for better house partners.

Thank you to my trivia team—Dr. Adam Silverman, Dr. Jasmine Hershewe, Bon Ikwuagwu, Adam Sandler (not the famous one, the good one), and Will Dearden—for all of the memories and winnings we had at Nevin's, Whiskey Thief, and now virtually. From "Dat Asymptote" to "Danny DeVito, Mutant Yeti" to "Frisky Lemurs, Wide-Eyed", we crushed it. In particular, thanks to Adam Silverman for being a wonderful friend and fellow Oldies fan who has supported me, joked with me, written many trivias with me, and been the smartest person I know. Thanks to Bon for being an absolute joy to get to know—all of your opinions are the worst, but you're the best. And thanks to Jazzy for being a dork, a metalhead, and a friend. Thanks to Go4It Entertainment (*Sports!*) and Whaddyaknow? for the opportunity to make some great friends, eat some good food, and answer some niche questions!

Thank you also to all the folks at May I Have This Dance for the wonderful community, shared dances, and lessons learned. West Coast Swing has been an outlet and a joy.

Thank you to my lifelong love, Billy Joel, for your fantastic music that I torture everybody else with. Thank you to the PEZ Company for continuing to make the dispensers that fill my collection for a candy that nobody likes. Without you both, who even would I be, and what would people make fun of me for.

Thank you to my best friends, Reece Leonard and Ariel Bailey-Mills, for your lifelong friendship and love. It has been the greatest joy to have you both in my life since 6th and 1st grade, respectively. I owe so much of who I am to both of you. You taught me to be radical, to be kind, and how to be a friend. There are not enough words to describe my love for you both. You're like family—no, you are family. And you taught me so much about who I want to be and what I value.

Thank you to Anna Adami, Sarah Wesselius, Danielle Ury, and again Ariel for being my Chicken Sisters, my coolnerds, my united turkeys. Even though we all took wildly different paths in life, we maintain a friendship that spans states and time. You're all so wonderfully accomplished, and I'm so excited to be part of this group. I know we will be the closest of friends until we become old ladies together.

To my family—Dr. Gayle Prybutok, Dr. Victor Prybutok, and Sara Prybutok—I love you. You all are some of the most brilliant, motivated, devoted, loving, kind-hearted, loud, weird, Jewish, and pet-crazy people I know. You have inspired so much of who I am and who and what I want to be. Dad, thank you for taking care of me and the family. Mom, thank you for your empathy but also for pushing me. Sara, thank you for your endless kindness and patience. You're all insane, in the best way. Our house is loud, direct, and filled with food, and I wouldn't want it any other way.

To my tiny, four-legged family—Katy, Bella, Phoebe, Leo, Simon, Ellie, and our two unofficial pets, the opossums that live in our backyard that my mother feeds every night—you're all so adorable and nothing makes me happier than seeing you all be happy. Katy, Bella, and Phoebe, never stop being tiny sausages with ridiculous teeth. Leo, you didn't make it with me to the end of my Ph.D., but you were there for the majority of the rest of my life, and I miss you. Simon and Ellie, keep causing trouble. Opossums, please don't get eaten by a hawk, you're too cute to die. Y'all taught me that pets are family just as much as people.

To my partner Travis Marmon and our cat Sushi, I love you both. Travis, thank you for accepting me and loving me for who I am, letting me annoy you with weird dancing, and supporting me always. You're an endless vat of comfort, reason, and animal facts. I am so excited for our life together in Seattle. Sushi, thanks for being so sweet and affectionate. I really wish you would eat more you weirdo.

Last, but not least, thank you to all the cats, and one hamster, I have had the pleasure of watching during my time in graduate school. Thank you to Juno, Moon-Pie, Maple, Honey, Kiwi, Lila, Prince, Louie, Kasi, Miko, Mimi, Schatzi, and Nugget the hamster, and to all your owners for entrusting me with your care. You all got me through some hard times. My Ph.D. would not have been the same without you.

Table of Contents

List of Figures

List of Tables

1 Introduction

1.1 Motivation and context

Throughout my life I have had an interest in both medical science and treatment as well as education, and while the first part of my Ph.D. focused on the former, by the end my focus shifted to the latter. My simultaneous interest in understanding cell- and population-level biological phenomena that emerged in disease or dysfunction, aversion to blood, and interest to help treat or inform human health drove me to purse a career in chemical engineering with research focused on disease treatment. As an undergraduate, I worked as a researcher Dr. Jennifer Maynard's Protein Immunoengineering lab, studying the synergy of two antibodies used in combination to treat pertussis (whooping cough) in infants too young to receive the vaccine. While I enjoyed the motivation behind this work, I found myself drawn to solving and debugging problems on a computer rather than at a lab bench. This interest, along with a chance meeting with a professor conducting research in engineering education, drove me to pivot my undergraduate research by joining Dr. Maura Borrego's research group to focus on how engineering students form engineering identities, ultimately contributing to retention and sense of belonging in the degree and profession. As I went to join a graduate program, I strongly debated between earning a Ph.D. in chemical engineering vs in engineering education, ultimately with the goal of becoming a teaching professor in chemical engineering. I decided ultimately to take the path in which I would earn my Ph.D. in chemical engineering, taking the graduate level chemical engineering courses, conducting biological research, but also honing my teaching skills and interests by serving as a teaching assistant and finding opportunities to engage in teaching scholarship and pedagogy.

For my Ph.D. thesis work, I joined a co-advisement between Dr. Joshua Leonard and Dr. Neda Bagheri, to purse computational medically focused research. For this project, I extended an agent-based model (ABM) of tumor growth developed by my graduate mentor, Jessica Yu, to include CAR T-cells to investigate how tunable features of CAR T-cells and inherent tumor properties affect treatment outcomes. It was during this time that I was simultaneously gaining experience and training in teaching and engineering education. I gained direct teaching experience as a teaching assistant (TA) or as a co-instructor working with Dr. Linda Broadbelt through the Teaching Apprentice Program (TAP). Additionally, I dove into the scholarship of

learning and teaching by serving in various roles at the Northwestern University Searle Center for Advancing Learning and Teaching, including as a Graduate Student Teaching Conference Workshop Leader, a participant in the Teaching Certificate Program (TCP), and as a Graduate Teaching Mentor for the (TCP). As I learned more about inclusive teaching pedagogy, where that learning coincided with the onset of the ongoing COVID-19 pandemic and the resurgence of the Black Lives Matter movement following the murder of George Floyd, I began to realize the lack of incorporation not only of inclusive teaching practices, but also of social justice principles and context in chemical engineering classrooms. Driven by a desire to foster increased community engagement with the ideas of anti-racism, diversity, equity, and inclusion (ARDE) and social justice, I helped co-found the ChBE Department ARDEI Committee. As a member of this committee and in collaboration with many others, I engaged in many initiatives, many of which particularly focused on those related to enhancing and radicalizing engineering education. One project that resulted from this committee—led by me along with Dr. Jennifer Cole, undergraduates Ayinoluwa Abegunde, Lauren Simitz, Kenzie Sanroman Gutierrez, and fellow graduate student Chloé Archuleta—focused on training faculty to incorporate ARDEI and social justice context into course homework problems and surveying students on the impacts of engaging with these questions. This work has been substantial and is thus integrated into my thesis with equal weight to that of my CAR T-cell agent-based modeling work. Overall, my time as a graduate student has given me the opportunity to not only explore, but to contribute to, the two fields that have comprised my life-long interests.

In this dissertation, each aspect of my work is given equal space. **Chapter 1** comprises separate background sections for CAR T-cell and agent-based modeling and for social justice in engineering education. **Chapter 2** includes the development and use of an agent-based model to investigate how CAR T-cell therapy design interacts with tumor properties and contexts to impact treatment outcome. **Chapter 3** includes the development and implementation of a workshop to implementation to train ChBE faculty to integrate ARDEI and social justice context into their course homework and lectures as well as the student response to engaging with this context. **Chapter 4** highlights the conclusions, future work, and perspectives on both aspects of this collective work, separated into separate sections for each aspect.

1.2 Background on chimeric antigen receptor (CAR) T-cell therapies and agent-based models (ABMs)

1.2.1 CAR T-cell therapies are a novel engineered cell-based therapy to treat cancer

Engineered cell therapies show promise for treating diseases, such as cancer, but require a deeper understanding to increase their efficacy. These therapies use cells as living drugs and must therefore balance the cells' vital needs while performing a therapeutic function. Cells present an unlimited number of design features, which cannot be feasibly tested exhaustively *in vitro* and *in vivo*. This constraint limits our understanding of how each design feature affects treatment outcomes. There exists a need to efficiently and systematically explore cell-therapy features in relevant clinical-contexts to enhance cell therapy development by revealing which biological phenomena most impact cellular responses.

Chimeric antigen receptor (CAR) T-cell therapy, one of the most prominent engineered cell therapies, marries advances in cellular engineering and personalized medicine to provide patient-specific, targeted cancer treatments [1,2]. This therapy involves collecting, purifying, and genetically modifying a patient's own T-cells to contain a CAR protein that specifically targets the patient's tumor(s) [1,2]. These engineered cells are expanded *ex vivo* and then re-infused into the patient where the CAR T-cells target and kill antigen-expressing tumor cells. Created in the 1980s, the first CAR-molecule was engineered to combat tumor immune escape via downregulation of major histocompatibility complex (MHC) surface proteins that ordinarily trigger immune system activation [3]. This first-generation CAR contained two parts: a single-chain antibody fragment (scFv) for recognizing the target antigen and an intracellular signaling domain, commonly CD3ζ, for activating the T-cell [1]. First-generation CARs exhibited low efficacy in clinical trials due to limited anti-tumor function, modest persistence, and low expansion capabilities [4]. To improve these functions, second-generation CARs include the addition of an intracellular co-stimulatory signaling domain (ICD), often either CD28 or 4-1BB, to enhance receptor signaling [1,4]. Compared to first-generation CARs, second-generation CARs exhibited enhanced persistence and proliferation but comparable tumor-recognition [4-6]. Overall, second-generation CARs proved efficacious in clinical trials, and some are now approved and on the market; however, there still exists room for improvement. Third-generation CARs,

which are primarily in the pre-clinical stage, contain two co-stimulatory domains rather than one for enhanced activation and effector function [1]. These enhanced CARs show great promise, with improved function in all areas, but still require development and further testing [4].

1.2.2 FDA-approved CAR T-cell therapies to date treat blood cell cancers

Thus far, the six FDA-approved CAR T-cell therapies exclusively target blood cancers, where four of these approved therapies and many studies expanding CAR designs focus on $CD19^+$ B-cell cancers [1,7-9]. All healthy B-cells produce and require surface receptor CD19 for development, but malignant B-cells often overexpress CD19 [4]. Thus, the CD19 CAR targets not only malignant B-cells but also healthy B-cells through on-target off-tumor effects, leaving most successfully treated patients with B-cell aplasia [4,10]. Medical replacement of B-cell function through repeated infusion of antibodies treats this affliction, which makes the resulting consequences of the CAR T-cell therapy tolerable [1,4,8]. CD19 CAR T-cell therapies showed great success in the clinic with response rates between 70% and 90% reported [4]. As the first child to receive CD19 CAR T-cell therapy, Emily Whitehead is one of the most commonly referenced cases of therapeutic success [11]. Emily was diagnosed with acute lymphoblastic leukemia in 2010 at age five and after a series of failed standard treatments, including chemotherapy, enrolled in a CD19 CAR T-cell therapy study as a last resort. The treatment proved strikingly effective, and she remains cancer-free to this day. This case study highlights both the potential enhanced efficacy over conventional treatments and long-lasting effects of CAR T-cell therapy.

1.2.3 Solid tumors are more challenging to treat with CAR T-cell therapy

Targeting B-cell malignancies provided a perfect first-step in developing this therapeutic strategy. CD19 served as a nearly ideal target, as only B-cells express this receptor, and the off-tumor effects are manageable with treatment. Targeting solid tumors is more challenging due to (i) tumor microenvironment (TME) barriers preventing CAR T-cell infiltration [7], (ii) a lack of unique tumor antigens for selective targeting [12], and (iii) safety issues from cross-reactivity with healthy tissues [4]. Additional factors, such as the need for site-specific trafficking of T-cells to solid tumors, which is not an issue in blood cell cancers, and tumor antigen heterogeneity further complicate designing solid-tumor CAR T-cell therapies [4].

Early in the tumor formation process, proliferating tumor cells orchestrate the construction of a tumor-promoting, immunosuppressive tumor microenvironment (TME) that dampens or inhibits optimal CAR T-cell function. Altering the TME is recognized as a broad challenge for many types of solid-cancer treatment, and work in this area recently gained high recognition when the creators of immune checkpoint inhibitors, which aim to stimulate the immune system in an immunosuppressive TME, won the 2018 Nobel Prize in Medicine [13]. The TME encompasses a variety of cell types, related structures, and a unique metabolite composition. Besides the tumor cells and healthy tissue cells, the TME contains the tumor infiltrate [14], a mixture of tumor-suppressing lymphocytes, commonly $CD4^+$ and $CD8^+$ T-cells, and tumor-promoting anti-inflammatory cells, commonly T regulatory cells [15]. Tumor cells upregulate receptors like PD-L1 to hide from the immune system and drive immune cells into exhausted states [14,16]. Physical and chemical barriers include the extracellular matrix, blood vessels, hypoxia, and lack of glucose and other nutrients [7,15]. These TME components prevent immune cell infiltration and proliferation into the solid tumor. The CAR T-cell community has taken on the challenge of remodeling the immunosuppressive TME. “Armored” CAR T-cells are under development that constitutively express cytokines to promote immune activation [4,17]. Other attempts to combat the TME include creating CAR T-cells engineered to inhibit suppressive signals by releasing or expressing PD-1-blocking proteins [18-20] and combining CAR T-cell therapy with intravenous checkpoint inhibitor therapy or cytokines [4,17].

Another challenge in designing solid-tumor CAR T-cells is selecting appropriate antigen targets; few antigens exist that are exclusively expressed by tumor cells [12]. Unlike the on-target off-tumor effects of B-cell cancer treatment, those associated with targeting solid tumors can be harmful or even fatal [12,21]. To combat these challenges, engineering efforts focus on (i) increasing CAR specificity by tuning the affinity of receptor-antigen interactions to avoid healthy cells [22-24], (ii) designed CAR T-cells that target multiple antigens simultaneously to prevent formation of antigen escape variant tumors [25-27], and (iii) creating CAR T-cells that perform Boolean logic to enhance tumor recognition specificity [7,27-30].

In addition to the work conducted to improve solid-tumor CARs, CD19 CAR engineering experiments suggest other important factors that could enhance solid-tumor CAR T-cell therapies. Studies find that therapeutic efficacy is highly impacted by CAR T-cell effector and persistence behaviors, meaning how

effectively the cells perform immune tasks and how long the cells survive, respectively. These behaviors are conferred by (i) $CD4^+$:$CD8^+$ CAR T-cell ratios [31,32], (ii) choice of intracellular co-stimulatory domain (ICD) in the CAR [33-35], and (iii) the stage in differentiation at which T-cells are engineered to express the CARs [31]. Additionally, T-cell biology suggests that metabolism plays a critical role in dictating these behaviors [36-40]. Each of these design choices could affect or be affected by the underlying CAR T-cell metabolism. Though therapies that systematically target patient cell metabolism are being investigated [40]. there exists little work exploring the benefit of engineering CAR T-cells from a metabolic perspective.

Between antigen affinity-tuning and metabolism engineering, systematically identifying and testing all possible CAR design features is both difficult and time-consuming *in vitro* and *in vivo*. Computational investigations uniquely overcome challenges that can limit experimental investigations. Agent-based models (ABMs, also called agent-driven models), in particular, provide an ideal testbed to examine how features of individual CAR T-cells and the local tumor microenvironment affect population-level dynamics of anti-tumor immunity.

1.2.4 Agent-driven modeling paradigms enable investigation of emergent phenomena

This section contains text that appeared in the following publication [41]:

> Prybutok AN, Cain JY, Leonard JN, Bagheri N. Fighting fire with fire: deploying complexity in computational modeling to effectively characterize complex biological systems. *Current Opinion in Biotechnology* 2022, 75:102704.

Agent-driven models—simulations designed around the behavior of autonomous agents—facilitate studying emergent functions. Rules guiding agent behavior are abstracted from observed or hypothesized behaviors of individuals within populations. These models can serve as intuitive testbeds to understand how different rules impact emergent behavior. This paradigm is synonymous with agent-based models (ABMs), which include the common subtypes of cellular automata and cellular Potts. Depending on context and scale, agents typically represent individual cells (e.g., in immunological applications) or individual organisms/people (e.g., in epidemiology or sociology applications) [42,43]. In contrast to other modeling paradigms (data-driven and mechanism-driven), agent-driven design does not rely on training, but it does

rely on accurate characterization of higher-level dynamics. These models enable researchers to evaluate how hypothesized rules underlying biological phenomena give rise to observed emergent behavior.

Increasing model complexity increases computational cost. ABM design can be as simple as the two agent states and four rules included in Conway's Game of Life (a common, low-cost case study of the phenomenon of emergence) [44]. Other agent-based model designs are more complex, computationally costly (run time and memory usage), and difficult to parameterize [42]. Computational cost results from biological detail, scaling with the number of agents and agent properties in the simulation. Model reduction or abstraction can help avoid development of intractable models.

In systems immunology, ABMs with abstracted, rule-guided agents link subcellular or cellular-level changes to population-level emergent phenomena. ABMs with rule-guided agents that take on limited states and actions—such as proliferation, migration, death, genetic mutation, and/or environmental interaction—have revealed how tumor microenvironment conditions [45] and cell migration rate [46] affect tumor morphology, growth, and genetic diversity. ABMs can also be used to compare hypotheses. One modeling framework supported two different rule sets to compare how competing hypotheses on genetic mutation can drive the evolution of aggressive phenotypes in cancer progression [45]. Both rule sets resulted in a few aggressive phenotypes dominating tumor genetic makeup. Relatively simple agent descriptions can provide profound insight when recapitulating complex biological behavior.

Designing an ABM to describe intricate processes—such as intercellular interactions, sensing, signaling, environmental features, and trafficking—may necessitate reducing complexity to manage computational cost. One strategy is to lump functionally related features (e.g., intracellular signaling mediators) into aggregate signals, an approach applied to generate a simple representation of tumor-macrophage interactions [47]. This reduction facilitated a multiparametric sensitivity analysis that identified parameters influencing tumor survival and helped propose cell therapy strategies. Another study employed a simplified model of vasculature structure and dynamics (omitting details used in other ABMs [48,49]) to simulate checkpoint inhibitor therapy and identify biomarkers that may be useful for guiding treatment [50]. A useful approach for integrating phenomena involving fine-grained detail is a Potts model, which explicitly describes

cell boundaries and surface interactions. Potts models have been used to incorporate pMHC-TCR interactions and build understanding of anti-tumor $CD8^+$ T-cell responses in heterogenous contexts [51]. Designing ABM complexity to fit the specific questions of interest helps manage computational cost and generate relevant insights.

1.2.5 Agent-based modeling could aid in exploration of CAR T-cell therapy designs

The agent-based modeling framework provides single-cell spatial resolution, incorporates quantitative and qualitative experimental observations, and enables tuning and measuring properties of interest during *in silico* experiments [42,43,52,53]. To date, ABMs have been used to model cancer growth [45,46,54-56], cancer vasculature dynamics [49], T-cells infiltration of tumors [42,57], checkpoint inhibitor cancer immunotherapies [50], and native macrophage-based tumor therapies [58], yet there is no ABM to model CAR T-cells. An ABM of CAR T-cells would accelerate solid-tumor CAR development by identifying the CAR T-cell properties that most impact treatment outcome and help match inherent tumor features to required CAR T-cell properties for optimal treatment.

1.3 Background on social justice context in engineering education curriculum

1.3.1 Engineering lacks diversity due to systemic inequities and lack of support for marginalized students

While it is generally recognized that diversity in the engineering workforce results in better and more equitable solutions that meet societal needs [59], university engineering degree programs in the United States lack diversity. Women and racial/ethnic minorities are underrepresented and receive the minority of engineering degrees awarded [59-61]. In 2020, 23.10% of bachelor's degrees in engineering were awarded to women [62]. In the same year, white populations (59.4% of degrees awarded) received the majority of degrees awarded compared to racial/ethnic minority groups, including Black or African American (4.5%), Hispanic (13.1%), Asian American (14.9%), Multiracial (3.9%), American Indian/Alaskan Native (0.3%), and Native Hawaiian/Other Pacific Islander (0.2%) [62]. These stark differences in percent of degrees awarded

between majority and minority populations point to significant and systemic barriers to equity in engineering education.

The lack of inclusion of minoritized groups results in part from historical context related to gatekeeping policies barring these populations access to higher-education [63]. For example, The Morrill Land-Grant College Acts resulted in race-conscious exclusion by selling public land (stolen from Indigenous people) to fund the establishment of colleges and universities that were required to offer programs furthering government needs and that often excluded or actively prohibited women and Black populations from attending unless through racially segregated institutions [64]. Other policies that appeared race-neutral resulted in race-conscious exclusion in practice. The Servicemen's Readjustment Act of 1944 (G.I. Bill) provided funds for WWII veterans to adjust back to society, and while Black students were not excluded from receiving G.I. Bill support, many were denied admission to historically white institutions, and Historically Black Colleges and Universities (HBCUs) were too poorly funded to accommodate the influx of Black servicepersons [64]. Similarly, the National Defense Education Act (NDEA) helped propel the space race by putting federal funds into STEM improvement at primary, secondary, and higher education levels, but most of this money went to research institutions which were already predominantly white [64]. Malcom-Piqueux notes that "racially minoritized populations are the only groups to have their exclusion from higher education codified in law and enforced by federal and state governments" [64]. Even modern systems for determining school ranking, which influences admissions, reinforce existing systemic inequities by incentivizing schools to value students' selectivity, test scores and grades, and intuitional resources, which ultimately equate to student and family affluence [65]. Engineering programs and workforces still suffer as a result of systemic racism and prejudice against minoritized populations.

Another factor influencing this lack of diversity is a failure to support minoritized students in identifying with the field of engineering [61]. Each engineering student develops their own engineering identity, a term which has many definitions across the literature [66], but that Godwin and Lee define well as how a student "positions themselves and are positioned by others as the kind of people that engage in engineering, mathematics, or physics" [67]. Engineering identity develops within the context and under the influence of the larger student identity [68], which encompasses an array of intersectional social and personal identities

such as race/ethnicity, gender, sexual orientation, and socioeconomic status, to name a few. Engineering identity is recognized to be influenced by the following features: interest, performance/competence, and recognition by self and others as an engineer [66]. Engineering programs could better support minoritized students along each of these dimensions, resulting in increased inclusion, engagement, and retention of these students in the program and downstream workforce.

1.3.2 Increased use of inclusive teaching practices would support marginalized students

Increased use of inclusive teaching pedagogies and practices would better support marginalized students in developing a connection with the field of engineering and development of engineering identities by making learning accessible and welcoming to all students [59,69,70]. While inclusive practices are an evidence-based way to support all student learning and enhance equity, one particularly relevant strategy in the context of supporting minoritized students is to integrate culturally diverse and relevant examples [70,71]. This strategy helps students feel that diverse cultures, communities, and perspectives, including those matching their own, are welcome and represented in their field of study. Integrating culturally diverse and relevant examples can include highlighting contributions from diverse engineers, investigating case studies from a variety of regions, acknowledging imbalances in the discipline, and providing examples of scholars or figures to serve as role models to students with different identities [70,72]. Additionally, it is important to acknowledge and include contexts that capture and reflect student interests and experiences [72,73] and that interrogate or aim to address inequities caused by or related to engineering content [74].

1.3.3 Chemical engineering curriculum lacks connection to social justice context and principles

Chemical engineering, like all fields of engineering, encompasses work in an array of technical areas—including catalysis, polymer engineering, synthetic biology, bioengineering, and data science—that advance energy, medical, and commercial technologies. The work of engineers not only impacts, but ideally aims to improve, global societal challenges, including mitigating climate change, improving human healthy and quality of life, and increasing economic outcomes of a process. While all members of society are affected by and interact with the results of these engineering efforts, traditional engineering curriculum has ideologically supported depoliticization, meritocracy, and the “technical/social dualism” [59,75]. Farrell et.

al. define depoliticization as “an ideology that promotes engineering as a purely ‘technical’ space where ‘social’ or ‘political’ issues such as inequality are tangential (at best) or irrelevant to engineer’s work” [59]. They define meritocracy as “the belief that inequalities are the result of a well-functioning social system that rewards talent and hard work”, which legitimizes, rationalizes, and prevents reform of social inequities [59]. Cech describes technical/social dualism as one that “devalues ‘social’ competencies such as those related to public welfare” [75]. Incorporating these ideologies into engineering curriculum is harmful to student learning and identity development and deepens existing inequities. Unmarrying engineering work from and devaluing caring about the societal context in which it takes place prevents students from engaging with and understanding how engineering applications and technologies differentially affect communities with varying identities. Specifically, not all communities or members of society equally experience benefits of, harm from, or access to these technologies, nor can all communities contribute equally to their development [59,75,76]. Engineering curriculum instead should intertwine technical content with the principles of anti-racism, diversity, equity, and inclusion (ARDEI) and social justice [76,77].

Educators and students alike must engage with ARDEI and social justice context throughout engineering curriculum, focusing on the intersection of chemical engineering content with marginalized communities, to enhance engineering technologies and student ethics. This engagement will provide students with opportunities to consider how engineering decisions can positively, negatively, or even differently impact communities, where it is particularly important for students think about the impacts on communities with identities different from that of their own [76]. Without training engineering students to think about other communities, engineers in research and the workforce may fail to develop technologies that work equitably for and are accessible to all populations. For example, machine learning algorithms for automated facial analysis exhibit substantial disparities in classifying and bias against women and darker-skinned people [78]. These facial recognition algorithms can have harmful downstream consequences on the lives of marginalized people, highlighted by the wrongful arrest of Robert Williams, a Black man from Detroit, due to a false face recognition match [79]. In another example of inequitable technology, Sunter et. al. found that Black and Latinx communities deploy significantly less solar power compared to white populations despite controlling for factors such as income disparity, home ownership status, and community buy-in [80].

These examples highlight the critical need to design for and with marginalized communities in mind, and to teach this to students from the outset. If entire engineering curricula are reframed through a social justice lens, students will eventually learn to design solutions that meet needs equitably. Of equal importance, this curricula change will change how students define problems, as most predefined decontextualized problems don't allow space for critical thought or development of problem-framing skills [76] that require taking community-engaged approaches that center and include affected communities in engineering efforts [81].

1.3.4 Some educators have successfully integrated social justice context into their courses

Some engineering educators have successfully integrated real-world context, current issues, and diverse communities into their chemical engineering courses. In alignment with the teachings of inclusive pedagogy, Hirshfield and Mayes wrote homework questions for reaction engineering courses that span various real-world applications, focus on engineering ethical considerations, and ask students to reflect on current issues [73]. To capture diverse student interests, their examples include analyzing Maillard reactions in baking and the kinetics of diamond rings. Examples focusing on ethical considerations highlight the development and controversial use of flame retardants and developing less-toxic antifreeze. Finally, the current event problem asked students to focus and reflect on the Flint water crisis.

Other educators have overhauled entire courses with equity ideals in mind. Riley implemented pedagogies of liberation when teaching engineering thermodynamics by considering aspects of course development assignments, and classroom dynamics [82]. Liberative pedagogies—used as a term to encompass elements of feminist pedagogy, bell hooks' engaged pedagogy, and Paulo Freire's critical/radical pedagogy—is a student-centered approach that focuses on developing student reflection and critical thinking to end oppressive systems. Riley designed the course to connect to student experiences, give students authority in the classroom, integrate ethics and policy considerations, and de-center Western and male civilization. A few years later, Riley famously wrote a textbook that reframes thermodynamics, a topic often thought of theoretical, as energy, which is a basic human need [83]. The textbook also emphasizes student engagement, engineering ethics, social context, and communication.

Faculty have taken similar strides to incorporate social justice in other core engineering classes. Riley emphasized the use of life cycle assessment (LCA) in a first year mass and energy balances course, asking students to analyze and green products, processes, and consumerism [84]. Leydens et. al. incorporated and assessed student perceptions of social justice in a feedback control systems course [76]. Catalano et. al. integrated social justice ideas into a bioengineering numerical methods course, where case studies focused on wealth distribution, the costs of health care in the U.S., and poverty trends in the U.S. and around the world [85]. Sociotechnical considerations have also been integrated into energy- and sustainability-focused courses [86]. LaChance et. al. integrated a one-week course module on environmental justice principles into a unit operations course, where students affected by climate injustice and environmental racism, as well as students who participate in climate activism, were invited to help contribute to the development and delivery of this module [87]. Together, these examples highlight the progress engineering educators have made in integrating or centering social justice in their courses to enhance student learning, engagement, and ethics.

1.3.5 Faculty need scalable, low-cost, low-barrier training to support integration of ARDEI and social justice context into engineering courses

Integrating ARDEI and social justice into engineering curriculum is currently limited to the classrooms of select educators who are adept in this space. Thus, few students engage with this discourse, and those who do likely can only do so in a small subset of courses within their entire degree. There are a variety of reasons why the majority of faculty are not currently engaging in this effort. First, many faculty lack or don't have access to the training, background, resources, or time necessary to transform their course content to include this context. Additionally, while many faculty have good intentions with regards to enhancing DEI and may have a desire to undergo this work, fear of causing harm or lack of confidence in the subject limits engagement [74]. The engineering education community needs a scalable way to support many or all faculty in development and teaching of a contextualized curriculum that meets the needs and constraints of faculty.

Trainings programs, courses, or seminars are a scalable way to support faculty development. Some DEI-specific trainings geared toward helping faculty understand and incorporate equity in their roles and classrooms have been provided to the larger chemical engineering community. For example, the American Institute of Chemical Engineers (AIChE) provides access to an Equity, Diversity, and Inclusion Certificate Program that is free for college and university faculty [88]. This three-part training covers why DEI in engineering is important and how unconscious bias manifests and affects academia, offers techniques for reducing the prevalence and effect of bias in engineering, and encourages a growth mindset for DEI. Dr. Donna Riley and Dr. Sindia M. Rivera-Jiménez offered a workshop, Liberating Learning: Social Justice in The Chemical Engineering Curriculum, at the 2021 AIChE National Conference and provide access to the workshop resources for free online [89]. This workshop focused on defining why social justice is important for the chemical engineering practice and education, providing strategies participants can use to integrate context into their courses, and discussing common challenges in this effort. These workshops provide a good starting point for understanding the importance of and thinking about general strategies to integrate ARDEI and social justice context into chemical engineering curriculum. However, they still require significant work on the part of faculty after the workshop to transform their specific courses, as they don't provide faculty with tangible course materials that can be directly applied to their specific classrooms upon completion of the workshop. There still exists the need for a sustainable, accessible, action-driven solution that gives faculty examples and materials for use within the direct context of their own courses.

Integrating ARDEI and social justice context into homework problems is a low-cost, low-barrier, scalable method that faculty can use and be trained in to begin transforming their curriculum. This method presents multiple avenues for embedding this context into problems: either by (1) appending the context in the form of background or additional subparts to an existing homework problem from a textbook or other source or (2) writing new problems from scratch. The first option may be particularly appealing, as textbooks present technical material within a given course written at an appropriate level to benefit student learning, a task that can otherwise be time consuming and difficult. In general, developing ARDEI-context homework problems presents faculty with an option that is a manageable time commitment and that creates a lasting, reusable, adaptable, and sharable resource. If enough faculty within a department were to implement this

approach, students would be able to consistently engage with this context in many courses across their degrees.

There exists a need for an interactive workshop that trains faculty in how to adapt/write, collect resources for, and discuss these ARDEI-context homework problems and results in immediately implementable course materials. Additionally, the workshop could help increase faculty confidence and comfort in engaging in these important conversations. Overall, this presents and attractive, but currently absent, avenue to large-scale integration of ARDEI and social justice context into chemical engineering curriculum.

2 Mapping CAR T-cell design space using agent-based models

This section contains text that appears in the following publication:

> Prybutok AN, Yu JS, Leonard JN, Bagheri N. Mapping CAR T-cell design space using agent-based models. *Frontiers in Molecular Biosciences* Under review.

This manuscript is also published on bioRxiv [90]:

> Prybutok AN, Yu JS, Leonard JN, Bagheri N: Mapping CAR T-cell design space using agent-based models. bioRxiv 2022:2022.2004.2007.487561.

2.1 Abstract

Chimeric antigen receptor (CAR) T-cell therapy shows promise for treating liquid cancers and increasingly for solid tumors as well. While potential design strategies exist to address translational challenges, including the lack of unique tumor antigens and the presence of an immunosuppressive tumor microenvironment, testing all possible design choices *in vitro* and *in vivo* is prohibitively expensive, time consuming, and laborious. To address this gap, we extended the modeling framework ARCADE (Agent-based Representation of Cells And Dynamic Environments) to include CAR T-cell agents (CAR T-cell ARCADE, or CARCADE). We conducted *in silico* experiments to investigate how clinically relevant design choices and inherent tumor features—CAR T-cell dose, $CD4^+$:$CD8^+$ CAR T-cell ratio, CAR-antigen affinity, cancer and healthy cell antigen expression—individually and collectively impact treatment outcomes. Our analysis revealed that tuning CAR affinity modulates IL-2 production by balancing CAR T-cell proliferation and effector function. It also identified a novel multi-feature tuned treatment strategy for balancing selectivity and efficacy and provided insights into how spatial effects can impact relative treatment performance in different contexts. CARCADE facilitates deeper biological understanding of treatment design and could ultimately enable identification of promising treatment strategies to accelerate solid tumor CAR T-cell design-build-test cycles.

2.2 Introduction

Chimeric antigen receptor (CAR) T-cell therapy combines advances in cellular engineering and personalized medicine for patient-specific, targeted cancer treatment [1,2]. This therapy involves collecting, purifying, and genetically modifying a patient's own T-cells to express a CAR that specifically targets the patient's tumor(s) [1,2]. These engineered cells are expanded *ex vivo* and then re-infused into the patient where the CAR T-cells target and kill antigen-expressing tumor cells. The two FDA-approved CAR T-cell therapies and many studies expanding CAR designs exclusively target "liquid" cancers derived from $CD19^+$ B-cells [1,7,8]. CD19 CAR T-cell therapies have shown great success in the clinic with response rates between 70-90% reported [4]. In contrast, response rates for solid cancers are significantly lower at 4-16% [91].

CAR T-cells are currently less effective for treating solid tumors due unique complexities of both the tumor microenvironment (TME) and tumors themselves. First, TME barriers prevent CAR T-cell infiltration [7]. These barriers include the intricate influence of both tumor-suppressing and tumor-promoting cells on the TME [14,15], immune-evading cell markers promoting tumor escape [14,16], and physical and chemical barriers that impact spatial dynamics and nutrient availability [7,15]. Thus, developing CAR T-cells that remodel the immunosuppressive TME has been an active area of research [4,17-20]. Second, solid tumors often lack unique tumor antigens for selective targeting [12]. Cross-reactivity with healthy tissues present harmful or fatal off-tumor effects [4,21]. Cellular engineering efforts have focused on increasing CAR specificity by tuning the affinity of receptor-antigen interactions to avoid healthy cells [7,22-24]. Similarly, creating CAR T-cells that perform Boolean logic can enhance tumor recognition specificity [7,27-30]. Designing CAR T-cells that target multiple antigens simultaneously can also prevent formation of antigen escape variant tumors [25-27]. Finally, additional factors that have not proven problematic for "liquid" cancers, such as the need for site-specific trafficking of CAR T-cells to solid tumors and tumor antigen heterogeneity, further complicate solid-tumor CAR T-cell therapy design [4].

In combination with the array of engineering design choices presented by addressing the constraints above, additional design choices impact CAR T-cell effector functions and long-term persistence regardless of

tumor type. These features include $CD4^+$:$CD8^+$ CAR T-cell ratios [31,32,35], choice of intracellular co-stimulatory domain (ICD) in the CAR [33,34], and the stage of T-cell differentiation [31]. Collectively, the vast number of design choices complicates interpreting and comparing studies of and iteratively tuning CAR T-cell therapies.

Simultaneously tuning multiple features of a CAR T-cell therapy and forecasting their impact on emergent population dynamics remains a grand challenge. Exploring the multidimensional design space becomes prohibitively expensive and laborious *in vitro* and *in vivo*, particularly when considering the time and resources required for mouse experiments. Additionally, some design aspects and emergent properties are difficult to interrogate experimentally, such as cell-level behavioral states that impact treatment efficacy. Employing *in silico* experiments has proven to be a resource-saving and valuable way to understand how underlying biological processes impact CAR treatment outcome and hypothesizing new design features to improve efficacy. Recent CAR T-cell modeling efforts have used ordinary differential equation (ODE) models to understand factors influencing CAR T-cell receptor signaling and downstream activation [92-94]. Other CAR T-cell ODE modeling efforts aim to optimize patient pre-conditioning with chemotherapy [95]. However, these models lack spatial resolution, test a limited set of features, and do not assess emergent cell population dynamics; these important contributions do not yet enable predictions of the sort needed to guide the design of CAR T-cell therapies.

Agent-based models (ABMs) provide ideal *in silico* testbeds for interrogating emergent population dynamics. ABMs are bottom-up computational frameworks that describe the behavior of autonomous agents through defined rules that guide agent actions and interactions within their local environment. The ABM framework provides single-cell spatial and temporal resolution, incorporates quantitative and qualitative experimental observations, and enables tuning and measuring properties of interest through *in silico* experiments [42,43,52,53]. Past ABMs have explored how cell properties influence tumor growth [46,54-56], vasculature and microenvironment dynamics [45,49], immune response to infection and tumors [57,58], and tumor response to checkpoint inhibitor therapy [50]. However, to our knowledge, no ABM reported to date has characterized CAR T-cell dynamics in solid tumors, or explored how CAR T-cell and tumor features impact outcomes.

In this study, we systematically explore CAR T-cell therapy designs in solid tumor contexts by adding CAR T-cell agents to an established ABM (Agent-based Representation of Cells And Dynamic Environments, or ARCADE) comprising tissue cell agents [56] and dynamic vasculature [49]. We use this model—CAR T-cell ARCADE (CARCADE)—to simulate CAR T-cell interactions with tissue cells and analyze a multidimensional design space. We demonstrate that CARCADE recapitulates known observations and predicts responses to new designs for solid tumor CAR T-cell therapies.

2.3 Results

2.3.1 CARCADE characterizes CAR T-cell behavior, metabolism, and effector function

CARCADE provides a flexible framework for characterizing and exploring hypothesized dynamics of population-level tumor responses to CAR T-cell treatment by defining individual CAR T-cell, cancer, and healthy cell features and rules.

2.3.1.1 CAR T-cell agents recapitulate CAR T-cell behavior

ARCADE comprises tissue cell agents with individual subcellular metabolism and signaling modules that influence the cell-level decision making rules and drive emergent population- and environment-level dynamics (**Figure 2.1A**). Tissue cell agent rules and parameters can be tuned to represent either cancer or healthy cells. We introduce a new cell agent representing CAR T-cells into this framework (**Figure 2.1A**). All cell agents are simulated in a microenvironment that comprises either constant nutrient sources (representing a dish context) or vasculature (representing a vascularized tissue context). To distinguish between simulation and experiment, we denote simulated dish and tissue contexts as `dish` and `tissue`, respectively.

Agents navigate through a set of defined, cell-type specific states and rules derived from experimentally observed states and transitions. Each tissue cell can be in one of six states—migratory, proliferative, quiescent, senescent, necrotic, and apoptotic—at each time step. CAR T-cell agents follow a unique rule set with additional states designed to capture T-cell behaviors (**Figure 2.1B**). There are two subtypes of CAR T-cell agents: $CD8^+$ T-cells that primarily provide cytotoxic functions and $CD4^+$ T-cells that primarily

provide stimulatory functions [31,96,97]. Although both T-cell subtypes can provide cytotoxic and stimulatory functions, for simplicity, we specified that each of these T-cell subtypes would perform only their primary function. CAR T-cell agents can enter ten different subtype-dependent states, broadly categorized as desirable and undesirable during treatment. Desired states include migratory, proliferative, stimulatory ($CD4^+$ only), cytotoxic ($CD8^+$ only), and paused. Undesired states include apoptotic, senescent, exhausted, anergic, and starved. Cells change state according to the rule set and to their current state (**Supplementary Figures A.1** and **A.2**, **Appendix A.4 Supplementary Methods Details**). All new model parameters are listed in **Supplementary Table A.1** [24-26,33,49,50,56,98-120].

Each agent utilizes subcellular modules to capture underlying metabolic and signaling states. ARCADE tissue agents use two subcellular modules that control metabolism and signaling. The metabolism module uses stoichiometric equations to determine cellular uptake of glucose and oxygen, which is then converted to energy and cell mass. The signaling module uses an ODE model with regulatory nodes to determine the influence of tumor growth factor alpha (TGFα) on a tissue cell's decision to proliferate or migrate. CAR T-cell agents use the tissue cell metabolism module with modifications to capture the influence of IL-2 signaling and antigen-induced activation on T-cell metabolism: (i) increased metabolic preference for glycolysis; (ii) increased glucose uptake rate; and (iii) increased fraction of glucose used to produce cell mass (**Figure 2.1C**, **Appendix A.4 Supplementary Methods Details**) [36,38-40,101,109,121,122]. CAR T-cell agents also contain an inflammation module to capture the impact of IL-2 binding and antigen-induced activation on IL-2 production in $CD4^+$ CAR T-cells [123-125] and on granzyme production in $CD8^+$ CAR T-cells [96] (**Figure 2.1C**, **Appendix A.4 Supplementary Methods Details**). For both CAR T-cell subtypes, the inflammation module uses an ODE model to determine the amount of IL-2 bound to various IL-2 receptor species [123,124,126].

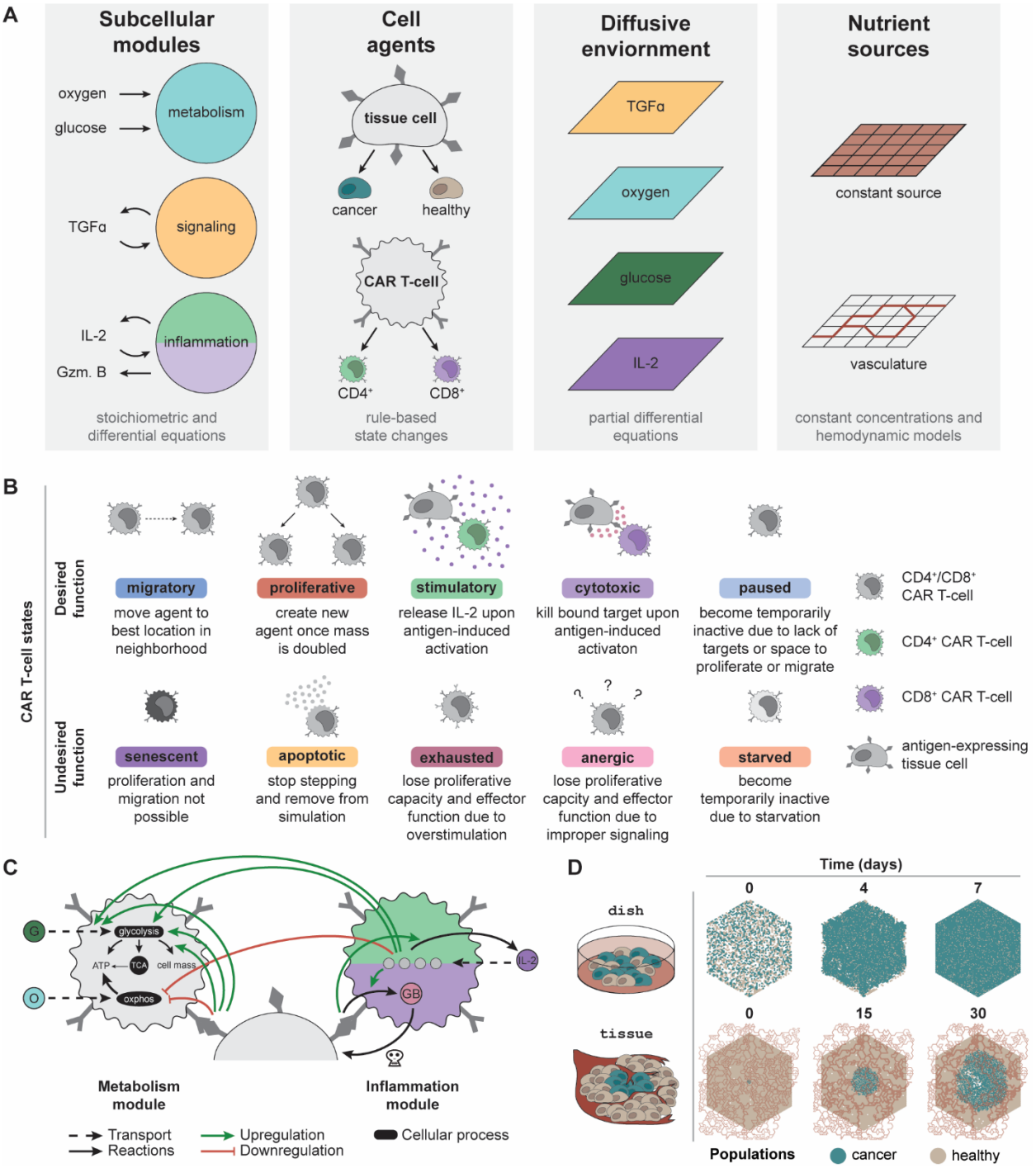

FIGURE 2.1. CARCADE structure and CAR T-cell agent design. (A) Depiction of CARCADE components. Subcellular modules guide underlying cellular function to influence behavior (Gzm. B: granzyme B). Agents include tissue cell and CAR T-cell agents, each of which has separate rule sets and is depicted with surface ligands and CARs (dark gray). Tissue cells include both healthy cells and cancer cells. Agents exist in an environment where diffusion is controlled by partial differential equations and constant sources or vasculature provide nutrients. **(B)** Descriptions of each CAR T-cell agent state, separated by whether the state is desired or undesired for efficacious treatment. **(C)** Diagram of CAR T-cell metabolism and inflammation module interactions with small molecules, proteins, and regulatory edges.

The inflammation module diagram is broken into two parts, showing differences between $CD4^+$ CAR T-cells (light green, top) and $CD8^+$ CAR T-cells (purple, bottom). All CAR T-cells use identical metabolism modules. Regulatory edges (upregulation: green arrow, downregulation: red flathead arrow) result from IL-2 binding and antigen-induced activation. G: glucose, O: oxygen, GB: granzyme B., OXPHOS: oxidative phosphorylation. Legend for cell color is consistent with panel B. **(D)** An example of a single `dish` and `tissue` simulation of untreated cancer cells shown at select time points. For `tissue`, the dynamic vasculature architecture is overlaid.

2.3.1.2 *In silico* experiments mimic *in vitro* and *in vivo* contexts

To provide an *in silico* testbed that can be related to physical experiments, simulations were designed to represent two experimental contexts: `dish` and `tissue` (**Figure 2.1D**). Each configuration utilizes an environment in which four nutrient and signaling molecules—oxygen, glucose, TGFα, and IL—diffuse. Additionally, the environment contains distinct sources from which oxygen and glucose are produced. `Dish` uses a constant nutrient source environment to represent the well-mixed cell media of an *in vitro* experiment. These simulations are initialized with a defined number of tissue cells placed randomly in the environment. CAR T-cells are introduced after 10 min and simulated for 7 d of treatment. `Tissue` uses vasculature to represent realistic hemodynamics of nutrients diffusing through the environment to represent an *in vivo* solid tumor experiment. Vasculature can be degraded and collapse due to cancer cell crowding and movement. These simulations are initialized with a confluent bed of healthy cells and a small colony of cancer cells added to the center of the simulation environment. The cancer cell colony grows for 21 d to form a tumor before CAR T-cells are added and simulated for 9 d of treatment. Untreated `dish` and `tissue` simulations highlight how *in silico* experimental design leads to diverse outcomes (**Figure 2.1D**).

2.3.2 Monoculture and co-culture simulations are consistent with *in vitro* observations

CAR T-cell agents were developed *de novo* based on established cell-level observations; resulting emergent dynamics of the simulation were used for model validation. The comparison between *in silico* and *in vitro/in vivo* experiments is a critical and common method for validating ABMs. To confirm that emergent dynamics follow experimental observations, we tested how outcomes vary as a function of four CAR and tumor features—CAR T-cell dose [127], $CD4^+$:$CD8^+$ CAR T-cell ratio [31,32], CAR-antigen affinity [22-24,128-130], and antigen density on cancer cells [24,111,131,132].

In a clinical setting, CAR T-cells necessarily interact with both healthy and cancer cells, and healthy cell antigen expression can impact off-target effects [116]. It is critical to consider how these CAR and tumor features impact both cancer and healthy cell populations. We simulated CAR T-cell treatment in three different contexts—(i) monoculture with only cancer cells, (ii) ideal co-culture with cancer cells and antigen-negative healthy cells, and (iii) realistic co-culture with cancer cells and low-level antigen expressing healthy cells—modulating CAR T cells and tumor features in each context to assess how *in silico* dynamics compare to observations *in vitro*. Using `dish` removes confounding effects of nutrient constraints and TME factors. We simulated 10 replicates of each combination of features (**Supplementary Table A.2** for monoculture, and **Supplementary Table A.3** for co-culture). In monoculture, `dish` was randomly plated at t = 0 s with 2 x 10^3 antigen-expressing cancer cells. At t = 10 min, treatment begins by adding a dose of CAR T-cells, each expressing 5 x 10^4 CARs with a defined CAR affinity and $CD4^+$:$CD8^+$ ratio. We simulated 7 d of treatment. Co-culture is identical except initial plating uses 1 x 10^3 cancer cells and 1 x 10^3 healthy cells. Simulation trajectories—including each cell's location, state, volume, and average cell cycle length—were collected every half day. The input files used to generate `dish` simulations are described in the **Appendix A Supplementary Information for Chapter 2** (**Supplementary Data A.1** and **Supplementary Table A.4** for monoculture and **Supplementary Data A.2** and **Supplementary Table A.5** for co-culture).

2.3.2.1 Cancer cell and CAR T-cell dynamics are independent of context

We first consider the impact of individual features on cell counts and behavior in `dish` (holding other features constant at intermediate values). In all simulations, cancer cell and CAR T-cell counts follow experimentally observed trends, including conditions with effector-to-target (E:T) ratios less than one where cancer cell killing occurs over several days (**Figure 2.2A** for monoculture, **Supplementary Figure A.3A** for ideal co-culture, **Supplementary Figure A.3B** for realistic co-culture) [117,128]. Increasing CAR T-cell dose increases T-cell counts and accelerates cancer cell killing [127,133]. Our simulations mirror this trend; when E:T ratios are increased beyond the initial range explored (i.e., to explore ratios greater than one), substantial cancer cell killing occurred in monoculture in half the time (all other features are held at intermediate values) (**Supplementary Data A.3** and **Supplementary Figure A.4A**). Increasing the E:T ratio brings closer parity in rate of cancer cell killing between our simulations and experimental analyses,

but we acknowledge that there remains a discrepancy based on time to complete elimination of cancer cells. This difference can be attributed to unaccounted for contact-independent mechanisms of killing, potentially including exosomes [134]; these additional mechanisms were not included in the model for simplicity. Intermediate $CD4^+$:$CD8^+$ ratios maximize cancer killing and increase CAR T-cell proliferation [31,32]. Higher fractions of $CD8^+$ CAR T-cell treatments prove less effective because cytotoxic $CD8^+$ cells need the support of the cytokines primarily produced by $CD4^+$ cells [96,97]. We tested an expanded range of $CD4^+$:$CD8^+$ ratios to include 90:10 and 10:90 in monoculture and co-culture; these extensions further validated observed trends and provided no additional treatment benefit, and thus we do not carry these conditions forward in subsequent analyses (see **Supplementary Note A.1**, **Supplementary Data A.4**, and **Supplementary Figure A.5**). Increasing CAR affinity increases the chances of CAR T-cell antigen binding and subsequent activation, resulting in increased cancer cell killing [24,128,135]. This increased activation also leads to increased proliferation and thus increased T-cell count [22]. Increased antigen expression on cancer cells increases cancer cell killing [24,117,128,131]. Similarly, because CAR T-cells are more likely to be activated by high antigen density cancer cells, CAR T-cell proliferation, and thus counts, increase with increasing antigen count [135]. $CD8^+$ T-cells counts exceed $CD4^+$ T-cell counts even when cells are delivered at a 50:50 ratio, especially in conditions where cells are more likely to be activated [31,32]. The lowest CAR T-cell counts occur when we treat with only one subset of CAR T-cells. Cancer cells cannot be killed off without $CD8^+$ cells. $CD8^+$ cells have limited killing and proliferative capacity without cytokines produced by $CD4^+$ cells, and lack of cancer cell killing presents spatial limitations on CAR T-cell proliferation. Overall, all `dish` simulations, regardless of healthy cell context, support experimental observations of cancer and CAR T-cell dynamics, suggesting that healthy cell presence and antigen expression do not strongly influence cancer and CAR T-cell dynamics or individual feature trends *in vitro*.

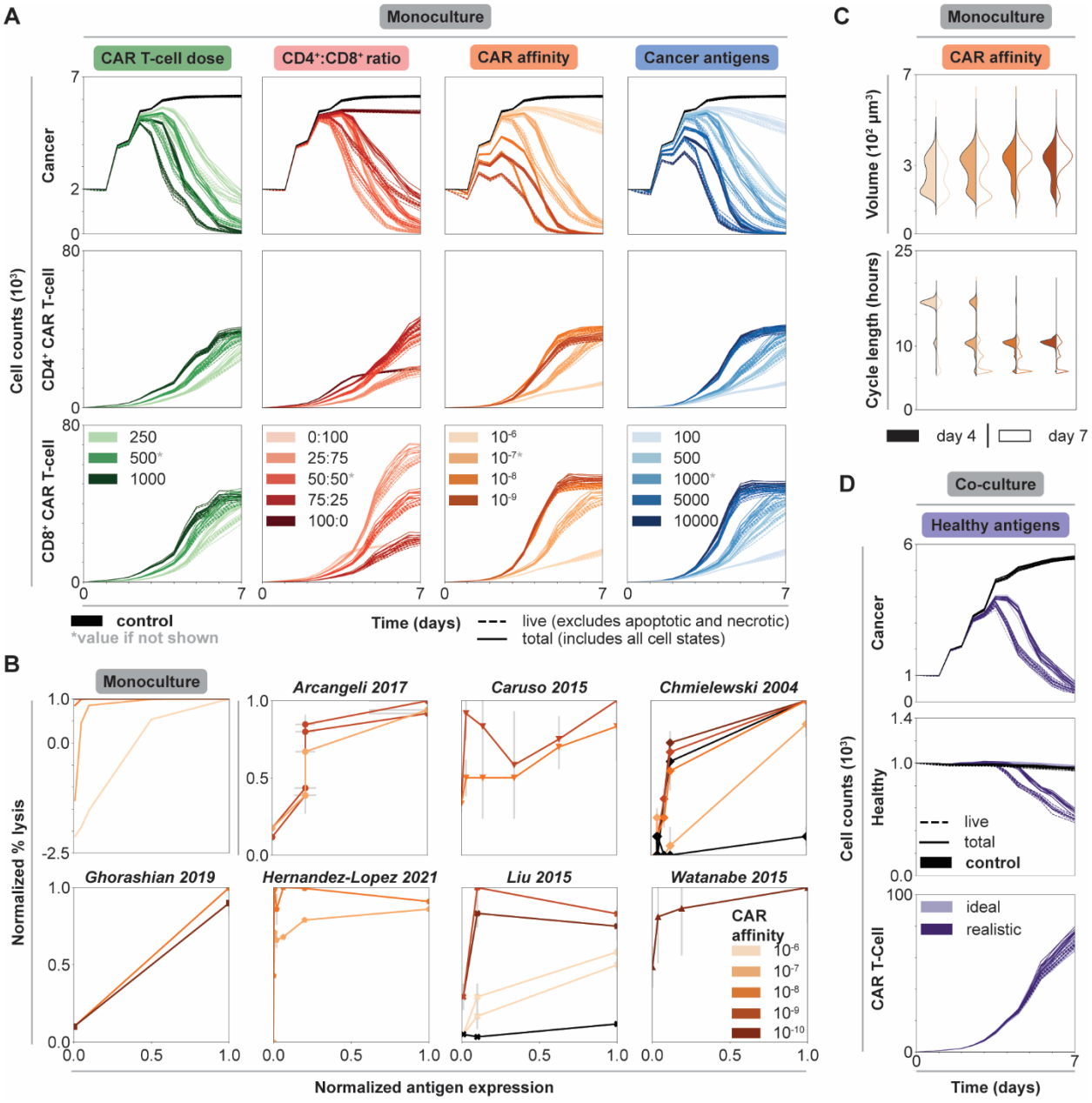

FIGURE 2.2. Impact of individual CAR T-cell and tumor features on cytotoxicity and CAR T-cell growth in `dish`. (A) Cell counts over time of untreated (black) and treated conditions (graded hues) holding all but one feature constant. Each column shows the axis being changed, where all other features are held constant at indicated intermediate values (indicated by asterisk, CAR T-cell dose–500 CAR T-cells, $CD4^+$:$CD8^+$ ratio–50:50, CAR affinity–10^{-7} M, cancer antigens–1000 antigens/cell), while rows show the cell type being plotted. **(B)** Normalized percent lysis curves for *in silico* and published experimental *in vitro* data. Plot for simulated data shows percent lysis for each set of CAR affinity values across normalized cancer antigen values. All other axes were held constant, and the data were averaged across replicates. Simulations with negative percent lysis indicate cancer cell growth. Experimental data—representing an array of CAR types, effector to target (E:T) ratios, ICDs, and cancer cell lines (**Supplementary Table A.6** and **Supplementary Data A.5**)—were normalized to maximum percent lysis and antigen levels with estimated error bars. The plots show percent lysis for each set of CARs tested per paper, each with unique CAR affinity and tested across a range of antigen target values. **(C)** Volume and cell cycle distributions for

CAR T-cell populations at t = 4 d (filled) and t = 7 d (outline) holding all but CAR affinity constant at an intermediate value in monoculture. Legend is consistent with panel B. The data for cancer cell populations and for all other features can be found in the in supplement. **(D)** Cell counts over time of untreated (black) and treated conditions (graded hues) holding all features constant at an intermediate value. Legend is consistent with panel B for both ideal and realistic co-culture. Solid lines represent total cell counts, dashed lines represent live cell counts.

2.3.2.2 Monoculture data qualitatively recapitulate a range of *in vitro* CAR T-cell studies

Quantifying percent lysis as a function of cancer antigen density is a common experimental analysis. In monoculture, percent lysis increases as a function of both antigen count and CAR affinity. This qualitative trend and the general shape of the data agrees with prior *in vitro* observations (**Figure 2B**) [22,24,117,128,130,131,135]. Additionally, for monoculture and most *in vitro* data, higher CAR affinities promote higher percent lysis across all antigen expression values. Our simulations reproduce general trends observed across diverse *in vitro* studies varying in CAR, intracellular co-stimulatory domain, effector to target ratio, and cell lines (**Supplementary Table A.6** and **Supplementary Data A.5**). Notably, CARCADE captures known experimental trends relevant to many different experimental CAR T-cell scenarios without being trained to any specific CAR T-cell experiment. Consistency in these emergent dynamics provides baseline validation that supports our use of the model to interrogate CAR T-cell design.

2.3.2.3 Trends in cell-level features support population-level observations and model validation

Treatment efficacy can be evaluated by volume [105] and cell cycle length [107] distributions, which serve as proxies for CAR T-cell growth and proliferation resulting from antigen-induced activation and IL-2 binding. As an increasing number of CAR T-cells undergo antigen-induced activation, CAR T-cell volumes increase and cycle lengths decrease both over time and with increasing CAR affinity (**Figure 2.2C**). In T-cells, antigen-induced activation and IL-2 binding influence metabolism to help T-cells rapidly proliferate by increasing nutrient uptake, metabolic preference for glucose, and flux of nutrients towards producing cell mass [36-40,101,105,109]. These internal cellular changes increase cell growth rates, increase volumes, and decrease cell cycle lengths [105,107,109,114,136]. The cell cycle length observed *in silico*—an emergent property of the simulations—ranged from around 6-24 h and falls within the range of 2-24 h found *in vitro, in vivo,* and for other *in silico* models [50,102,107,109,114,136]. Cancer cell volumes increase slightly and cycle lengths decrease slightly with increasing CAR affinity and over time, as cancer cells

proliferate to compensate for cell death (**Supplementary Figure A.6A**). Similar trends in volume and cell length distributions are observed across all other modulated features, where conditions with more activated CAR T-cells result in increased CAR T-cell volume and decreased cell cycle lengths (**Supplementary Figure A.6B-D**). Altogether, the model recapitulates known *in vitro* observations, and furthermore, it enables us to observe single cell-level properties that are non-trivial to measure experimentally.

2.3.3 Varying individual features highlights tradeoffs within co-culture

Due to the lack of unique tumor antigens, CAR T-cell designs must rely on target antigens that are more highly expressed on cancer cells than healthy cells [116]. Investigating the difference in treatment outcomes—cancer cell killing, healthy cell sparing, and CAR T-cell growth—between the ideal co-culture (containing antigen-negative healthy cells) and realistic co-culture (containing antigen-expressing healthy cells) is critical for understanding successful CAR T-cell design [22].

2.3.3.1 Healthy cell antigen expression and tumor/CAR T-cell features impact healthy cell killing.

Healthy cell antigen density does not affect cancer cell killing, CAR T-cell proliferation, or previously noted trends across individual features for these populations (**Supplementary Figure A.3**). However, healthy cell antigen density dramatically impacts healthy cell killing (**Figure 2.2D**) [117]. The seeming lack of influence that minimal healthy antigen expression has on CAR T-cell proliferation is demonstrated by a lack of clear difference in CAR T-cell volume and cell cycle length distributions (**Supplementary Figure A.7**) or fraction of cells in the proliferative state (**Supplementary Figure A.8**) between the ideal and realistic co-culture. In general, we hypothesize that the low healthy cell antigen level is too weak to impact these other factors but enables the CAR T-cells to target healthy cells. Thus, healthy cell antigen expression only needs to be considered in avoiding healthy cell death and not in tuning CAR T-cell behavior or cancer cell killing.

To further investigate the impact of healthy cell antigen expression on feature trends, we directly compare cell counts between the ideal and realistic co-culture along the CAR affinity feature axis (**Figure 2.3A**). Cancer cell killing dynamics are nearly identical in both contexts, increasing with increased CAR affinity. In contrast, healthy cell dynamics differ dramatically between contexts. When healthy cells do not express antigen, increasing CAR affinity leads to increased healthy cell count as healthy cells grow to fill the space

left behind by targeted cancer cells. However, when healthy cells do express antigen, healthy cell killing increases with increasing CAR affinity. Additionally, healthy cell counts begin to decrease at increasingly earlier time points with increasing CAR affinity. Comparing cell counts along other features exhibits similar trends: presence of healthy cell antigen generally only impacts healthy cell dynamics, resulting in varying degrees of healthy cell killing (**Supplementary Figure A.3**). These data are consistent with experimental studies demonstrating a detrimental effect of high CAR affinity designs on healthy cells [22,116]. Low affinity CARs successfully target tumors that overexpress the desired antigen and produce minimal off-tumor effects when healthy cells express low antigen levels [22-24]. When healthy cells express antigen, it is not always desirable to have the strongest affinity CAR T-cells.

2.3.3.2 Cell dynamics reveal potential new treatment strategy that spares healthy cells

Comparing trends in cell dynamics between ideal and realistic co-culture provides insight as to why each feature differentially impacts healthy cell killing. In ideal co-culture, increasing CAR affinity and cancer antigen expression level leads to healthy cell growth beyond their original numbers. Increasing CAR T-cell dose and $CD4^+$:$CD8^+$ ratio leads to healthy cell counts similar to those in the untreated control (**Supplementary Figure A.3**). Interestingly, increasing CAR affinity results in more healthy cell growth compared to the case in which cancer cell antigen expression is increased. We hypothesize that this difference occurs because cancer cell killing is more strongly impacted by CAR affinity than cancer antigen density, providing healthy cells more opportunity to grow as more cancer cells die. However, in realistic co-culture, increasing cancer antigen level results in more healthy cell growth before being killed off compared to the scenario in which CAR affinity is increased. Cancer antigen expression primarily impacts cancer cell killing, which gives healthy cells the ability to grow before being targeted after cancer cell populations decline. Meanwhile, CAR affinity impacts both cancer and healthy cell killing, so healthy cells are killed at the same time as cancer cells. These data highlight how each feature differentially impacts the dynamics of this system. A large difference in cancer and healthy cell antigen levels can create a time delay between when cancer killing completes and when healthy cell killing starts, whereas tuning CAR affinity cannot create such a window. This time delay is an emergent phenomenon that occurs in some scenarios—it is not a trained, optimized, or hard-wired parameter in the model. One can design a strategy to take advantage

of this time delay in scenarios when it occurs, for example, by deactivating CAR T-cells with an antibody or small-molecule induced off-switch that shuts down effector function after cancer cells are killed but before lower antigen expressing healthy cells are targeted.

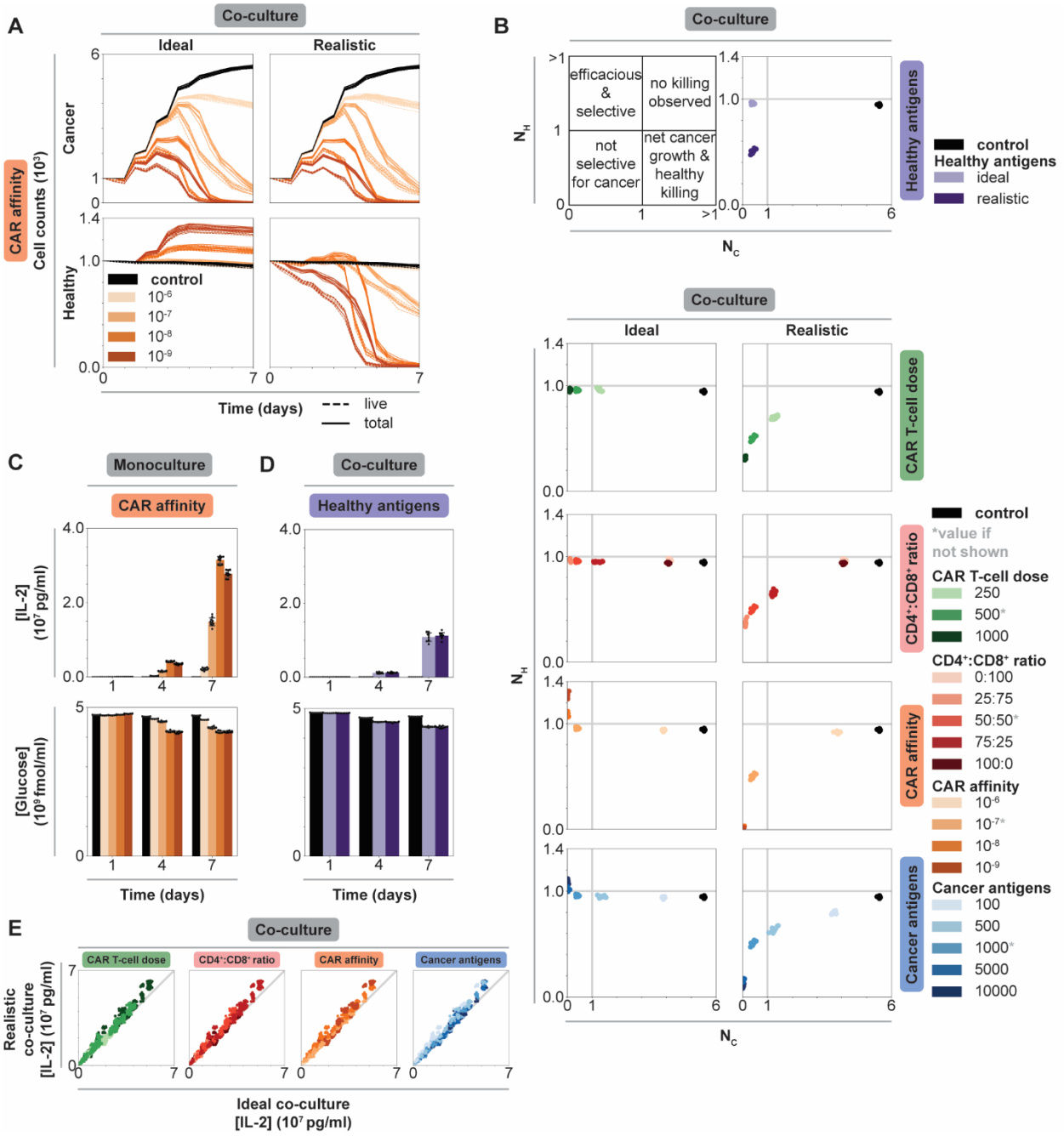

FIGURE 2.3. Impact of individual CAR T-cell and tumor features on efficacy, selectivity, and cytokine production in monoculture vs co-culture. (A) Cancer and healthy cell counts over time of untreated (black) and treated (graded hues) conditions holding all but CAR affinity, which is reported in units of M, constant at an intermediate value and separating data by co-culture context. Column shows co-culture type,

row shows cell type. Solid lines represent total cell counts, dashed lines represent live cell counts (live, excludes necrotic and apoptotic states as in **Figure 2.2**). Intermediate values of other features indicated by asterisk in panel B: CAR T-cell dose–500 CAR T-cells, $CD4^+$:$CD8^+$ ratio–50:50, cancer antigens–1000 antigens/cell. **(B)** Scatter plots of normalized live healthy cell count (N_H) vs normalized live cancer cell count (N_C) for untreated (black) and treated conditions (graded hues) holding all but one axis constant at an intermediate value. Upper left plot shows quadrant meanings. Upper right plot shows scatter plot for different co-culture contexts. Columns show co-culture type, and each row indicates which feature is being plotted. **(C)** IL-2 and glucose concentrations over time holding all but CAR affinity constant at an intermediate value in monoculture. Legend is consistent with panel B. **(D)** IL-2 and glucose concentrations over time varying CAR affinity while holding all features constant at an intermediate value in ideal and realistic co-culture. Legend is consistent with panel B. **(E)** Parity plot of IL-2 concentration at final time point (t = 7 d) for all conditions in realistic (y-axis) vs ideal (x-axis) co-culture colored by each feature (column). Legend is consistent with panel B.

2.3.3.3 Individual feature analysis highlights tradeoffs in a Pareto curve

To quantify cancer and healthy cell killing, we use two metrics: normalized live healthy and cancer cell counts. The normalized count for each population (N_P) is calculated as follows:

$$N_P = \frac{n_F}{n_T}$$

where n_F and n_T are the total number of live cancer or healthy cells at the final (t = 7 d) and treatment start (t = 0 d) timepoints, respectively. Values below one indicate net killing, and values above one indicate net growth. Together, these metrics place treatment outcomes within quadrants that can be used as guidelines for classifying efficacy (**Figure 3B**). Ideally, treatment conditions would appear in the upper left quadrant with maximal healthy cell sparing and maximal cancer cell killing. In both contexts, the trends match those of experimental observations—more aggressive treatments with more overall killing result from increasing CAR T-cell dose, intermediate $CD4^+$:$CD8^+$ ratio, increasing CAR-antigen affinity, and increasing cancer antigen density. These conditions allow for healthy cell maintenance or growth in ideal co-culture, nearing or entering the efficacious and selective treatment quadrant. However, in realistic co-culture, there exists a dramatic tradeoff between cancer cell killing and healthy cell killing, presenting a Pareto curve across each feature. Aggressive treatments exist toward the lower left quadrant (not selective for cancer cells). This observation suggests that it is not possible to optimize both efficacy and safety when healthy cells express antigen, and the most useful strategies—typically less aggressive treatments—balance these objectives [22-24].

2.3.4 IL-2 production is more strongly impacted by tuned features than context

IL-2 production is a standard *in vitro* measurements to quantify T-cell activation [24,31,117]. Similarly, glucose consumption can quantify T-cell activation through nutrient usage and competition [101]. We compare nutrient consumption and cytokine production across features and contexts to identify strategies for understanding, and potentially controlling, IL-2 production.

2.3.4.1 Tuning CAR affinity modulates IL-2 production by balancing CAR T-cell proliferation and effector function

In `dish` (**Figure 2.3C** and **Supplementary Figure A.9A** for monoculture; **Supplementary Figure A.10A** for co-culture), IL-2 increases over time and with increasing values of CAR T-cell dose, $CD4^+$:$CD8^+$ ratio, CAR affinity, and cancer antigen expression level due to increased numbers of activated $CD4^+$ CAR T-cells. Across all contexts and features, glucose decreases as IL-2 increases, indicating that glucose consumption follows CAR T-cell activation and proliferation (**Figure 2.3D**, **Supplementary Figure A.9B**, **Supplementary Figure A.10B**).

Unintuitively, IL-2 concentration is not maximized at the highest CAR-antigen affinity in monoculture where CAR T-cell activation is maximized. At the highest CAR affinity, more CAR T-cells spend time in effector, non-proliferative states (**Supplementary Figure A.11**), resulting in fewer total $CD4^+$ T-cells producing IL-2 (**Figure 2.2A**). This decrease is not observed in co-culture where cancer cell numbers are lower, reducing the likelihood that CAR T-cells will be activated. Decreased activation in co-culture produces lower IL-2 concentrations compared to monoculture. Thus, CAR T-cells in co-culture remain outside of the regime at which this tradeoff between activated and proliferating T-cells is observed. We hypothesize that maximum IL-2 production occurs at intermediate CAR affinity where these exists a balance between proliferation and frequent antigen binding. Excessively high CAR affinity leads to frequent target antigen binding, causing CAR T-cells to spend more time in effector rather than proliferating states, leading to fewer total CAR T-cells that can later produce cytokines. On the other hand, very weak affinity CARs drive cells primarily into states other than proliferative and effector states. Maximizing CAR-antigen affinity can therefore prove

counterproductive for achieving CAR T-cell proliferation, survival, and cytokine production at the tumor site; moderate CAR-antigen affinities may be more effective.

2.3.4.2 IL-2 production is independent of healthy cell antigen expression

In co-culture, healthy antigen expression minimally impacts IL-2 production and glucose consumption over time (**Figure 2.3D**). We speculate that healthy antigen expression is too low to strongly impact CAR T-cell proliferation and thus IL-2 production. Comparing final IL-2 concentration in all ideal versus realistic co-culture conditions reveal that IL-2 levels are independent of context for a given condition, further supporting this hypothesis (**Figure 2.3E**). CAR T-cell IL-2 production and overall glucose consumption are more strongly impacted by the higher level of antigen expression on the cancer cells than by the low antigen expression on healthy cells. When considering desired IL-2 levels produced by CAR T-cells in patient treatment, IL-2 production can be mostly attributed to and designed around cancer cells in isolation as healthy cell antigen expression does have a significant impact.

2.3.5 Multidimensional data analysis reveals context-specific treatment strategies

Since tuning individual features has different impacts on treatment efficacy based on the type of `dish`, we rank-ordered treatment outcomes across all individual simulated conditions, tuning all features simultaneously, within each context. Comparing the strongest treatments between monoculture and co-culture will enable us to determine how optimal treatments vary between contexts.

2.3.5.1 Aggressive feature choices additively benefit treatment in monoculture

For monoculture, outcome is sorted by normalized live cancer cell count (**Figure 2.4A**). The best outcomes typically occur at the highest CAR T-cell doses, at a 25:75 $CD4^+$:$CD8^+$ ratio, at moderate to strong CAR affinity, and with high cancer cell antigen density. These trends are consistent with individual feature analyses in monoculture, and the same trends are observed in scenarios in which we considered expanded CAR T-cell doses (**Supplementary Figure A.4A** and **A.4B**) and $CD4^+$:$CD8^+$ ratios (**Supplementary Figure A.5F**). Choosing aggressive values for all features and using large E:T ratios yield cancer cell killing rates that are comparable with those observed in most experimental studies that use E:T ratios greater than one

(i.e., killing most cancer cells occurs within hours), (**Supplementary Figure A.4A**). Worse outcomes, in which cancer cells grow beyond their initial plated count, occur at low CAR T-cell doses, at 100:0 and 0:100 $CD4^+$:$CD8^+$ ratios, with the weakest CAR affinity, or with lower cancer cell antigen expression. Overall, combining aggressive choices for individual features additively benefits treatment outcome in monoculture. Effective CAR T-cell designs in the absence of healthy cells combine design choices from individually optimized features.

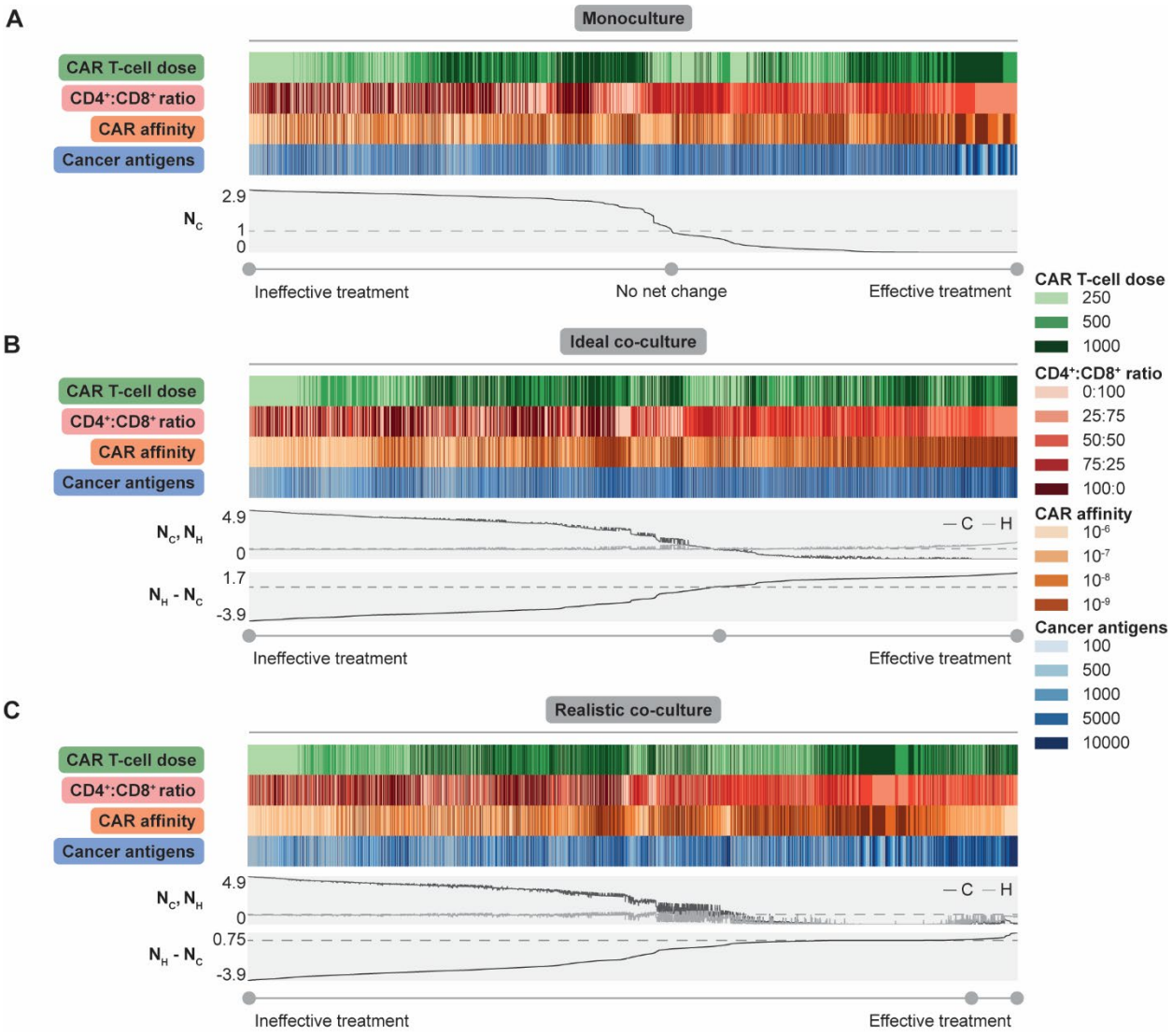

FIGURE 2.4. Collective impact of CAR T-cell and tumor features on `dish` outcomes. (A) Heatmap showing values for each feature with line plots showing normalized live cancer cell count (N_C) sorted from highest (left) to lowest (right). The dashed line indicates value of N_C = 1, meaning no net change due to treatment. Values of N_C > 1 indicate net growth and values of N_C < 1 indicate net killing. **(B)** Heatmap showing values for each feature with line plots showing normalized live cancer cell count (N_C) and

normalized live healthy cell count (N_H) (dashed line indicates normalized live cell count of 1) and the difference in normalized live healthy and cancer cell counts ($N_H - N_C$) for each ideal co-culture simulation individually (dashed line indicates $N_H - N_C = 0$). The heatmap has been sorted from lowest (left) to highest (right) difference. All metrics were calculated at the final time point (t = 7 d). **(C)** Heatmap and normalized cell counts for realistic co-culture. Labels are consistent with panel B. Each feature is reported in the following units; CAR T-cell dose–500 CAR T-cells, $CD4^+$:$CD8^+$ ratio–50:50, CAR affinity—M, cancer antigens–1000 antigens/cell.

2.3.5.2 Addressing off-target effects requires tuning multiple parameters

To identify general conclusions across diverse co-culture conditions, we considered treatment outcomes across all individual simulated conditions, sorted by the difference in the normalized live healthy and cancer cell count at the endpoint (**Figure 2.4B** for ideal co-culture, **Figure 2.4C** for realistic co-culture). This difference is maximized when healthy cells are spared and cancer cells are killed. We expect aggressive treatments to be most effective in the ideal cases, as healthy cells that do not express antigen cannot be killed. Trends in ideal co-culture match those in monoculture, supporting the idea that “invisible” healthy cells do not change observed trends.

However, the realistic co-culture where healthy cells express antigen, and can therefore be targeted by CAR T-cells, is more clinically relevant. In this context, there is a distinct tradeoff between cancer cell killing and healthy cell sparing. Conditions with the lowest normalized live cancer cell counts also show the lowest normalized live healthy cell counts (**Figure 2.4C**). Treatments with a positive difference all have some amount of healthy cell killing, but this killing is minimal compared to other conditions. Effective treatments have the highest doses of CAR T-cells, weaker CARs, $CD4^+$:$CD8^+$ ratios of 25:75 or 50:50, and higher cancer cell antigen count (**Figure 2.4C**). These observations agree with experimental findings that optimization of CAR T-cell therapy design yields different conclusions when balancing cancer cell killing and healthy cell sparing, versus focusing on the former objective alone [22-24]. Though choosing high doses of weak CAR T-cells might seem unintuitive, using weak CARs minimizes the probability of targeting healthy cells while the high dose maximizes the probability that these weaker CARs successfully interact with high antigen density cancer cells. These results suggest that delivering higher doses of weaker CAR T-cells with $CD4^+$:$CD8^+$ ratios of 25:75 or 50:50 kill more cancer cells and spare more healthy cells for tumors where on-target off-tumor killing is undesired or detrimental.

2.3.6 Spatial dynamics drive vascularized `tissue` treatment efficacy

CAR T-cell therapy has great potential for use in solid tumor contexts, which include a complex tumor microenvironment, vasculature, spatial dynamics, and potentially antigen-expressing healthy cells. Predicting how the *in vitro* behavior conferred by various CAR T-cell designs corresponds to *in vivo* performance is not straightforward. We investigate the translation and efficacy of select treatment strategies in vascularized `tissue` where a solid tumor exists in a bed of antigen-expressing healthy cells within a dynamic microenvironment. We chose a subset of simulations—the realistic co-culture conditions deemed effective after averaging across replicates (**Supplementary Table A.7**)—to analyze in `tissue`. Effective treatments were those that met the following two conditions: (1) cancer cells did not grow beyond the initial number, and (2) no more than 50% of the initial healthy cells were killed off.

A `tissue` is initialized with a bed of healthy cells in vascularized tissue that was inoculated with cancer cells and grown for 30 d. At t = 21 d, treatment began by adding a specified total dose of CAR T-cells, each expressing 5 x 10^4 CARs with the given CAR affinity, and $CD4^+$:$CD8^+$ ratio. CAR T-cells were spawned at locations adjacent to vasculature to mimic intravenous trafficking to the tumor; they were not spawned adjacent to vessels that are too small in diameter for CAR T-cells to pass through. Files used to generate `tissue` simulations are described in **Supplementary Data A.6** and **Supplementary Table A.8**.

2.3.6.1 Tested treatments are effective in `tissue` but differ in healthy cell killing

All treated tumors resulted in far fewer cancer cells and somewhat fewer healthy cells compared to untreated conditions, indicating that all strategies identified as effective in realistic co-culture proved effective in `tissue` (**Figure 2.5A**). In `dish`, healthy cell killing occurred primarily after most cancer cells were removed. This again motivates treatment strategies in which CAR T-cells include an inducible off-switch that shuts down effector function after cancer cells are killed but before lower antigen expressing healthy cells are targeted.

Comparing normalized live cancer and healthy cell counts at treatment endpoint enables direct comparison of treatment efficacy (**Figure 2.5B**). Notably, the primarily difference between treatment strategies is in

degree of healthy cell killing. CAR affinity and cancer antigen expression, but not CAR T-cell dose or $CD4^+$:$CD8^+$ ratio, dictate this difference. In general, increasing CAR T-cell dose and using higher $CD4^+$:$CD8^+$ ratio treatments results in increased CAR T-cell counts, but it has little effect on cancer and healthy cell killing. Interestingly, most of the simulations that show the highest CAR T-cell production use the highest CAR T-cell doses and the weakest CAR affinity (**Supplementary Figure A.12**, **Figure 2.5A**), indicating that designs with high doses of weak CAR T-cells result in the highest CAR T-cell growth rate *in vivo*. Overall, these observations reinforce the previously identified treatment strategy: use weaker CARs and select antigens with the highest differential between cancer and healthy cell expression. With this strategy, even though the CAR is weaker, the cancer antigen density is high enough to result in effective, selective treatment.

2.3.6.2 Cancer cells with higher antigen density shield healthy cells from CAR T-cell killing

Though changing multiple features simultaneously complicates analysis, we noted an interesting pattern in which increasing cancer cell antigen density spares more healthy cells in tissue, representing a stark contrast to our `dish` findings. We thus investigated the spatial dynamics of each cell type to probe whether the mechanism by which CAR T-cells navigate within the solid tumor gives rise to this observation. At t = 21 d, cancer cells exist primarily in the center of the simulation, between the center and a radius of about 0.39 mm, while healthy cells are evenly spread across the simulation (**Figure 2.5C**). In untreated conditions, cancer cells grow to cover a radius of 0.58 mm by t = 30 d and healthy cell count remains unchanged over time. In treated conditions, cancer and healthy cell counts decrease over time, primarily starting from the center where most CAR T-cells are initially spawned and moving outward. Cancer cell counts decrease with increasing cancer antigen density. CAR T-cell counts increase as a function of time and cancer cell count, but not as a function of cancer antigen density. Meanwhile, higher cancer antigen levels result in decreased healthy cell killing. We hypothesize that this phenomenon occurs when high antigen density cancer cells effectively outcompete healthy cells for CAR T-cell effector function due to large differences in the probability of CAR-antigen binding between these two potential target cell types. In such scenarios, CAR T cells that successfully traffic to a tumor core are more likely to selectively target cancer cells even if healthy cells are present.

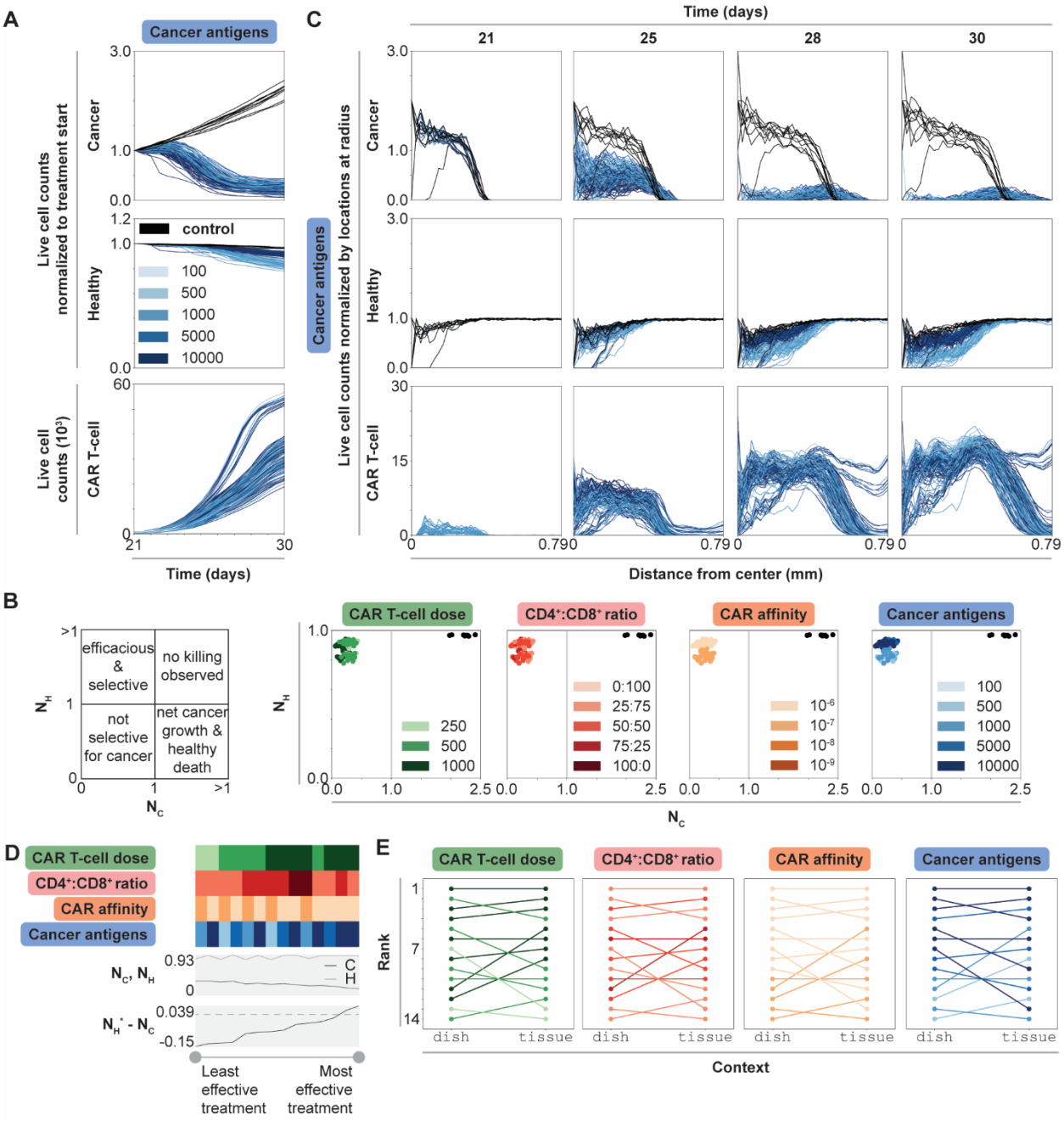

FIGURE 2.5. Dynamic, spatial, and ranked outcomes for selected promising treatment combinations in `tissue`. (A) Live cell counts over time of untreated (black) and treated conditions (graded hues) normalized to cell count at start of treatment (t = 21 d), for all simulations, colored by cancer antigens (other features may be changing as well). Cancer antigens reported in antigens/cell. The same data colored by other features are shown in Supplementary Figure 12. **(B)** Scatter plots of normalized live cancer cell count (N_C, x-axis) vs. normalized live healthy cell count (N_H, y-axis), each normalized to initial value at start of treatment (t = 21 d), for untreated (black) and treated conditions (graded hues) for all simulations, colored by one feature at a time. Each feature is reported in the following units; CAR T-cell dose–500 CAR T-cells,

CD4+:CD8+ ratio–50:50, CAR affinity—M, cancer antigens–1000 antigens/cell. **(C)** Normalized live cell counts over time (t = 21 d, 25 d, 28 d, and 30 d shown) for untreated (black) and treated conditions (graded hues), normalized to locations per radius, for all simulations, colored by cancer antigens. The columns indicate the timepoint in the simulation (day), while the rows indicate cell type plotted, and the x-axis for each plot shows the distance from the center. Legend is consistent with panel B. **(D)** Heatmap showing values for each feature with line plots showing normalized live cancer and healthy cell counts and difference in normalized live healthy and cancer cell counts ($N_H^* - N_C$, where healthy cell value is multiplied by the ratio of cancer to healthy cells at the start of treatment to ensure equal weighting since initial cell population sizes are not equal; dashed line indicates value of 0) at final time point averaged across replicates. The heatmap is sorted from lowest (left) to highest (right) difference. Feature legends are consistent with panels A and C. **(E)** Ladder plots of condition rankings in both `dish` and `tissue`, where condition outcome (averaged across replicates) is colored by each corresponding feature.

2.3.6.3 Spatial differences between `dish` and `tissue` explain treatment performance

Comparing simulation rankings between `dish` and `tissue` reveals how context impacts treatment efficacy. To rank treatment strategies in `tissue`, we consider treatment outcomes across simulations (averaged across replicates) sorted from best to worst outcome in terms of difference in healthy and cancer cell counts normalized to start of treatment (**Figure 2.5D**). Nearly all highest ranked simulations use the highest CAR T-cell dose, a $CD4^+$:$CD8^+$ ratio of 25:75, the lowest CAR affinity, and the highest cancer antigen level. The four highest ranked treatment conditions in `dish` remain the four highest ranked treatment conditions in `tissue` (**Figure 2.5E, Supplementary Table A.9**). The rankings for the mid and lower tier ranked simulations (5^{th}-14^{th} in `tissue`) are shuffled from their original rankings in `dish`. One of the worst ranked treatments in `dish` (11^{th}) jumped to 5^{th} in `tissue`, while a middle-ranked simulation (7^{th}) fell to 13^{th} in `tissue`. These data predict that the most effective treatment conditions in `dish` will perform similarly in `tissue` assuming perfect CAR T-cell trafficking. Even with perfect trafficking, performance in `dish` does not exactly correlate with performance in `tissue`. Certain conditions may outperform in *in vivo* conditions compared to their performance *in vitro*.

Trends in how each feature impacts relative rank reveal which features most strongly dictate performance in `tissue` (**Figure 2.5E**). There are no distinct trends as a function of $CD4^+$:$CD8^+$ ratio. Most conditions that improve in rank use the relatively higher (though still objectively moderate) CAR affinity and higher CAR T-cell dose, and nearly all conditions that decrease in rank (from `dish` to `tissue`) have higher cancer antigen expression level. This finding is surprising given earlier observations that lowest CAR affinity with highest cancer antigen expression level combinations were most effective.

We hypothesize the differences in `dish` and `tissue` trends/rank result from differences in spatial dynamics. In `dish`, both healthy and cancer cells are well-mixed across the simulation, even after treatment, which results in an even spatial distribution of CAR T-cells (**Supplementary Figure A.13**). In `tissue`, cancer cells sit in the center of the simulation surrounded by a large bed of healthy cells, with few healthy cells in the tumor core. When CAR T-cells are spawned with bias towards locations with more cancer cells to mimic perfect trafficking, the probability that spawn locations are adjacent to that of a healthy cell is higher in `dish` compared to `tissue`. Analyzing CAR T-cell state dynamics in both realistic co-culture `dish` and `tissue` for the selected promising treatment strategies further informs this spatial analysis. When we examine the distribution of CAR T-cell states only considering T-cells that are adjacent to a cancer cell (i.e., somewhat controlling for the local environment that a T-cell experiences), we find similar distributions of cells in effector states across `dish` and `tissue` simulations (**Supplementary Figure A.14**). Small numbers of exhausted and anergic cells accumulate in `tissue`, which is notable as these states are not observed in the `dish` context. These states are rare, which is unsurprising as they are expected to accumulate over longer time courses than were used in these experiments, but their presence in `tissue` indicates that they are more likely to appear in *in vivo* experiments compared to *in vitro* experiments. Thus, CAR T-cells in proximity to cancer cells exhibit similar behavior independent of experimental setup, and differences in overall trends/rank between contexts result from differences in collective cancer and healthy cell spatial distributions. Overall, this spatial difference in cancer and healthy cell distribution parallels comparisons between physical *in vitro* and *in vivo* experiments, even if CAR T-cell trafficking deviates from the perfect mechanism employed in our simulations, reinforcing the key role that spatial dynamics play in treatment outcome.

2.4 Discussion

We developed CARCADE as an open-access *in silico* testbed that enables systematic interrogation of the multidimensional design landscape of cellular engineering strategies, therapeutic optimization, and hypothesis generation. After verifying that the developed model recapitulates known trends *in vitro*, we explored design strategies in both `dish` and `tissue` contexts to gain insight into CAR T-cell design.

Tuning individual features in `dish` revealed key insights as to how these features impact CAR T-cell design. For example, we determined that healthy cell antigen expression results in healthy cell killing but has no impact on CAR T-cell or cancer cell dynamics. Modulating individual features recapitulated known tradeoffs between cancer cell killing and healthy cell sparing in realistic co-cultures. A new observation uniquely enabled by our model's high resolution is that maximizing CAR affinity not only increases healthy cell killing but can also be counterproductive to CAR T-cell proliferation and cytokine production. In a related finding, we observed that IL-2 production is influenced more by tunable CAR T-cell design features than by healthy cell-related context.

Multidimensional analysis revealed that the relative performance of various treatment strategies is context dependent. Aggressive treatments are more effective in monoculture and ideal co-culture experiments, but effective treatment in realistic co-culture requires balancing all tuned features. We identified a particularly effective treatment strategy that balances cancer cell killing and healthy cell sparing when healthy cells express antigen. Specifically, we identified that the use of high doses of weak CAR T-cells with intermediate $CD4^+$:$CD8^+$ ratio and a maximized difference between cancer and healthy cell antigen expression produces the most effective treatments. By investigating these effective treatments in `tissue` context, we determined that differences in spatial distributions of cancer and healthy cells in `dish` and `tissue` contexts explain differences in treatment performance between contexts.

CARCADE is a first pass toward demonstrating the utility of models for generating hypotheses and informing design strategies for this class of problem, and it is important to consider that this model makes several assumptions and simplifications. First, the model is not tuned to a specific context. Results are general and might not hold in specific tumor contexts. A major strength of the model is that it can be easily tuned to a specific CAR and/or tumor type, and to interrogate specific design questions of interest. For example, CARCADE does not currently specify the CAR construct's intracellular co-stimulatory domain (ICD), which is known to be an important factor in dictating CAR T-cell efficacy, persistence, and dynamics; rather, we approximate CAR behavior independent of ICD and find that broad trends hold despite not accounting for this factor explicitly. The model could be tuned to capture the effect of different ICD choices on CAR T-cell function. Similarly, the analysis can be tuned to change the definition of effective treatment

outcomes to further penalize healthy cell killing (e.g., when considering treatments in which damage to CAR target antigen-expressing healthy cells is less tolerable from a safety standpoint). When treating B-cell cancers, off-tumor effects like B-cell aplasia are manageable with treatment, and healthy cell killing is less of a concern. In glioblastomas, EGFR is expressed on cancer cells, healthy brain cells, and other tissues, making healthy cell killing a greater risk of morbidity and mortality [22]. Another assumption made in the current CARCADE model is that there is no T-cell-mediated killing of bystander cells unless those bystander cells express the target antigen, which represents an ideal case. This assumption could easily be relaxed to interrogate the consequences of various forms of non-ideal T-cell killing. Additionally, the process by which CAR T-cells traffic to the tumor has been simplified and idealized, as CAR T-cells spawn at sites closest to cancer cells. The model could be adjusted to contemplate other scenarios, such as spawning CAR T-cells at the simulation edge while including CAR T-cell and environmental features that influence CAR T-cell trafficking to the tumor.

Expanding the agents, environment, or subcellular functions included in CARCADE offers opportunities for future model development and use in the field of CAR T-cell engineering. The present model comprises CAR T-cells and cancerous and healthy tissue cells; addition of macrophages, regulatory T-cells, natural killer cells, and other regulatory or supporting cell types or environmental factors could enable investigation of CAR T-cell therapy in a more complete and complex immune environment. In future studies, it may be particularly important to include the cell and environmental factors that contribute to immunosuppressive environments, as this is a common issue faced with *in vivo* CAR T-cell therapy. Additionally, while the current model was designed to facilitate analysis of treatments for solid tumors, particularly through the use of the `tissue` simulations, the `dish` simulations could be adapted to investigate liquid cancer treatment strategies. Future expansions could also incorporate trogocytosis, a processes by which CAR T-cells pick up tumor antigens from cancer cells and then experience fratricidal killing by other CAR T-cells, to investigate how this phenomena affects CAR T-cell persistence [133].

Overall, we believe that CARCADE will prove valuable for CAR T-cell designers and enable cross-cutting collaborations to facilitate further model development or tuning to specific contexts and questions of interest. By further refining the model using experimental data, CARCADE could help suggest potential promising

strategies for experimental pursuit by testing strategies in `dish` and/or `tissue` contexts. CARCADE is designed to enable interrogation of questions and phenomena that are beyond the scope of the current study. For example, future studies using the current model could include a more granular consideration of CAR T-cell trafficking within the tumor by removing the assumption of perfect trafficking. Tumor immune escape could be investigated by creating multiple tumor subpopulations with variable antigen expression levels or susceptibly to killing. Additionally, inter- and intra-tumor heterogeneity could be integrated by simulating tumors that comprise multiple populations with different parameters and/or differing levels of heterogeneity. Ultimately, integrating CARCADE into the CAR T-cell design process could accelerate the design-build-test cycle, saving resources and time associated with new therapeutic development.

2.5 Materials and Methods

CARCADE was developed by extending ARCADE, an existing multi-scale, multi-class agent-based model that includes tissue cells and hemodynamic environments. We used CARCADE to generate *in silico* experiments where we treated monoculture `dish`, ideal and realistic co-culture `dish`, and `tissue` contexts with CAR T-cells. All model details, including adaptation of tissue cell agents, development of CAR T-cell agents, development and adaptation of subcellular modules, development of `dish` plating, and all simulation setups and analyses are described in detail in the Supplementary Methods Details section of the **Appendix A Supplementary Information for Chapter 2** [16-20,24-26,31,33,36-40,49,50,56,96-120,122-126,128,135,137-149].

The agent-based model developed during this study is available at the Bagheri Lab GitHub CARCADE repository: https://github.com/bagherilab/CARCADE.

The scripts developed to process and analyze the data during this study is available at the Bagheri Lab GitHub carcade_mapping_design_space repository: https://github.com/bagherilab/carcade_mapping_design_space.

2.6 Conflict of Interest

The authors declare that the research was conducted in the absence of any commercial or financial relationships that could be construed as a potential conflict of interest.

2.7 Author Contributions

A.N.P., J.N.L, and N.B. conceived the project. A.N.P developed CARCADE by extending the ARCADE model, originally created by J.S.Y. J.S.Y. provided mentorship on the model development process. A.N.P. designed and conducted *in silico* experiments; processed data; and analyzed and plotted results. A.N.P. prepared the initial draft of the manuscript; A.N.P., J.S.Y., J.N.L, and N.B. wrote, refined, and edited the manuscript. J.N.L and N.B. supervised the project.

2.8 Funding

This work was supported by a National Science Foundation Graduate Research Fellowship Program (A.N.P.); the National Science Foundation CAREER award CBET-1653315 (N.B.); and by the Washington Research Foundation (N.B.).

2.9 Acknowledgments

The authors acknowledge computational resources and staff contributions by the Quest high performance computing facility at Northwestern University, which is jointly supported by the Office of the Provost, the Office for Research, and the Northwestern University Information Technology. The authors also thank members of the Leonard and Bagheri Labs for invaluable project discussions and feedback.

2.10 Data Availability Statement

The *in silico* datasets generated and analyzed for this study can be provided upon request.

2.11 Supplementary Material

The Supplementary Material for this article are included with the online publication and include (i) an extended dataset of monoculture simulations with two additional $CD4^+$:$CD8^+$ ratios tested (**Appendix A.2 Supplementary Notes**); (ii) a detailed description of the methods including details on the model framework, tissue cell agents, new CAR T-cell agents, model environment, cell placement and treatment, simulated experiment setups, and data analysis (**Appendix A.4 Supplementary Methods Details**); (iii) figures describing CAR T-cell agent function, details on monoculture/co-culture/tissue simulation time courses and treatment outcomes not shown in main text, such as cell counts and states over time, cell cycle and volume distributions, and environmental IL-2 and glucose concentrations over time, and `dish` spatial dynamics (**Appendix A.3.1 Supplementary Figures**); (iv) and tables showing model parameters, simulation setups, and co-culture/tissue treatment ranking and live normalized cell outcomes (**Appendix A.3.2 Supplementary Tables**).

3 Creating and implementing course content contextualized with anti-racism and social justice in chemical engineering: how faculty and students engaged in the process

This section contains text that is in a manuscript being prepared for the following publication:

> Prybutok AN, Abegunde A*, Sanroman Gutierrez KM*, Simitz L*, Archuleta C, Cole J. Creating and implementing course content contextualized with anti-racism and social justice in chemical engineering: how faculty and students engaged in the process. *In Preparation.* *co-second authorship.

My specific contributions include preparing the ARDEI-Context Question Writing Workshop Canvas page, helping to collect and write content for the asynchronous pre-work, writing an example ARDEI-context question, making some of the videos that accompany the Canvas pages, helping host and facilitate the workshop, helping to write the surveys for both students and faculty, conducting all survey analyses, and writing the manuscript.

3.1 Abstract

Engineering curriculum often fails to connect content and decisions to impacts on diverse, particularly marginalized, communities. Given that integration of social justice ideas into curriculum is currently uncommon among most faculty, we provide resources in the form of a workshop to help catalyze these efforts by teaching faculty how to incorporate social justice into homework and example problems. Through faculty and student surveys, we show the feasibility of this work and benefits on student learning.

3.2 Introduction

The field of chemical engineering interacts strongly with various technical areas that advance energy, medical, and commercial technologies to impact and ideally improve climate change, quality of life, and economic outcomes. Each of these areas intersects with all members of society, but traditional engineering

curriculum engages in depoliticization and decontextualization. Removing this context obscures how these technologies differentially harm, benefit, are developed by, or reach communities with varying identities, where these differences either result from or further societal inequities [59,75,76]. Thus, engineering curriculum often fails to engage with the principles of anti-racism, diversity, equity, and inclusion (ARDEI) and social justice (defined in **Table 3.1**) and how these concepts can be fostered, or hindered, by engineering decisions [76].

There is a great need to reflect on and engage with this ARDEI and social justice context in our classrooms, particularly reflecting on the intersection of chemical engineering content with marginalized communities. At a minimum, integrating this context into coursework will give students the chance to consider the positive, negative, and/or disparate impacts of engineering decisions on communities, particularly for communities with identities different from that of their own [76]. In the long-term, reframing engineering curriculum through a social justice lens will not only help students learn to design robust solutions that meet needs equitably, but also encourage critical thinking about how to *define* problems [76] and taking community-engaged approaches that center and include affected communities in engineering efforts [81].

Some educators have made significant strides in integrating real-world context, current issues, and diverse communities into engineering curriculum, often utilizing inclusive teaching pedagogies in tandem. Inclusive teaching practices and pedagogy already highlight how integration of diverse contexts, interests, contributors, and experiences increase inclusivity and engage students [70,71]. Hirshfield and Mayes wrote homework questions for reaction engineering courses that capture varied student interests (e.g., kinetics of baking, diamond rings, ethical considerations of commercial products) and current events (e.g., the Flint water crisis) [73]. Riley implemented pedagogies of liberation by encouraging students to challenge traditional assumptions, power structures, and terminology often found in engineering curricula when teaching engineering thermodynamics [82], and subsequently wrote a textbook that reframes thermodynamics as energy, a topic that is more inclusive by nature of being a basic human need, and that emphasizes student engagement [83]. Faculty have also incorporated social justice in core engineering classes such as mass and energy balances [84], unit operations [87], feedback control systems [76], and numerical methods [85].

While the above examples highlight the significant work done to integrate ARDEI and social justice contexts into curriculum, this integration hasn't been done in a scalable way such that many or all faculty can teach a contextualized curriculum and students can continue this discourse throughout their degree. This is in part because faculty don't necessarily have the training, background, time, access to resources, or even confidence necessary to contextualize their curriculum. While some trainings that highlight the importance of this work and general strategies to begin it have been provided to the larger chemical engineering community [88,89], there exists the need for a sustainable, accessible, action-driven solution that gives faculty a starting point using the direct context of their own courses.

One low-cost, low-barrier, scalable option to integrate ARDEI and social justice context into curriculum is to embed this context into homework problems. Context can be added either by appending it within existing problems or writing problems from scratch. This approach has several benefits. First, it presents an option that is a manageable time commitment, as writing technical problems at the appropriate level for students in any given course can be time consuming and difficult. Additionally, development of ARDEI-context homework problems would create a lasting and reusable resource that can be shared among faculty. Through this approach, students can consistently engage with this context in many courses if many faculty within a department commit to this work. Finally, this approach lends itself well to collecting feedback and adapting over time.

We created a workshop and lasting resource to help faculty engage in the work to provide faculty with a starting point for centering anti-racism and social justice in their engineering curriculum. The workshop, which is freely and publicly available via a website, provides faculty with training on how to incorporate ARDEI and social justice context into homework problems. We subsequently surveyed students on the impact of engaging with these questions and surveyed and interviewed faculty on the process of developing these questions. In this paper, we detail the content and format of the workshop, as well as the positive effects that engaging with these questions had on students, to provide resources and motivation for other institutions to implement this approach as a first step to integrating ARDEI and social justice into engineering curriculum.

3.3 Research Design

We, the members of the ARDEI Committee, focused on initiatives related to engineering education, developed the following workshop, and conducted the following surveys to carry out this study.

3.3.1 Glossary of terms used

First, we define a glossary of common terms used in this text and within the workshops to provide readers with the same definitions and background we provided to participants (**Table 3.1**).

TABLE 3.1. Glossary of terms.

Term	Definition
Anti-racism	An active and conscious effort to work against multidimensional aspects of racism
Diversity	Having a people of different backgrounds, ethnicities/races, genders, sexualities, perspectives, and mental and physical ability present; note that the presence of a diverse group does not necessarily mean each member is being treated equitably or being supported as needed.
Equity	Providing support to people on an individual basis to ensure that each member of a group or community can participate equally
Inclusion	The active, intentional, and ongoing engagement with diversity (in the classroom or broader communities) in ways that increase awareness, knowledge, and understanding of the complex ways individuals interact within systems and institutions. We note that this is a more traditional definition of inclusion, but we want to incorporate the idea that we are trying to create an environment and culture where members who have historically been excluded or marginalized are welcomed and accommodated within an organization or group.
Social justice	The idea that all people, regardless of identity, deserve equal access, opportunity, rights, and to be treated fairly. Justice often includes the actions that lead to the dismantling of systems and structures that uphold inequality.

3.3.2 Faculty workshop

The workshop for faculty was hosted in two parts consisting of an asynchronous pre-work portion and a synchronous virtual workshop portion. All resources for the asynchronous portion were hosted through Canvas (learning management system). The workshops and resources are described in detail below.

3.3.2.1 Asynchronous workshop and pre-work

We created an asynchronous pre-work section of the workshop, hosted through Canvas, to enable faculty to complete the workshop materials at their own pace and schedule. This pre-work took about 2-4 hours to complete during a 2–3-week span in advance of the synchronous workshop. The goal of this pre-work was

to provide context on the importance of integrating ARDEI context into courses, a baseline DEI terminology to provide sufficient background for all faculty, example ARDEI-context questions and corresponding analysis using a harm assessment worksheet created by the ARDEI Committee (details in **Table 3.2**). Additionally, after faculty successfully completed and deployed ARDEI-context questions in their classrooms, their completed questions and corresponding solutions were added to Canvas for the continuous updating of resources and sharing of ideas. The Canvas site included separate pages on each of the topics shown in **Table 3.2**. The asynchronous workshop and pre-work resources can be found in **Appendix B.1 Supplementary Workshop Content**.

TABLE 3.2. Asynchronous pre-work content.

Topic	Description	Resources
Definitions and Establishing Community Guidelines	Definitions of ARDEI-related terms; Explanation of community guidelines as a way to host discussions in a safe and inclusive way, leaving space for discomfort and reflection; Reflection on creating community guidelines in class	• Video explaining page contents • Definitions of common terms in the context of ARDEI discussions • Sample community guidelines
Reading: Incorporating ARDEI into Class Homework and Examples	Literature from *Chemical Engineering Education* about importance of integrating diverse topics into questions	• Video explaining page contents • During and post-reading reflection questions • Selected reading [73]
Example Problems	Example ARDEI-context questions written by ARDEI Committee members (fluids, kinetics, and separations) and a worksheet to help faculty reflect on whose voice is being uplifted by the added context in the question, and how the way the question is posed may prevent further harm to marginalized students.	• Video explaining example separations questions • Example fluids, kinetics, and separations questions • ARDEI Post-Question Review Sheet • Video explaining ARDEI Post-Question Review Sheet • ARDEI Post-Question Review Sheet filled out for separations question
Understanding and Preventing Harm	Explanation of why it is important to consider positionality and unconscious bias when discussing ARDEI topics, resources (Social Identity Wheel) for reflection on positionality and bias, and explanation of types of harm and the importance of understanding and preventing harm	• Video explaining the importance of considering positionality and bias and preventing harm • Social Identity Wheel [150]

Inclusive Teaching	Resources on inclusive teaching practices, a reading activity with reflection questions for a subset of the selected readings [73,151,152]	• Video explaining the importance and examples of inclusive teaching practices • Selected readings [73,151-154] • Links to inclusive teaching resources provided by the teaching center on campus

Additional Resources	Links to external resources at and beyond the university aimed at supporting students and further providing information on integrating ARDEI context into STEM curriculum and classrooms	• ChBE Department and University resources
		  ○ Use of visual art in teaching engineering (document compiled by A. Abegunde)
		  ○ The NU ChBE Department's ARDEI Committee Website [155]
		  ○ Handout compiled by teaching center on campus about campus resources for supporting students
		• General and STEM Education Resources [77,156,157]

Completed and Draft ARDEI-Context Question Bank	Contains all faculty-written ARDEI-context questions and solutions to enable faculty to share resources and ideas; this page is continually updated as more questions are completed	• ARDEI-Context questions and question solutions written and used by faculty who participated in the workshop and study (kept internal to institution's department)

3.3.2.2 Example questions

We provided faculty with three example ARDEI-context questions written to highlight different types of question development (i.e., written from scratch versus adapting a textbook problem), methods of ARDEI-context integration (i.e., background information, problem solving, resource providing), and question engagement (i.e., resource utilization, brainstorming, reflection, technical problem-solving). Example questions were provided in the topics of Fluid Dynamics, Separations, and Kinetics and Reactor Design, and details about each question's content and method of question development are described in **Table 3.3**. Questions and solutions can be found in **Appendix B.2.1 Example ARDEI-context questions**.

TABLE 3.3. Example ARDEI-context questions provided with asynchronous workshop content.

Course	Question Description	Question Development Process
Fluid Dynamics	This problem focuses on how simple fluid dynamics concepts can be used to estimate the speed of a river current. The question is modified to incorporate ARDEI concepts by asking students to estimate the speed of the current of a contaminated river, specifically in Navajo rivers facilitated by uranium mining on Navajo Nation and Lakota Nation lands. Students are asked to think about the negative effects of Uranium mining on the Navajo community as well as what safeguards could have been implemented to prevent such impact on communities. This should help students think beyond the financial benefit of chemical engineering projects and consider the social impact of their decisions.	Adapted from a textbook problem by adding additional context, resources, and subparts
Separations	This problem focuses on the separation of hydrogen sulfide (H_2S) from a feed gas. The existing textbook question provides technical information about the problem and asks students to do calculations to determine what the separation output and number of equilibrium stages are. The question is modified to incorporate ARDEI concepts by adding both background and additional question subparts. The first adaptation included a preface describing what H_2S is, where it is found in drilling processes, and its dangers to human health to emphasize why the separation is necessary. Additional subparts added to the problem ask students to answer questions related to (i) H_2S regulation, (ii) a current event related to H_2S exposure, (iii) utilize the tool Social Explorer [158], which gives students free (though a university sponsored account) access to past census data, to interpret the relationship between chemical plant locations and marginalized community locations by focusing on the area in the previously mentioned current event as a case study, and (iv) to make actionable recommendations to chemical systems producing H_2S above threshold levels.	Adapted from a textbook problem by adding additional context, resources, and subparts
Kinetics and Reactor Design	This problem focuses on how susceptible-infected-removed (SIR) ordinary differential equation models are used to understand the spread of disease. The problem walks through the kinetic equations describing the basic SIR model, and subsequently asks students to interrogate how population dynamics change as a function of changing transmission and recovery rates. Finally, to incorporate the ARDEI component, students are asked to think about these how the ideal SIR model would need to change in the context of something like the COVID-19 pandemic, where disease spread and treatment were not equitably distributed among populations, and factors such as socioeconomic status, race, environmental conditions, access to health care, and underlying health conditions caused differences in disease dynamics, often most negatively impacting marginalized groups.	Written from scratch

3.3.2.3 Synchronous workshop

The synchronous workshops were hosted as 1-hour virtual sessions and faculty were expected to have completed the pre-work and bring in a question idea or a fully written question along with the completed harm assessment worksheet. The workshop began with a brief introduction and then faculty were separated into breakout rooms with at least one other faculty and one workshop facilitator for discussion and feedback on their ARDEI-context question. The goal of this session was primarily to support faculty in question development through sharing resources and ideas, providing suggestions for edits or enhancements, and harm mitigation. Afterwards, faculty were asked to complete a brief survey, shown in **Table 3.4**, to assess utility and success of the workshop format and content at helping faculty develop ARDEI-context questions. The workshop has been given three times (twice in Summer 2021 and once in Winter 2022), and after receiving feedback from students on the ARDEI-context questions used in Fall 2021, we adapted the workshop slightly for Winter 2022 to address the student feedback, specifically encouraging and discussing adding lecture components to problems.

TABLE 3.4. Faculty post-workshop survey.

Question	Response Option/Type
Before the workshop (and pre-work), how confident did you feel incorporating ARDEI and social justice topics into course/homework questions?	Scale of 1-5 (1=Not confident at all and 5=Very confident)
After the workshop (and pre-work), how confident did you feel incorporating ARDEI and social justice topics into course/homework questions?	Scale of 1-5 (1=Not confident at all and 5=Very confident)
Do you intend to use the ARDEI question you wrote or brainstormed in your future course?	Yes, No, Maybe
If you answered No or Maybe to the previous question, please explain why.	Open-ended response
Do you intend to write other ARDEI questions for use in your future course?	Yes, No, Maybe
If you answered No or Maybe to the previous question, please explain why.	Open-ended response
How useful did you find the Canvas page in navigating through materials and pre-work?	Scale of 1-5 (1=Not very useful and 5=Very useful)
How useful did you find the pre-work in preparing you to write an ARDEI question?	Scale of 1-5 (1=Not very useful and 5=Very useful)
How useful did you find the virtual peer review/brainstorming session in preparing you to write an ARDEI question?	Scale of 1-5 (1=Not very useful and 5=Very useful)
What did you like about the workshop? What was done well?	Open-ended response
What didn't you like about the workshop? What could be improved?	Open-ended response
If you have any additional comments, please leave them here! Thanks for attending!	Open-ended response

3.3.3 Question deployment and student surveys

To assess the impact of ARDEI-context questions, we reached out to faculty teaching each quarter who participated in the workshop(s) to see if they planned to deploy the question in their course. For those who were, we provided faculty with a link to a Qualtrics survey, where no identifying information was collected, to give to their students in order to assess the success and impact of the ARDEI-context question on student learning and association with chemical engineering and social justice concepts (**Table 3.5**). Students given a survey on Qualtrics After reaching out to faculty, we occasionally provided additional feedback on the question was provided if edits were made after the synchronous workshop and feedback was requested.

TABLE 3.5. Student ARDEI-context question impact survey.

Question	Response Option/Type
What course are you filling this out for?	Drop down list of specific courses in which faculty deployed these questions
What quarter are you filling this out for?	Drop down list of quarters in which courses took place
Please rate how strongly you agree or disagree with the following statements: • I was familiar with concepts of anti-racism, diversity, equity, and inclusion (ARDEI) and social justice before taking this course. • Engaging with this question increased my awareness of and ability to recognize how ARDEI and social justice relate to chemical engineering/my field. • Engaging with this question increased my ability to critically evaluate how current engineering practices or theories have been used to promote or fight inequity. • Engaging with this question increased my awareness of how marginalized communities are impacted by engineering decisions. • Engaging with this question increased my desire to make change in chemical engineering/my field. • This question was very clearly related to ARDEI and social justice context. • This question brought up context that had not previously been brought up in my chemical engineering classes before. • Adding ARDEI and social justice concepts into chemical engineering course questions is a good way to promote social and/or environmental justice in engineering practice. • I would like to see more ARDEI and social justice focused content integrated into chemical engineering course questions.	Likert Scale including the following options: Strongly disagree, Somewhat disagree, Neither agree nor disagree, Somewhat agree, Strongly agree
What else do you want us to know about your experience engaging with this question?	Open-ended response

Faculty deployed these ARDEI-context questions in a range of core and elective courses, where classes contained undergraduate students only, graduate students only, or a mix of both. Typically, these questions were integrated into homework sets, however some faculty included lecture components or integrated ARDEI-context into course projects. The key-labeled list of courses per quarter where data was collected is listed in **Table 3.6**.

TABLE 3.6. Course information and survey response rate for courses where faculty deployed ARDEI-context questions.

Course Label	Core/ Elective	Quarter	Undergraduate/ Graduate/Mix	Number (%) of total responses	Response rate (% of class)
C1F21U	Core	Fall 2021	Undergraduate	36 (43.4%)	85.7%
C2F21U	Core	Fall 2021	Undergraduate	13 (15.7%)	48.1%
E1F21M	Elective	Fall 2021	Mix	6 (7.2%)	33.3%
C3F21G	Core	Fall 2021	Graduate	12 (14.5%)	36.4%
E2W22M	Elective	Winter 2022	Mix	12 (14.5%)	48.0%
C4W22U	Core	Winter 2022	Undergraduate	4 (4.8%)	44.4%
All courses	Mix	2021-2022	Mix	83	53.9% of enrolled students

3.4 Results

3.4.1 ARDEI-context question writing workshop built faculty confidence and supported question development

Quantitative responses to the post-workshop survey highlighted the impact of the workshop on supporting faculty in engaging with and writing ARDEI-focused content. After completing the workshop asynchronous pre-work and synchronous session, faculty reported increased confidence in incorporating ARDEI and social justice topics into course/homework questions compared to before the workshop (**Figure 3.1A**). Additionally, nearly all faculty reported that they intended to use the ARDEI-context question that they wrote or brainstormed during the workshop write additional questions for their future courses, highlighting the success of the workshop in helping faculty both with current and future question development (**Figure 3.1B**). Those who responded “maybe” to using and writing ARDEI-questions primarily indicated they wanted to do additional work to refine their questions rather than use them in their current form. Together, these findings speak to the success of the workshop in encouraging and preparing faculty to include ARDEI and social justice context into their course problem sets.

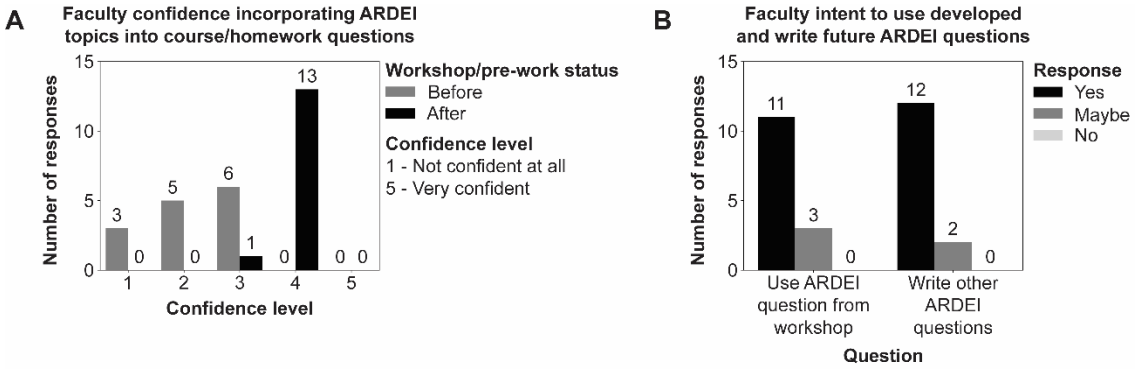

FIGURE 3.1. Faculty engagement with the workshop increased confidence in and intent to incorporate ARDEI and social justice topics into course questions and content.

Qualitative responses to the survey revealed the key aspects of the workshop that faculty found most beneficial. Faculty attributed the workshop's success primarily to both the compiled resources, which gave them ideas and a shared vocabulary and starting point, as well as the discussion, which helped provide feedback, ideas, and specific resource procurement regardless of question stage. Given the resources provided in this paper, this workshop format could be recreated and deployed at other university settings, further expanding this work and enabling other faculty to undergo this training.

3.4.2 Engaging with ARDEI-context questions supports student understanding of how ARDEI and social justice intersect with the field of chemical engineering

We surveyed students who engaged with ARDEI-context questions written by faculty who took the workshop and taught in Academic Year 2021-2022 to determine the impact of engaging with the question on student learning and ethics and to assess student's perspectives on if incorporating ARDEI-context into homework questions is a good way to engage with these important topics. We collected data on a total of 83 students across 4 core classes (3 undergraduate, 1 graduate) and 2 electives (open to both undergraduate and graduate) using the survey described in Table 4. Given the small sample size within any one class, we analyzed this data collectively to get a sense of generalizable success of this method.

We first assessed how engaging with the ARDEI-context question impacted student ability to connect ARDEI principles to chemical engineering concepts (**Figure 3.2A**, **Table 3.4**). Nearly all students (n=74/83, 89.1%) somewhat or strongly agreed with the idea that engaging with the questions increased their

awareness of and ability to recognize how ARDEI and social justice relate to CHE. A similarly high fraction (n=70/83, 84.3%) somewhat or strongly agreed with the idea that engaging with the question increased their ability to critically evaluate how current engineering practices or theories have been used to promote or fight inequity. Most students (n=72/83, 86.7%) also reported an increased awareness of how marginalized communities are impacted by engineering decisions. Finally, in assessing the longer-term impact of engaging with ARDEI-questions, most students (n=72/83, 86.7%) reported that engaging with the question increased their desire to make change in chemical engineering/their field. Notably, this question had the highest fraction of students who “strongly agreed” with the statement, further indicating the potential to have positive long-term impacts on student goals and role in the field. Overall, students, who comprise a mix of undergraduate and graduate students, had an overwhelmingly positive response to engaging with these ARDEI-focused questions. Engaging with the question increased their understanding of chemical engineering’s impact on inequities and marginalized communities. Perhaps most importantly, the question impacted students’ desire to make change in their field, which supports and directly relates to the overall goal of engaging with ARDEI-focused curriculum of creating ethical and anti-racist engineers.

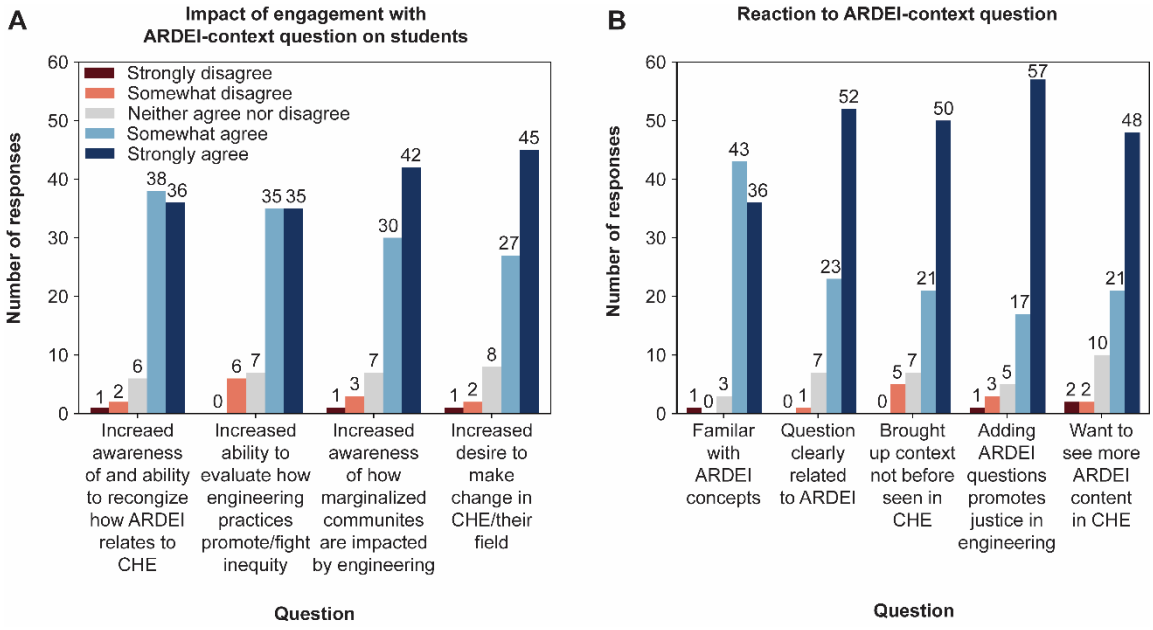

FIGURE 3.2. Student quantitative responses indicate the positive impact of engaging with ARDEI-context questions and the desire to see more of these types of questions in their courses.

To gauge student perspectives on this method of engaging with ARDEI-content, we asked questions about their existing familiarity with ARDEI and social justice concepts and if they'd already engaged with these topics or would like to see more questions like these in other courses (**Figure 3.2B**, **Table 3.4)**. While most students (n=79/83, 95.2%) reported being familiar with ARDEI concepts, students (n=71/83, 85.5%) confirmed that there is a lack of integrating this context into courses. Nearly all students (n=75/83, 90.4.9%) also reported that the question they engaged was clearly related to ARDEI, indicating the success of the faculty to write questions that directly address these topics. Following the indicated success of this question, students agreed that adding ARDEI and social justice concepts into chemical engineering course questions is a good way to promote social and/or environmental justice in engineering practice (n=74/83, 89.2%) and that they'd like to see more ARDEI and social justice focused content integrated into CHE course questions (n=69/83, 83.1%). These results highlight student's desire to engage with ARDEI content within their chemical engineering curricula and support this method as a low-barrier, low-cost and still successful method of facilitating this engagement.

When given the chance to leave additional, qualitative feedback, students reported both appreciating the effort being made to incorporate ARDEI into curriculum and a desire to see more than just integration of this content in homework problems. While some faculty integrated lectures related to their ARDEI-context problems, those who did not received feedback from students wishing for discussion of the topic rather than just encountering it on homework problems in isolation. For example, one student said, "*I think it would be more beneficial to use questions like these as a starting point for a larger class discussion rather than it simply being a homework problem*". Further supporting this point, one student in a course that used both a discussion and homework reported that "*the discussion of the question in class was a bit more useful than answering the question individually for homework, where we weren't discussing and learning collaboratively*". Meanwhile, other students in that same course asked for the discussion to be deeper, but still acknowledged that this was a great step. These findings speak to student desire to engage with this material frequently and critically. One student particularly highlighted this point, saying "*The ARDEI questions allowed me to have more of a connection with the impacts of research and engineering. This not only brings social justice topics forward but also helps me learn the material in a more memorable way.*"

Another student said, "*I really liked how this was incorporated into our homework problem set!*". Collectively, these responses highlight the benefit of integrating this content, and how this is a good first step of integrating social justice throughout engineering curriculum. Following this feedback, some of which was collected after Fall 2021, we recommended to all faculty deploying questions in Winter 2022 and Spring 2022 to integrate lecture components and updated the workshop's synchronous session to encourage and further support this recommendation.

One important note is student criticism of this work, which was minimal but highlighted important points. One student reported that they "*do value factoring ARDEI curriculum in chemical engineering courses, but I wish that other issues were more addressed…I wonder what more work ARDEI can do to address these issues and create a more diverse space*". Similarly, another student noted that "*I feel that even though the sentiment is the right one and the question was good, for those of us who are already familiar with these issues (personal background, international students, etc.) The question felt a bit disconnected…I think that it would be much more valuable to hold conversations/lectures/presentations on these issues where people can really ask questions and get enough information, because an out of context homework problem every other day does not feel very effective in this context*". These students brought up the previously mentioned desire for lectures, but also for other issues related to ARDEI beyond the curriculum to further foster equitable spaces. Additionally, their full comments highlighted the need to ensure ARDEI-questions and those writing them invest time learning about the topics discussed, don't reinforce stereotypes for marginalized communities, and to not oversimplify or characterize these topics without depth. Analyzing these questions to ensure they don't prevent further harm, such as by using the harm-assessment worksheet, is a first step at addressing these comments. Ensuring these needs are met will take time, effort, and critical thought, but the impacts and benefits to students are clear if this is done well.

3.5 Discussion

This paper outlines the process by which a low-cost, low-barrier method for integrating ARDEI and social justice context into chemical engineering curriculum. Specifically, we analyzed the impact and benefit of writing and engaging with ARDEI-context homework questions on faculty and students, respectively. After

the workshop, faculty reported an increased confidence in and intention to write homework or course questions contextualized in ARDEI and social justice. This finding speaks to the effectiveness of the workshop at training faculty in this endeavor. Students also reported the benefits of engaging with these questions, including increased ability to connect engineering decisions to societal inequities and motivation to make positive change in their field. The students' desire to see more of these questions in the classroom provides strong support for the need to incorporate ARDEI work into chemical engineering curriculum, and the collective faculty and student responses indicate this workshop as a successful method to facilitate this work.

We provided these resources in full in the hopes of sharing this work beyond the original institution. We acknowledge that development of and participation in this workshop and study was facilitated by being members of a private research intuition with the support of a teaching and learning center and commitment to DEI and of a department with a strong commitment to ARDEI. Unfortunately, not all members of academic institutions have this privilege, which may make implementation of this workshop more challenging. We hope that by sharing the overwhelming positive outcomes of this work, members of the chemical engineering education community will feel encouraged to begin integrating ARDEI and social justice principles into their courses.

Integration of social justice principles into curriculum is important for increasing student sense of belonging, understanding of inequity, and desire to support marginalized communities, but this integration needs to be handled with care. Faculty need to put concerted effort into the questions they write to ensure further harm is not being caused to students holding marginalized identities. This effort will entail engagement with more than just DEI trainings, but also a deep, critical thought on selected question topics, awareness of and reflection on positionality, and empathy for marginalized communities affected by inequities and engineering.

This workshop is only the first step in empowering widespread faculty to address the harm of allowing oppressive systems, biases, and inequities to remain uninterrogated. Since ABET requirements will soon mandate minimal inclusion of this work [159], this workshop can help engineering departments meet this

immediate need. Down the line, we hope that future changes centered on redesigning whole engineering courses and curriculum from a social justice lens will become the norm rather than the work of select few faculty.

3.6 Concluding Remarks

The collective positive response from students about the benefits of and desire to see more of these questions in the class provides strong support for the need to incorporate ARDEI work into chemical engineering curriculum independent of the updated ABET requirements. The reported success of this relatively low-time commitment workshop will hopefully inspire and enable implementation of this workshop at other universities. Given that development of high-quality, well thought through resources takes significant time and research, teaching faculty or others invested in this work, should be given tenure to help further fund and facilitate this work and devote the necessary time to development of these resources

3.7 Acknowledgements

We thank the Northwestern University ChBE ARDEI Committee for their support of this work and feedback on the workshop, resources, and the manuscript. Additionally, we would like to thank the Northwestern University Institutional Review Board for their support and suggestions. We thank all the faculty and students who engaged with the workshops and/or questions, gave their thoughtful feedback, and participated in interviews. Finally, we would like to thank the Searle Center for Advancing Learning and Teaching who curated many of the inclusive teaching materials that we linked in the workshop resources.

4 Conclusions, Future Work, and Perspectives

4.1 Conclusions

The advancements outlined in this body of work contribute both to the fields of chimeric antigen receptor (CAR) T-cell therapy design (detailed in Chapter 2) and chemical engineering education (detailed in Chapter 3). These contributions to both fields ultimately provide resources—in the form of an agent-based model and a training workshop for faculty, respectively—that can be used by future computational immunologists or engineering educators to further expand this work.

4.1.1 CARCADE enables exploring CAR T-cell therapy design strategies in varied contexts

Using the developed agent-based model (ABM)—a "bottom-up" computational model that utilizes first-principles to dictate probabilistic rules that guide agent behaviors and interactions within the context of a local environment—CAR T-cell therapy design strategies to treat solid tumors can be explored in `dish` and `tissue` contexts. This work builds upon a previously established ABM, Agent-based Representation of Cells and Dynamic Environments (ARCADE), to create CAR T-cell ARCADE (CARCADE). CARCADE agents include both cancerous and healthy tissue cells and $CD4^+$ and $CD8^+$ CAR T-cells, each equipped with metabolism and signaling modules, interacting within a vascularized and diffusive tumor microenvironment. Using CARCADE as a testbed, we investigated fundamental design questions that are difficult to address experimentally by exploring tunable CAR T-cell design parameters in a simulated monoculture `dish`, ideal (no healthy antigen expression) and realistic (low level of healthy cell antigen expression) co-culture `dish`, and `tissue` contexts. Specifically, we tested how CAR T-cell dose, $CD4^+$:$CD8^+$ CAR T-cell ratio, CAR affinity, and cancer cell antigen expression level affect cancer and/or healthy cell killing in each context both individually and in combination. Our *in silico* experiments qualitatively mimic experimental *in vitro* cell behaviors, and we subsequently used the model to uncover new treatment strategies and tested the best performing treatment conditions in an *in silico* tissue context to predict outcomes *in vivo*, uncovering the impacts of differences between `dish` and `tissue` spatial dynamics on treatment outcome. This work sets the foundation for future *in silico* experiments that use this

model as a flight simulator for elucidating design rules that may ultimately guide the construction of novel CAR T-cell therapies for solid tumors.

4.1.2 Workshop training enabled faculty to incorporate social justice context into chemical engineering course problems

Through development and facilitation of a workshop, chemical engineering faculty were supported through development of course homework problems that incorporated anti-racism, diversity, equity, and inclusion (ARDEI) and social justice context. This work addresses the common lack of connection between chemical engineering curriculum and how engineering decisions differentially impact various communities, specifically marginalized communities. The workshop proved an effect method of giving faculty the confidence and tools necessary to write and deploy ARDEI-context questions in their courses. Additionally, student reported the benefits of engaging with these questions, including increasing their awareness of the connection between engineering decisions and the impact on marginalized communities and increasing their desire to make change in their field. Overall, this workshop provides a starting point for a low-cost, low-barrier, and scalable way to empower faculty to integrate social justice into their courses, enhancing student engagement, inclusion, and critical thinking surrounding these issues.

4.2 Future Work

4.2.1 CARCADE facilitates exploring context-specific or novel CAR T-cell design strategies

4.2.1.1 CARCADE enables investigating CAR T-cell treatment strategies in heterogenous tumor contexts

CAR T-cells exclusively target tumor cell-surface antigens [4]. Due to a lack of unique tumor antigens, CARs must often target antigens more highly expressed on tumor cells than healthy cells [116]. Studies found that low antigen affinity CARs successfully target tumors that overexpress the desired antigen while minimizing off-tumor effects on healthy cells with low antigen levels [22-24]. However, tumor antigen expression heterogeneity could enable tumor variant escape through survival of low antigen density or

antigen-absent tumor populations [22,160]. Increased understanding of this tradeoff would aid in designing future CARs with increased efficacy and safety.

While the current work utilizes CARCADE to explore CAR T-cell treatment strategies in homogenous tumor contexts, the model could be used to elucidate CAR T-cell treatment strategies in heterogenous solid tumors to determine the tumor propensity to escape, therapeutic efficacy, and severity of off-tumor effects as a function of CAR-antigen affinity in a variety of tumor makeups. Tumor heterogeneity could be intra- or inter-population. Intra-population heterogeneity, such as the heterogeneity between cells of the same population that dictate differences in protein levels, would entail simulating a single population where parameter values at the sub-cell level are picked from a distribution rather than are identical as in the current work [56]. Inter-population heterogeneity, such as heterogeneity between two distinct populations of cancer cells within the same tumor, would entail simulating multiple populations with varying features [56]. These varied features could be antigen expression levels or parameter values for features paralleling known hallmarks of cancerous populations, such as increased metabolic preference for glycolysis or increased tolerance to crowding [56].

To begin this work, one might begin by taking a select few of the effective treatments found from the realistic co-culture `dish` context that were tested in the `tissue` context in the work presented in Chapter 2 and simulating how treatment efficacy of these conditions might change as a function of varying tumor heterogeneity at the cell, subpopulation, and vasculature level. Specifically, for the cell level heterogeneity, varying population heterogeneity parameter (where the value, in the form of a fraction, dictates the spread of the distribution from which parameters for new cells are drawn) for cancer and healthy cells would enable exploration of these treatments in tumors with varying and different levels of heterogeneity between and within cell populations. This experimental setup could entail testing each treatment condition (with already set CAR T-cell dose, $CD4^+$:$CD8^+$ ratio, CAR affinity, and cancer and healthy antigen expression levels) in every possible combination of varied cancer cell population heterogeneity (values: 10, 20, and 40%) and healthy cell population heterogeneity (values: 10, 20, and 40%), while setting the CAR T-cell population heterogeneity to a low level (value: 10%) and keeping the vasculature consistent setup S_{22} as used in the paper in Chapter 2, and vasculature seed 0 throughout all simulations, including replicates even if

simulation seed varies, so vasculature is identical in all simulations). This would enable isolating the effect of cell population level heterogeneity, and differences in cancer versus healthy cell population heterogeneity affect treatment outcome for a range of treatments. For the population-level heterogeneity, as previously mentioned it would be useful to simulate tumors with multiple cancer populations each expressing a different amount of antigen. This experimental setup could entail testing each treatment condition in simulations with two cancer populations where the first population expresses the antigen level from the original condition and the second population expresses either half the quantity or the same low level of antigens as the healthy cell population (value: 100 antigens/cell), where each option for the second cancer population can be tested separately. In these simulations, the heterogeneity level of the cancer, healthy, and CAR T-cell populations is set to a low level (value: 10%) to capture the idea that no populations exist without any heterogeneity, and the vasculature would be kept consistent (setup S_{22} as used in the paper in Chapter 2, and vasculature seed 0 throughout all simulations, including replicates even if simulation seed varies, so vasculature is identical in all simulations) to isolate the effect of having multiple, distinct tumor populations with varied level of antigen expression and understand how multiple populations might impact tumor escape. Finally, for the vasculature-level heterogeneity, varying the vasculature structure would enable understanding of how treatment efficacy is affected by vasculature features such as density and location relative to the tumor core. For varying the vasculature structure, the treatment conditions of interest could be simulated in three different vasculature setups, including the setup used in Chapter 2 (S_{22}) as well as two additional ones used by Yu. et. al. (L_{11} and S_{11}) [49]. For each simulation, including across replicates, the vasculature seed would be kept consistent (vasculature seed 0 throughout all simulations, including replicates even if simulation seed varies, so vasculature is identical in all simulations for a given vasculature setup) and the heterogeneity level of the cancer, healthy, and CAR T-cell populations is set to a low level (value: 10%). Each of these proposed computational experiments could be conducted using CARCADE and would enable interrogating how CAR T-cell treatment efficacy is influenced by heterogeneity that is innate to clinical contexts and between patients. Additionally, the proposed work here focuses on effective treatments, but it would be interested to extend this to treatments considered neutral or ineffective in the co-culture context to determine if the treatment robustness to heterogeneity is a function of treatment efficacy.

4.2.1.2 CARCADE enables investigating therapeutic benefits of tuning CAR T-cell metabolism

Currently, the relationship between design choices and underlying CAR T-cell metabolism that guides behaviors is poorly understood. T-cell metabolism plays a critical role in dictating differentiation, effector and persistence dynamics, and function efficacy [36-40]. Effector T-cells, like cancer cells, exhibit the Warburg effect, meaning they increase glucose uptake [38-40,97,101] and favor glycolysis [36,38-40] over mitochondrial metabolism [36,39]. Meanwhile, inactivated and memory T-cells preferentially make energy through oxidative phosphorylation (OXPHOS) and fatty acid oxidation (FAO) [36-40,97]. CAR T-cell design choices that affect effector and persistence dynamics are likely tightly intertwined with cell metabolism. For example, CARs with different ICDs, such as CD28 and 4-1BB, confer differing effector and persistence dynamics [33-35]. Studies suggest that 4-1BB CAR T-cells increase mitochondrial mass and upregulate genes involved in the electron transport chain and FAO, resulting in enhanced survival and memory [34,36]. This metabolic shift and resulting behaviors parallel those of memory T-cells. Conversely, CD28 naturally upregulates glycolysis and glucose uptake by increasing Glut1 expression [101], which could explain increased effector function and glycolytic metabolism in CD28 CAR T-cells [34]. Deliberately engineering CAR T-cell metabolism to confer desired behaviors could greatly enhance solid-tumor CAR T-cell efficacy.

Agent-based models uniquely offer a platform to explore how altering cell-level metabolism affects population-level behaviors and treatment outcomes. Since CARCADE explicitly models each agent's metabolism, it is feasible to change one aspect of the metabolism module across all individual CAR T-cell agents and measure changes in population dynamics. It is particularly relevant to change parameters that can be realistically and directly altered *in vitro*, such as the glucose uptake rate that serves as a proxy for Glut1 expression. However, changing *in silico* parameters that can be indirectly altered or that are unalterable experimentally still provides biological insight. Overall, varying CAR T-cell metabolism *in silico* will elucidate emergent phenomena and inform future designs.

4.2.1.3 CARCADE can be integrated with wet-lab experiments to facilitate model-guided design

While the proposed future work above primarily involves using the model in isolation to answer questions related to CAR T-cell treatment contexts and design, in the long term, CARCADE can be integrated and

iteratively enhanced using experimental data to provide specific, model-guided experimental and CAR T-cell design. For example, the Leonard lab is beginning to investigate CAR T-cell engineering in the wet-lab, which was not underway during my time in graduate school. These experiments could be used, in tandem with the lab's Keyence BZ-x800 microscope that can enable collecting cell spatial dynamics over time, to fine-tune the parameters in CARCADE to specific contexts of interest in the lab. This might entail tuning the heuristic guiding CAR-antigen binding, the CAR affinity itself to the specific value associated with the CAR used, or the cancer and healthy cell antigen expression levels to the specific cell lines of interest. After tuning, the model could then be used to help inform experimental design and identify experiments of interest. For example, the model could inform optimal $CD4^+$:$CD8^+$ T-cell ratios, CAR affinities, effector to target (E:T) ratios, or timing of experimental perturbations or stages. This iterative cycle between model refinement and experimental design has become core to tool development and understanding in the Leonard lab, but to date this cycle centers on the use of ordinary differential equation models. By bringing CAR T-cells into the wet lab, the model can become part of this iterative cycle. Other labs could similarly integrate experiments or clinical data to fine-tune the model or adapt the model to specific CAR-tumor contexts, as the current model is generalizable and was built from observations across many CAR studies. Overall, collaboration between wet-lab experiments and computational modeling could not only enhance the model, but subsequently enable the model to guide experimental design and enhance and expedite design-build-test cycles.

Additionally, the same principles used to design CARCADE to incorporate CAR T-cell modeling into ARCADE, could be used to eventually incorporate other synthetic biology tools into the model to explore the design space of other synthetic systems beyond CAR T-cells. Some of these tools include those key to the Leonard lab, such as the Composable Mammalian Elements of Transcription (COMET) [161] and the Modular Extracellular Sensor Architecture (MESA) [162-164], as well as those in the field more broadly, such as Synthetic Notch (SynNotch) receptors [163]. This integration and further model adaptation would enable similar, expedited investigation of how these synthetic tools behave in various contexts, such as varying cell types, spatial patterning, microenvironment conditions. Given that the Leonard lab has extensively modeled COMET and MESA systems [161,165,166], these models could be adapted into

subcellular modules for agents that guide agent rules and interactions. CARCADE serves as an example of how synthetic biology tools can be integrated into agent-based models, integrating experimental understanding with computational frameworks to map the design space of these synthetic systems. Eventually, these models may help enhance our understanding of or guide synthetic system genetic construct design, gene expression tuning, tool performance metrics or needs, and feedback control.

4.2.2 Further data collection on student and faculty engagement with ARDEI-context questions will facilitate continued integration of social justice context into chemical engineering courses

4.2.2.1 Interviewing faculty will further support question development and workshop facilitation at other institutions

While this workshop was successful at this institution, we hope to provide enough resources to motivate and support implementation of the workshop at additional institutions or learning spaces. Interviewing faculty on the process of engaging with the workshop and developing their ARDEI-context questions or lectures would support faculty at other institutions through the same process. We are in the process of interviewing faculty who participated in the workshop, and for some, who have deployed their ARDEI-context questions or lectures for inclusion into the manuscript prior to publication. These interviews will help elucidate the process, challenges faced, and resources used by faculty in the question development process and faculty perceptions of student responses in the question deployment process. These interviews will help encourage and support faculty who have yet to undergo this work by providing insight and solutions to challenges faced along the way.

4.2.2.2 Collecting additional student surveys will enable tailoring questions to course context

In addition to the data collected and presented in this work, collecting student surveys from additional core or elective courses that implement ARDEI-context questions would help increase the sample size and get broader student perspectives on this topic. At present, the relatively small sample size of student responses per course necessitated analyzing the data collectively, combining student responses across course makeup (undergraduate, graduate, and mixed populations) and context (core vs elective) and prohibiting meaningful results from analyzing courses in isolation. While we are in the process of collecting data from

students taking courses in Spring 2022 for publication of the manuscript, small course numbers and sizes will still limit larger analysis. If sufficient data were collected, comparing the data between student populations in undergraduate, graduate, or mixed courses could reveal different needs, approaches, or benefits to integrating ARDEI-context in courses for these populations. Further extending this, if additional universities participated in implementing this workshop, deploying ARDEI-context questions, and surveying students, student responses from students at each undergraduate level (e.g., freshmen, sophomores, juniors, and seniors) could be compared to determine differences in and types of engagement with these questions. Similarly, student responses from core and elective courses could be compared to determine if populations in elective courses are predisposed to engage with these questions more positively, particularly for courses that are inherently related to social justice concerning topics such as sustainability or global health. Overall, a larger sample size could enable more in-depth analysis across varying courses or student populations to further refine these ARDEI-context questions in accordance with student needs.

4.2.2.3 Adapting ARDEI-context questions and deployment based on students' survey responses would enhance the student learning experience

Since this study was run over the course of a single year, faculty were not able to use the feedback from students to enhance future versions of the ARDEI-context question. If this study were extended to future years, faculty could adapt their questions based on student feedback and determine if student outcomes increase over time. Additionally, while we conveyed overall student sentiments (i.e. largely students requesting a full lecture on the content or more frequent ARDEI-context questions) to faculty teaching each quarter based on updated data, we did not have a large enough sample size to compare student responses between quarters or between deployment strategies (i.e. question only vs full lecture). Future data analysis might collect sufficient data to determine if students who received ARDEI-context lectures, rather than just questions, report increased positive outcomes from engaging with the content.

4.2.2.4 Implementation of this workshop at additional institutions or learning spaces would expand the integration of ARDEI-context into chemical engineering courses

This study is limited in that it highlights a case study of deploying this workshop and these ARDEI-context questions at a single, private research-focused institution with a body of faculty who are largely supportive of DEI work. The true test of scalability of this resource and its benefits to students and faculty necessitates facilitating this workshop to faculty outside of this institution, whether by the current facilitators or by others who can use the resources outlined in this work. In accordance with the goal of spreading this work to the larger chemical engineering education community, we are presenting this workshop at the ASEE/AIChE Chemical Engineering Summer School for new faculty in Summer 2022. It would be interesting to subsequently (i) share the questions generated by workshop participants amongst each other to create a community-wide question bank for use in chemical engineering courses across the world and (ii) survey students who engage with these questions to see if results at the present institution hold at other institutions. Additionally, we intend to publish this work to serve as a resource for faculty at other institutions who may wish to hold this workshop, pairing with this publication a full repository of all the resources developed for the asynchronous pre-work and any resources necessary to analyze student responses to the questions. We hope that free access to these resources and public modeling of this workshop to other chemical engineering educators will help expand integration of ARDEI and social justice principles into chemical engineering curricula, making this a regular part of faculty and student learning and engagement.

4.3 Perspectives

4.3.1 CARCADE provides a novel tool for exploring CAR T-cell design strategies

While agent-based models have been used in other contexts, including tumor and native immune system modeling [45,56,58], CARCADE is the first agent-based model to incorporate CAR T-cell agents, thus enabling systematically and efficiently mapping the CAR T-cell design space in various tumor contests. The work presented here serves to justify and explain model development choices and show what insights could be gained from a generalized model that is not tuned to a specific CAR-tumor system. Maximizing the insights this model could provide may require close collaboration between experimentalists, clinicians, and

computationalists to tune or extend CARCADE to represent specific contexts of interest. Thus, there exist many exciting opportunities for future collaborations with the goal of extending this tool for system-specific insights, patient-specific treatment exploration, or expediting the design-build-test cycle of novel treatment strategies. Ideally and with sufficient tuning, CARCADE will help lower the labor, time, and resource costs of CAR T-cell therapy design. Down the line, it is my hope that expediting this design-build-test cycle could reduce the cost of CAR T-cell therapy treatment, making the treatment more equitable and accessible. While this is not possible with the model alone, as this is also largely a function of insurance and healthcare inequities, I hope that CARCADE can play some small role in achieving this goal, as engineers at every stage of health-application focused research should be consistently striving to make engineering decisions that reduce these inequities.

4.3.2 Integrating social justice context into chemical engineering course homework questions provides a starting point from which further curriculum-level changes can begin

While several engineering educators have made significant strides in integrating social justice into their own chemical engineering courses and curricula, many faculty remain unsure of how to approach this daunting and sensitive topic. We hope that by developing, implementing, and sharing this workshop on how to integrate ARDEI and social justice context into course questions, engineering faculty will feel empowered and confident in using this as a starting point to this integration. However, question integration alone is not sufficient to sufficiently address and interrogate the past, present, and future connections between engineering decisions and the differential impact on diverse, and particularly marginalized, communities. Recognizing and preventing future harm to marginalized communities requires consistent and frequent critical thought on not only how the *designed solution* affects people with different identities, experience, and access but also how the *problem itself* is defined, centering diverse voices and affected communities in these processes. We hope that wide-spread implementation of this workshop will help empower faculty not only to integrate these contextualized questions into their course, but to view this as the beginning of a process to reframing entire courses. This reframing will take time and will rely on the work of many important and radical scholars who came before us, but we hope this workshop can play some small role in enabling

faculty to intertwine chemical engineering and social justice principles and facilitating student growth, engagement, inclusion, and learning.

Appendices

A Supplementary Information for Chapter 2

A.1 Supplementary Data

SUPPLEMENTARY DATA A.1. Simulated monoculture `dish` setup files. Compressed (.zip) files containing .xml files needed to create untreated and treated monoculture `dish` simulations. Files correspond to those in **Supplementary Table A.4**.

SUPPLEMENTARY DATA A.2. Simulated co-culture `dish` setup files. Compressed (.zip) files containing .xml files needed to create untreated and treated co-culture `dish` simulations. Files correspond to those in **Supplementary Table A.5**.

SUPPLEMENTARY DATA A.3. Simulated monoculture `dish` setup files with expanded CAR T-cell doses (E:T ratios). Compressed (.zip) files containing .xml files needed to create untreated and treated monoculture `dish` simulations with expanded CAR T-cell dose range.

SUPPLEMENTARY DATA A.4. Simulated monoculture `dish` setup files with expanded $CD4^+$:$CD8^+$ ratios. Compressed (.zip) files containing .xml files needed to create untreated and treated monoculture `dish` simulations with expanded $CD4^+$:$CD8^+$ ratios.

SUPPLEMENTARY DATA A.5. Normalized antigen and percent lysis from cited papers shown in Figure 2.2B. This document (.xlsx) details estimated antigen and lysis data from the cited papers as well as the calculations and values of the normalized antigen and percent lysis for each paper. The figure from the paper where information was drawn and notes about the experimental context are noted for each reference.

SUPPLEMENTARY DATA A.6. Simulated `tissue` setup files. Compressed (.zip) files containing .xml files needed to create untreated and treated `tissue` simulations and corresponding graph simulations. Files correspond to those in **Supplementary Table A.8**.

A.2 Supplementary Notes

A.2.1 Supplementary Note A.1

Here we provide additional rationale as to how the range of ratios of $CD4^+$:$CD8^+$ CAR T-cells was selected following initial investigation in **Figure 2.2** and **Supplementary Figure A.3**. In these studies, expanding the range of tested $CD4^+$:$CD8^+$ ratios to include 90:10 and 10:90 in monoculture and co-culture, these more extreme ratio cases further validate trends observed in the originally tested set (**Supplementary Figure A.4**). The 90:10 ratio behaves in a way that is intermediate between the 75:25 and the 100:0 ratios, and the 10:90 ratio behaves similarly to the 25:75 ratio for trends across cell dynamics and killing (**Supplementary Figure A.4A-B**), IL-2 production (**Supplementary Figure A.4C-D**), and the holistic datasets (**Supplementary Figure A.4E-F**). The strong similarity in treatment efficacy between the 25:75 and the 10:90 ratio cases in `dish` indicates that they may perform similarly in `tissue`. The choice of which strategy to pursue *in vitro* or *in vivo* may eventually be guided by cost or feasibility with respect to $CD4^+$ and $CD8^+$ acquisition and culturing.

A.3 Supplementary Figures and Tables

A.3.1 Supplementary Figures

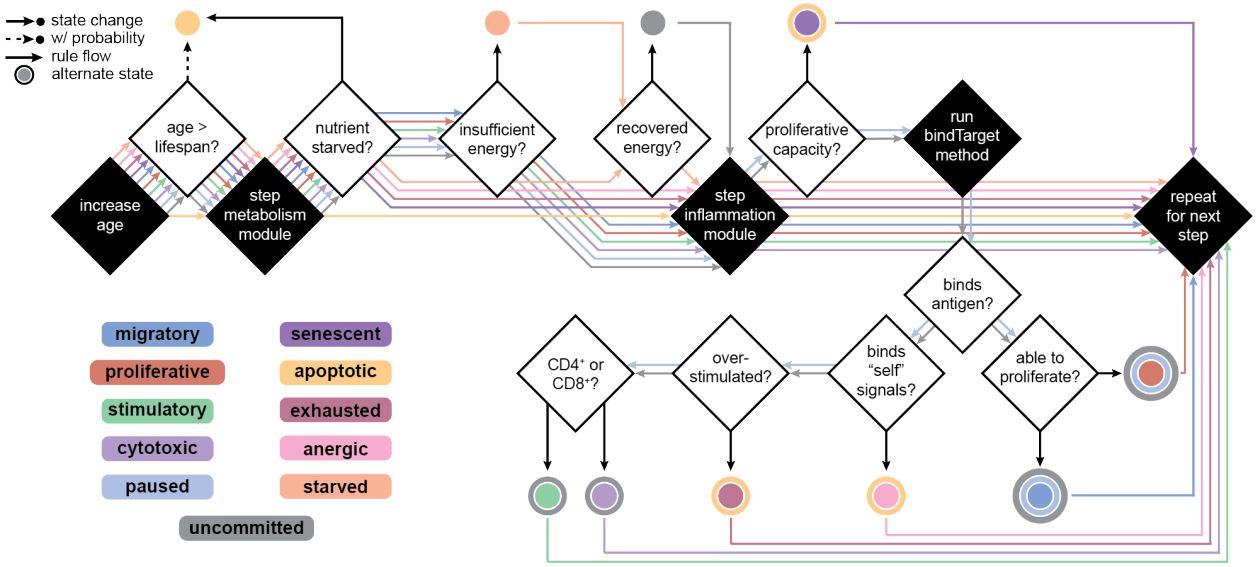

SUPPLEMENTARY FIGURE A.1. CAR T-cell state diagram flow chart. This flowchart outlines the rules governing CAR T-cell state transitions as a function of current cell state at each tick of the simulation. Black boxes indicate actions and white boxes indicate checks cells perform to change state. Some state transitions occur with probability, as indicated in the legend. Each agent first increases their age and then compares their age to their defined lifespan. If it is older than the lifespan, then the cell will become apoptotic with a given probability, and this probability increases with the age difference above the lifespan. Next, the metabolism module determines cell nutrient uptake and energy level. CAR T-cells that are nutrient starved become apoptotic. Those with low energy, but not below the starvation threshold, become starved until they can recover this energy or die. CAR T-cell agents then step their inflammation modules to determine how much IL-2 in the environment they've bound to, which has downstream effects on their metabolism and effector functions. Cells then either commit to a new cell state based on their surroundings or remain in the cell state that they are already committed to until their action is completed or they die. Cells in uncommitted or paused states will assess their surroundings and calculate the probability with which they bind to a neighboring tissue cell, giving the possibility of becoming activated (stimulatory or cytotoxic depending on cell type), dysfunctional (exhausted or anergic), or failing to bind and thus either migrating or proliferating. Each state is described in more detail in the **Supplementary Methods Details**.

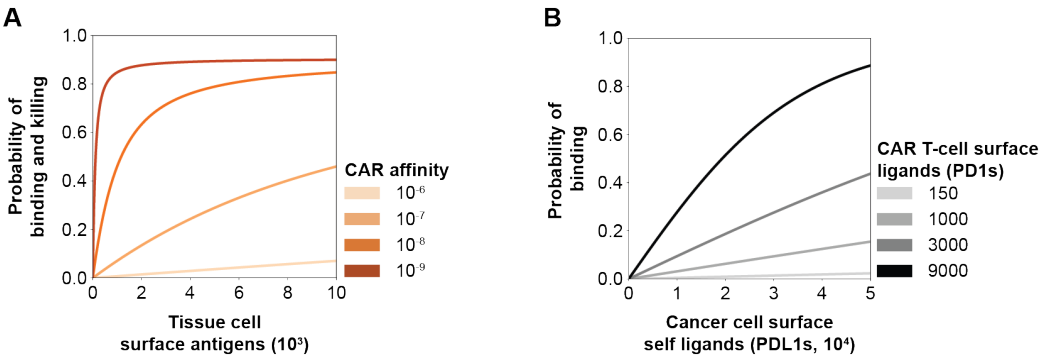

SUPPLEMENTARY FIGURE A.2. Binding probability heuristic function simulations. Binding probability heuristic function simulations for **(A)** binding and killing when CAR T-cells binding to target cell where CAR affinity is reported in units of M and **(B)** probability of CAR T-cell binding to self-ligands on cancer cell surface where CAR T-cell surface ligands and self-ligand are reported in units of ligands/cell.

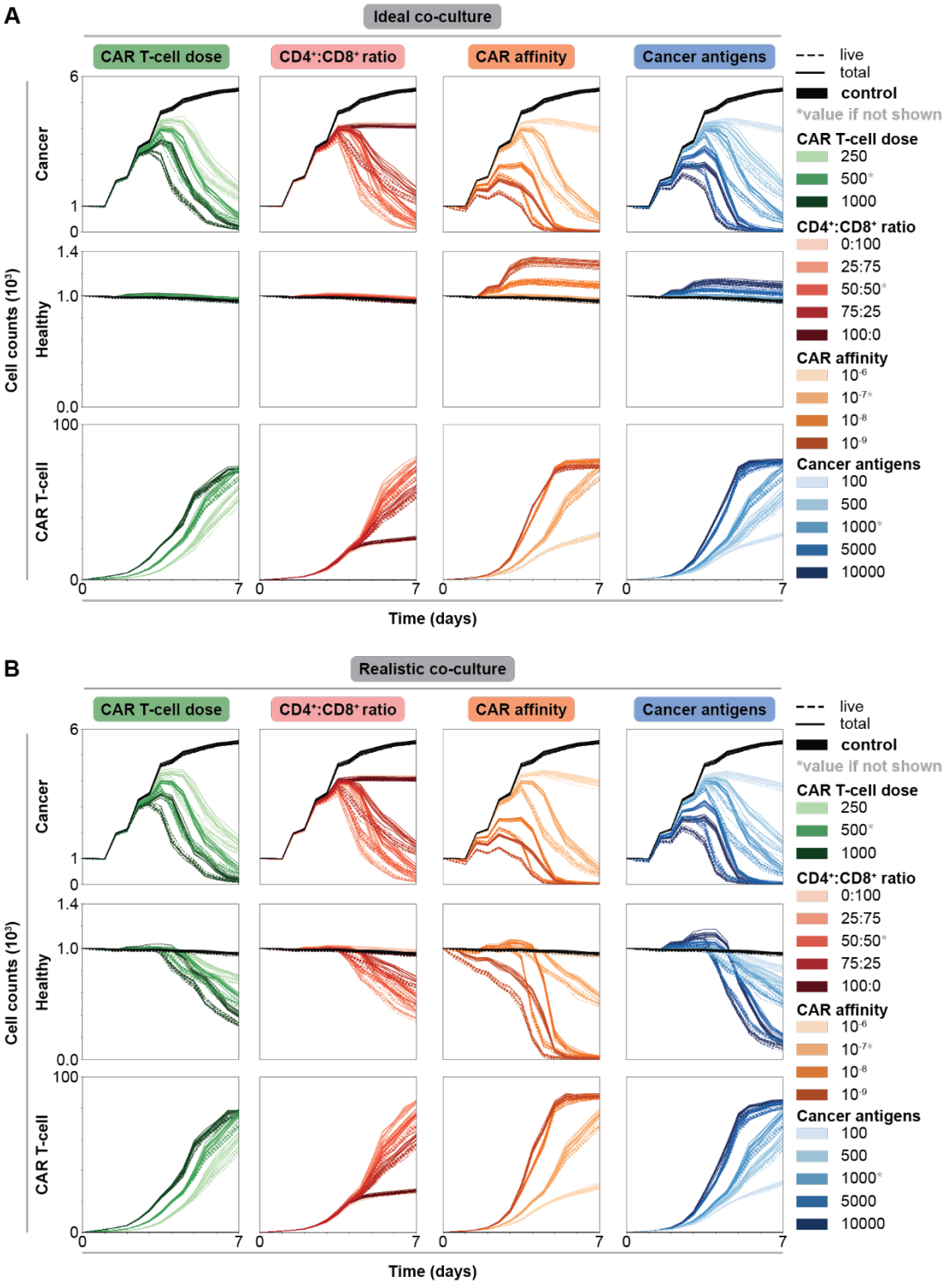

SUPPLEMENTARY FIGURE A.3. Impact of individual CAR T-cell and tumor features on cell dynamics in an ideal and realistic co-culture `dish`. Cell counts over time for **(A)** ideal and **(B)** realistic co-cultures. Each column shows the axis being changed, where all other features are held constant at indicated intermediate value (indicated by asterisk, CAR T-cell dose–500 CAR T-cells, CD4⁺:CD8⁺ ratio–50:50, CAR affinity–10^{-7} M, cancer antigens–1000 antigens/cell) while rows show the cell type being plotted.

The solid lines represent total cell counts (total), while dashed lines represent live cell counts (live, excludes necrotic and apoptotic states).

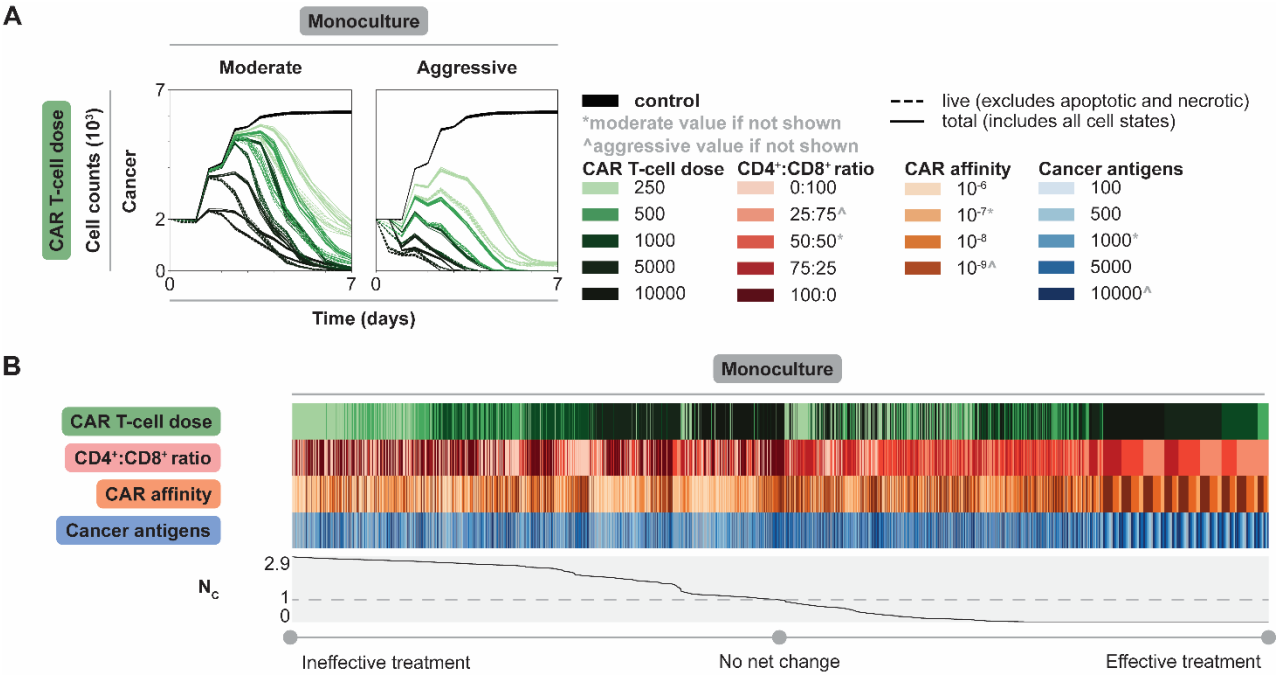

SUPPLEMENTARY FIGURE A.4. Increasing the effector-to-target (E:T) ratio results in increased and accelerated cancer cell killing. (A) Cancer cell counts over time colored by CAR T-cell dose with all other features set to moderate (indicated by asterisk, $CD4^+$:$CD8^+$ ratio–50:50, CAR affinity–10^{-7} M, cancer antigens–1000 antigens/cell) or aggressive (indicated by carrot, $CD4^+$:$CD8^+$ ratio–25:75, CAR affinity–10^{-9} M, cancer antigens–10000) values. **(B)** Heatmap reports values for each feature; the corresponding line plot shows normalized live cancer cell count (N_C) sorted from highest (left) to lowest (right). The dashed line indicates a value of 1, meaning no net change due to treatment. Values of N_C above 1 indicate growth and values below 1 indicate net killing. Legend is consistent with panel A.

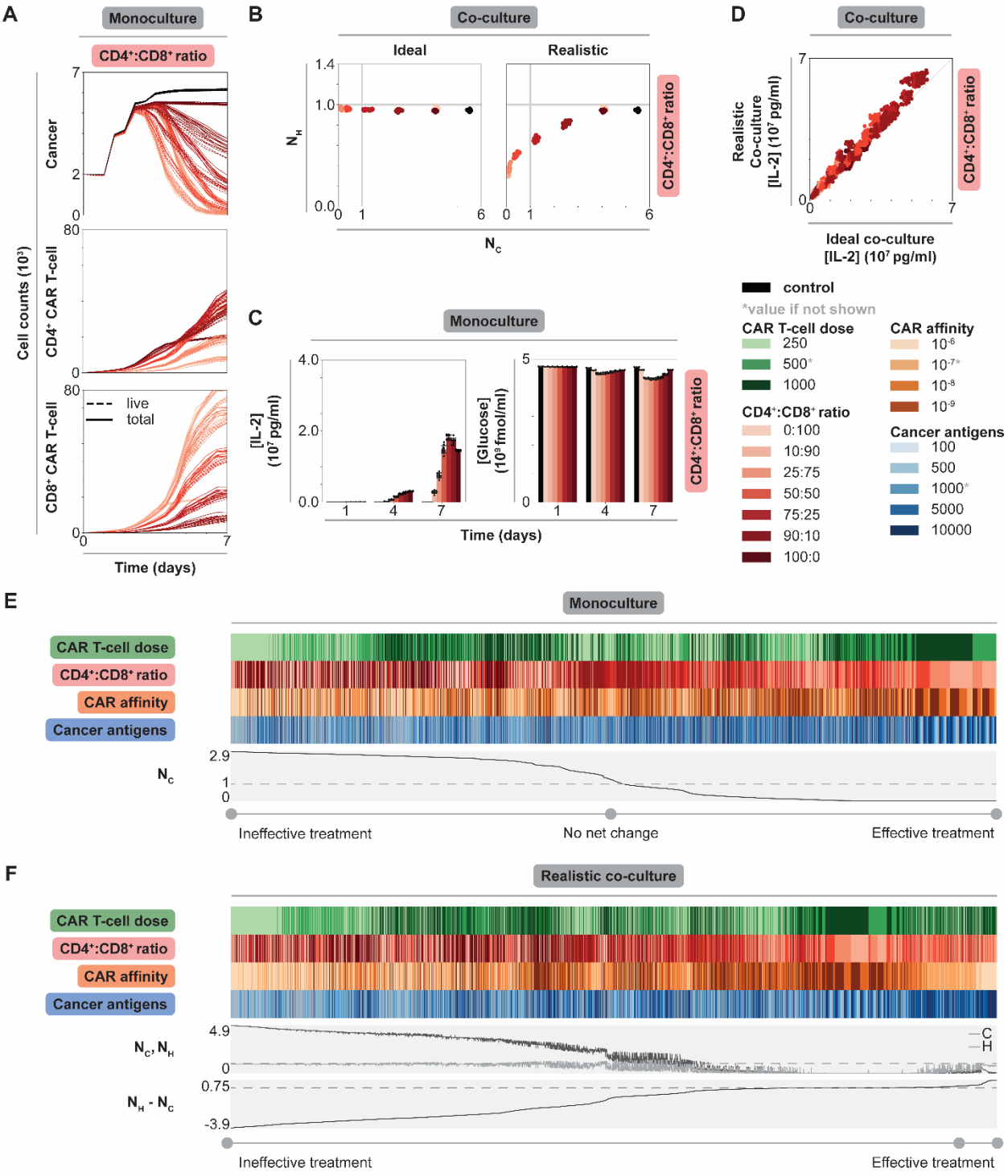

SUPPLEMENTARY FIGURE A.5. Treatment outcomes for additional edge case CD4⁺:CD8⁺ ratio conditions in monoculture and co-culture. (A) Cell counts over time of untreated (black) and treated conditions (graded hues) holding all but CD4⁺:CD8⁺ ratio constant at an intermediate value (indicated by asterisk, CAR T-cell dose–500 CAR T-cells, CAR affinity–10^{-7} M, cancer antigens–1000 antigens/cell) in monoculture. Each row shows the cell type being plotted. The solid lines represent total cell counts (total), while dashed lines represent live cell counts (live, excludes necrotic and apoptotic states). Legend is

consistent with panel C. **(B)** Scatter plots of normalized live cancer cell count (N_C, x-axis) vs normalized live healthy cell count (N_H, y-axis) for untreated (black) and treated conditions (graded hues) holding all but $CD4^+$:$CD8^+$ ratio constant at an intermediate value. Data are separated by ideal and realistic co-culture context. Legend is consistent with panel C. **(C)** IL-2 and glucose concentrations over time holding all but $CD4^+$:$CD8^+$ ratio constant at an intermediate value in monoculture. **(D)** Parity plot of IL-2 concentration at t = 7 d for all conditions in realistic (y-axis) vs ideal (x-axis) co-culture contexts colored by $CD4^+$:$CD8^+$ ratio. **(E)** Heatmap showing values for each feature with line plots showing normalized live cancer cell count (N_C) sorted from highest (left) to lowest (right). The dashed indicates value of 1, meaning no net change due to treatment. Values of N_C above 1 indicates growth and below 1 indicates net killing. Legend is consistent with panel C. **(F)** Heatmap showing values for each feature with line plots showing normalized live cancer and healthy cell count (N_C and N_H, respectively) (dashed line indicates value of 1) and the difference in normalized live healthy and cancer cell counts ($N_H - N_C$) for each realistic co-culture simulation individually (dashed line indicates value of 0). The heatmap has been sorted from lowest (left) to highest (right) difference. All the metrics shown were calculated at final time point (t = 7 d). Legend is consistent with panel C.

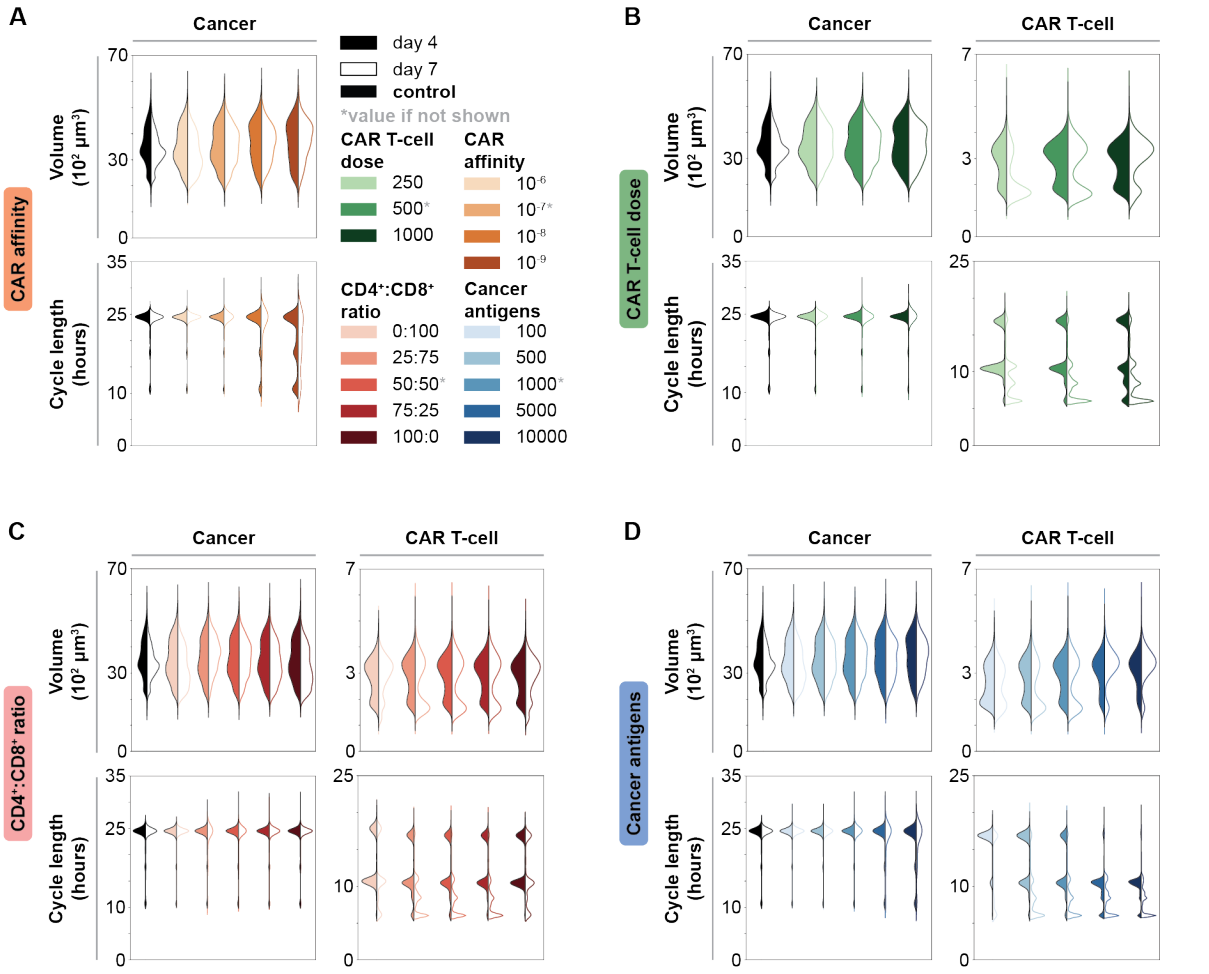

SUPPLEMENTARY FIGURE A.6. Impact of individual CAR T-cell and tumor features on cancer and CAR T-cell volume and cell cycle distributions over time in monoculture. (A) Volume and cell cycle length distributions for cancer cells when changing CAR affinity. Volume and cell cycle length distributions for cancer and CAR T-cell populations when changing **(B)** CAR T-cell dose, **(C)** $CD4^+$:$CD8^+$ ratio, and **(D)** cancer antigens. Legend for all is consistent with panel A. When one feature is changing, all other features are held constant at indicated intermediate value (indicated by asterisk, CAR T-cell dose–500 CAR T-cells, $CD4^+$:$CD8^+$ ratio–50:50, CAR affinity–10^{-7} M, cancer antigens–1000 antigens/cell). Each column shows the cell type being plotted, while rows show the distribution being plotted. Within each distribution, data are shown at t = 4 d (filled) and t = 7 d (outline).

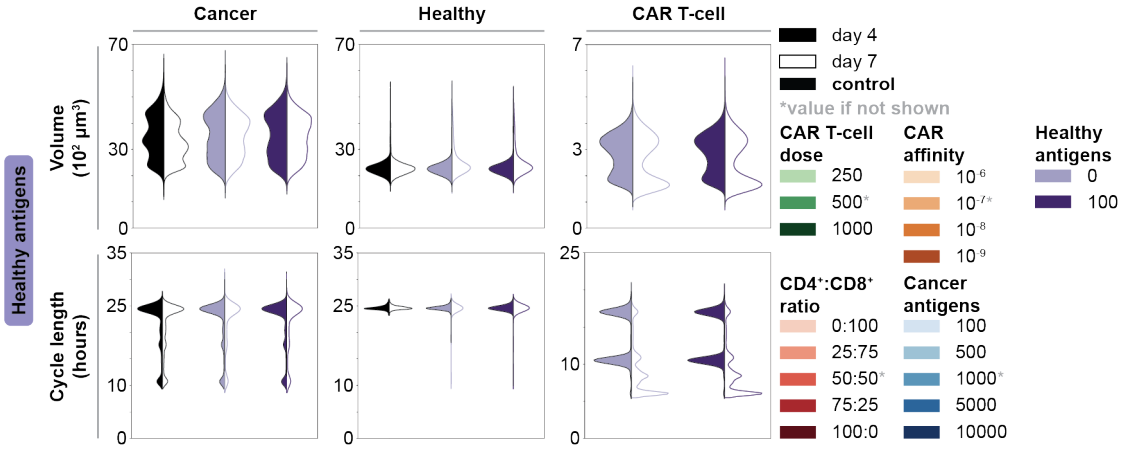

SUPPLEMENTARY FIGURE A.7. Impact of changing healthy cell antigen expression on cell volume and cell cycle distributions in co-culture. All features are held constant at indicated intermediate value (indicated by asterisk, CAR T-cell dose–500 CAR T-cells, $CD4^+$:$CD8^+$ ratio–50:50, CAR affinity–10^{-7} M, cancer antigens–1000 antigens/cell). Healthy antigens shown in units of antigens/cell. Each column shows the cell type being plotted, while rows show the distribution being plotted. Within each distribution, data are shown at t = 4 d (filled) and t = 7 d (outline).

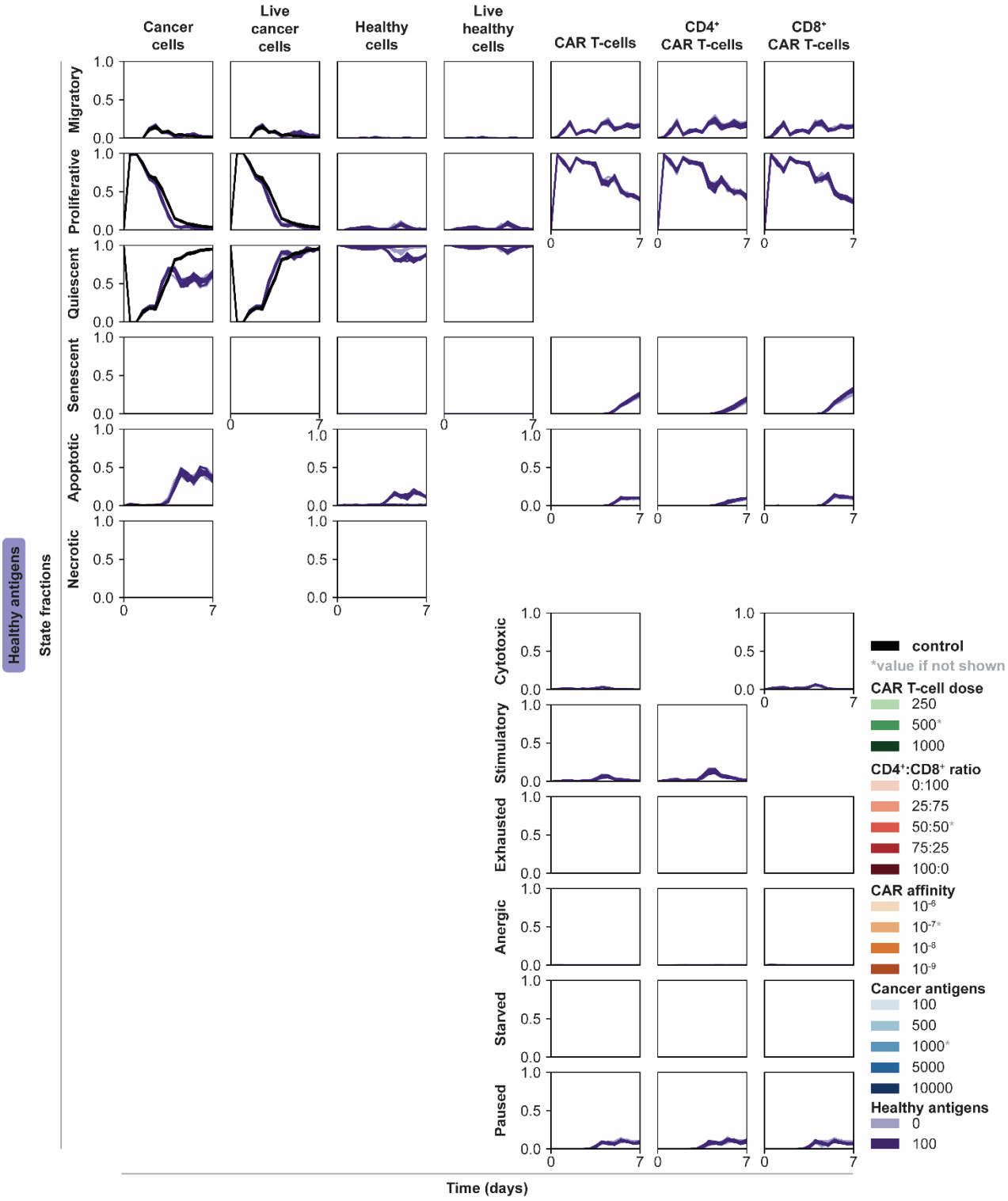

SUPPLEMENTARY FIGURE A.8. Impact of changing healthy cell antigen expression on cell states in co-culture. All features are held constant at indicated intermediate value (indicated by asterisk, CAR T-cell dose–500 CAR T-cells, $CD4^+$:$CD8^+$ ratio–50:50, CAR affinity–10^{-7} M, cancer antigens–1000 antigens/cell). Healthy antigens reported in units of antigens/cell. Each column shows the cell type being plotted, while rows show the cell state fraction being plotted.

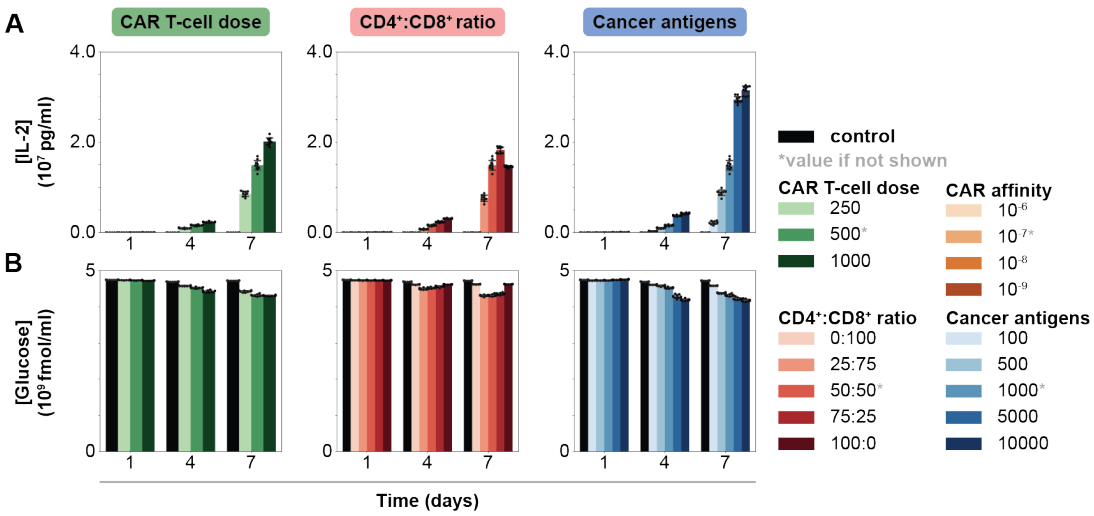

SUPPLEMENTARY FIGURE A.9. Impact of changing CAR T-cell and tumor features on IL-2 and glucose concentrations in monoculture. (A) IL-2 and **(B)** glucose concentrations over time as each specified feature is varied. Each column shows the axis being changed, where all other features are held constant at indicated intermediate value (indicated by asterisk, CAR T-cell dose–500, $CD4^+$:$CD8^+$ ratio–50:50, CAR affinity–10^{-7} M, cancer antigens–1000 antigens/cell), while rows show the environmental species being plotted.

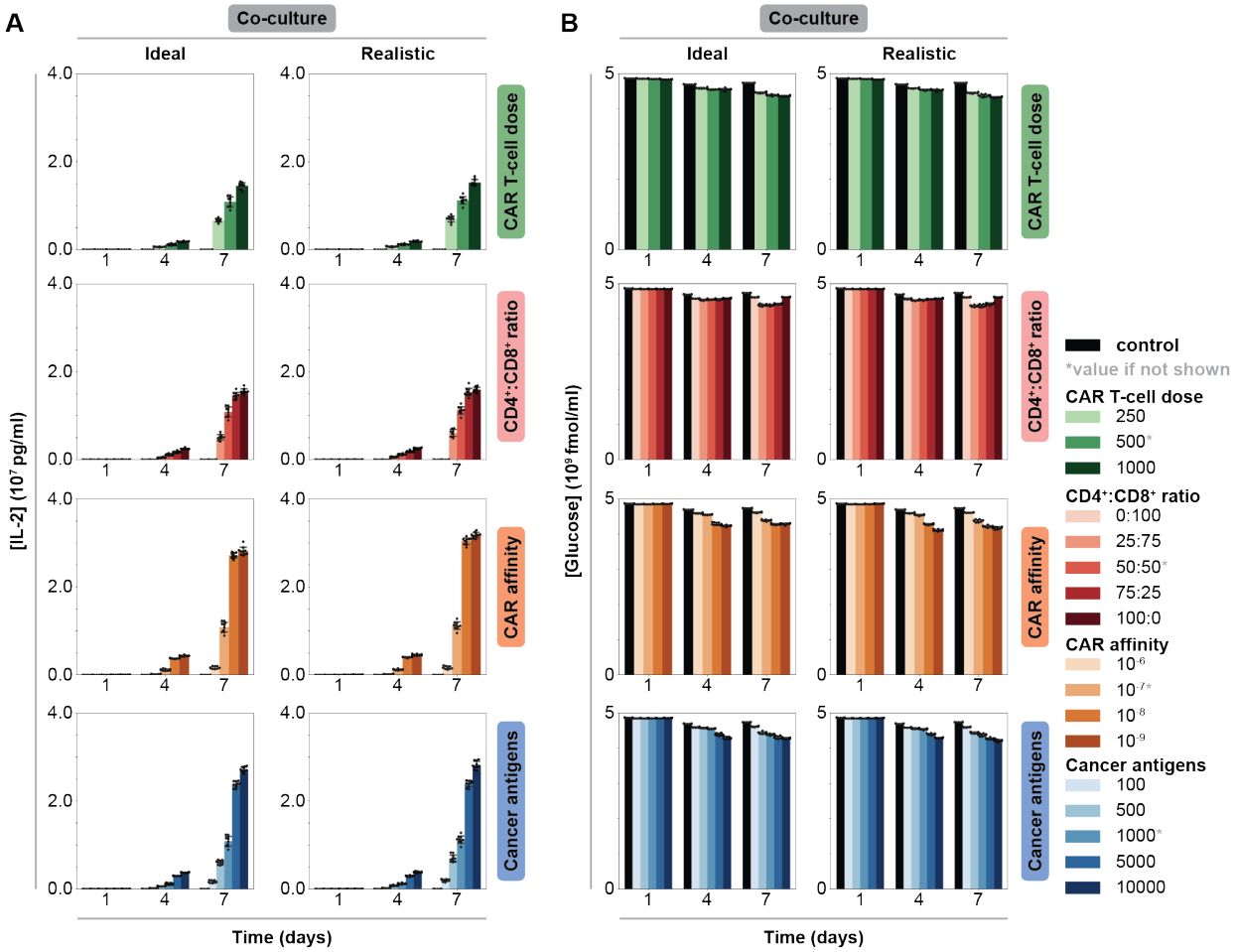

SUPPLEMENTARY FIGURE A.10. Impact of changing CAR T-cell and tumor features on IL-2 and glucose concentrations in co-culture. (A) IL-2 and **(B)** glucose concentrations over time as each specified feature is varied. Each column shows the co-culture context, while rows show the axis being changed, where all other features are held constant at indicated intermediate value (indicated by asterisk, CAR T-cell dose–500 CAR T-cells, $CD4^+$:$CD8^+$ ratio–50:50, CAR affinity–10^{-7} M, cancer antigens–1000 antigens/cell).

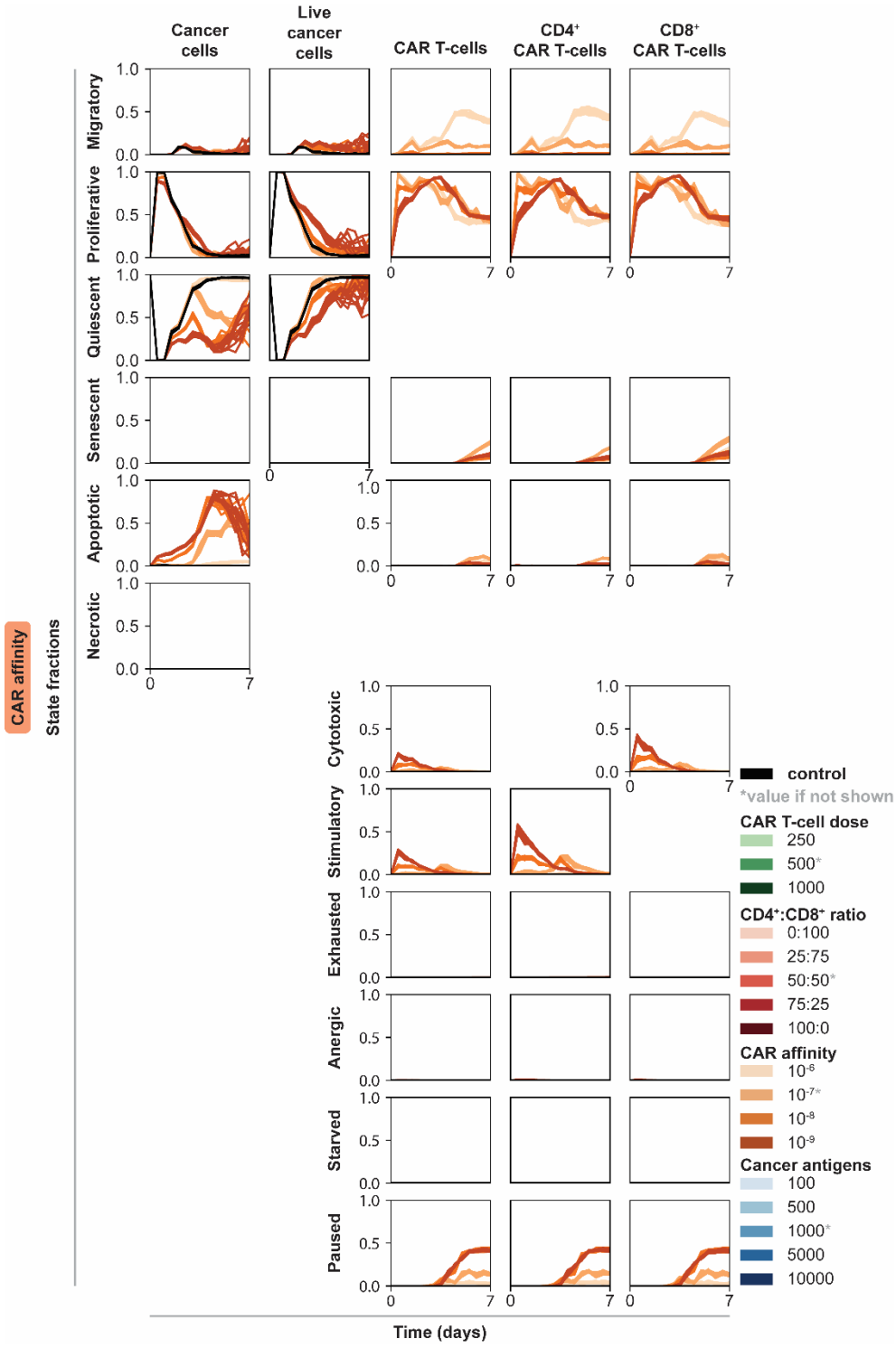

SUPPLEMENTARY FIGURE A.11. Impact of changing CAR affinity cell states over time in monoculture. All other features are held constant at indicated intermediate value (indicated by asterisk, CAR T-cell dose–500 CAR T-cells, $CD4^+$:$CD8^+$ ratio–50:50, cancer antigens–1000 antigens/cell). CAR affinity reported in units of M. Each column shows the cell type being plotted, while rows show the cell state fraction being plotted.

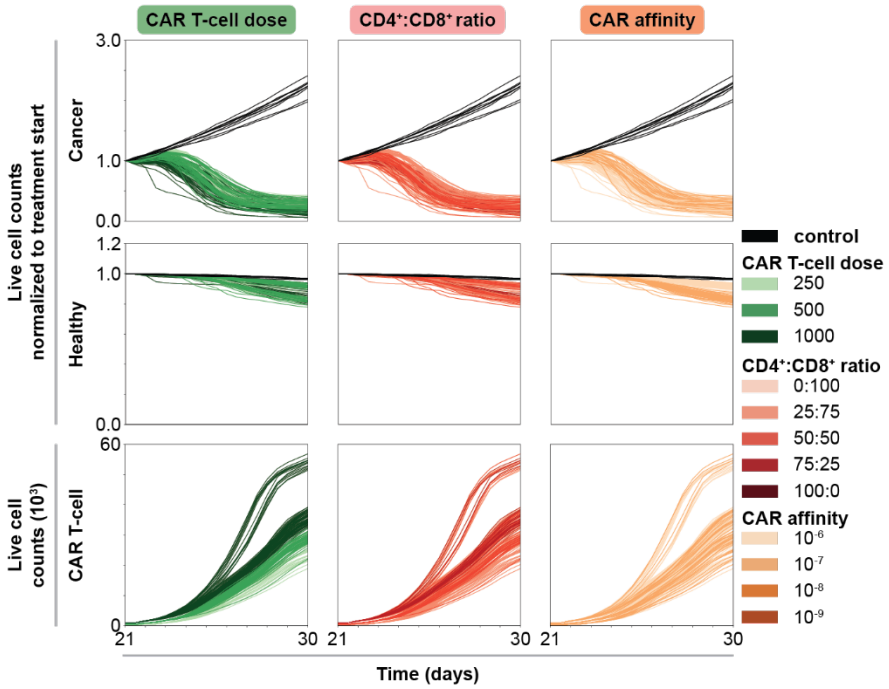

SUPPLEMENTARY FIGURE A.12. Dynamic and spatial outcomes for selected promising treatment combinations in `tissue`. Normalized live cell counts over time of untreated (black) and treated conditions (graded hues), normalized to live cell count at start of treatment (t = 21 d), for all simulations, colored by CAR T-cell dose reported in units of CAR T-cells, $CD4^+$:$CD8^+$ ratio, and CAR affinity reported in units of M. Note: not all combinations of features were simulated, see **Supplementary Table 6** for combinations tested.

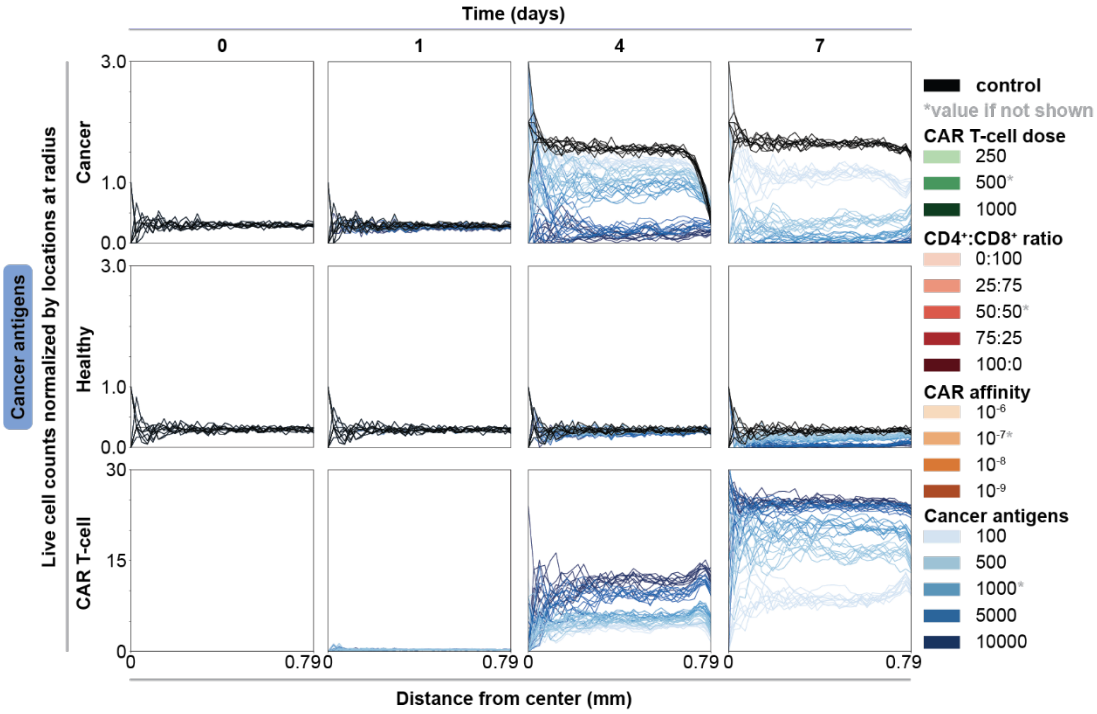

SUPPLMENTAL FIGURE A.13. Spatial dynamics for each cell type in realistic co-culture. Normalized live cell counts over time (t = 0, 1, 4, and 7 d shown) for untreated (black) and treated conditions (graded hues), normalized to locations per radius, for all simulations. Data are colored by cancer antigens while all other features are held constant at indicated intermediate value (indicated by asterisk, CAR T-cell dose–500 CAR T-cells, $CD4^+$:$CD8^+$ ratio–50:50, CAR affinity–10^{-7} M). Cancer antigens reported in units of antigens/cell. The columns indicate the timepoint in the simulation (day), while the rows indicate cell type plotted, and the x-axis for each plot shows the distance from the center.

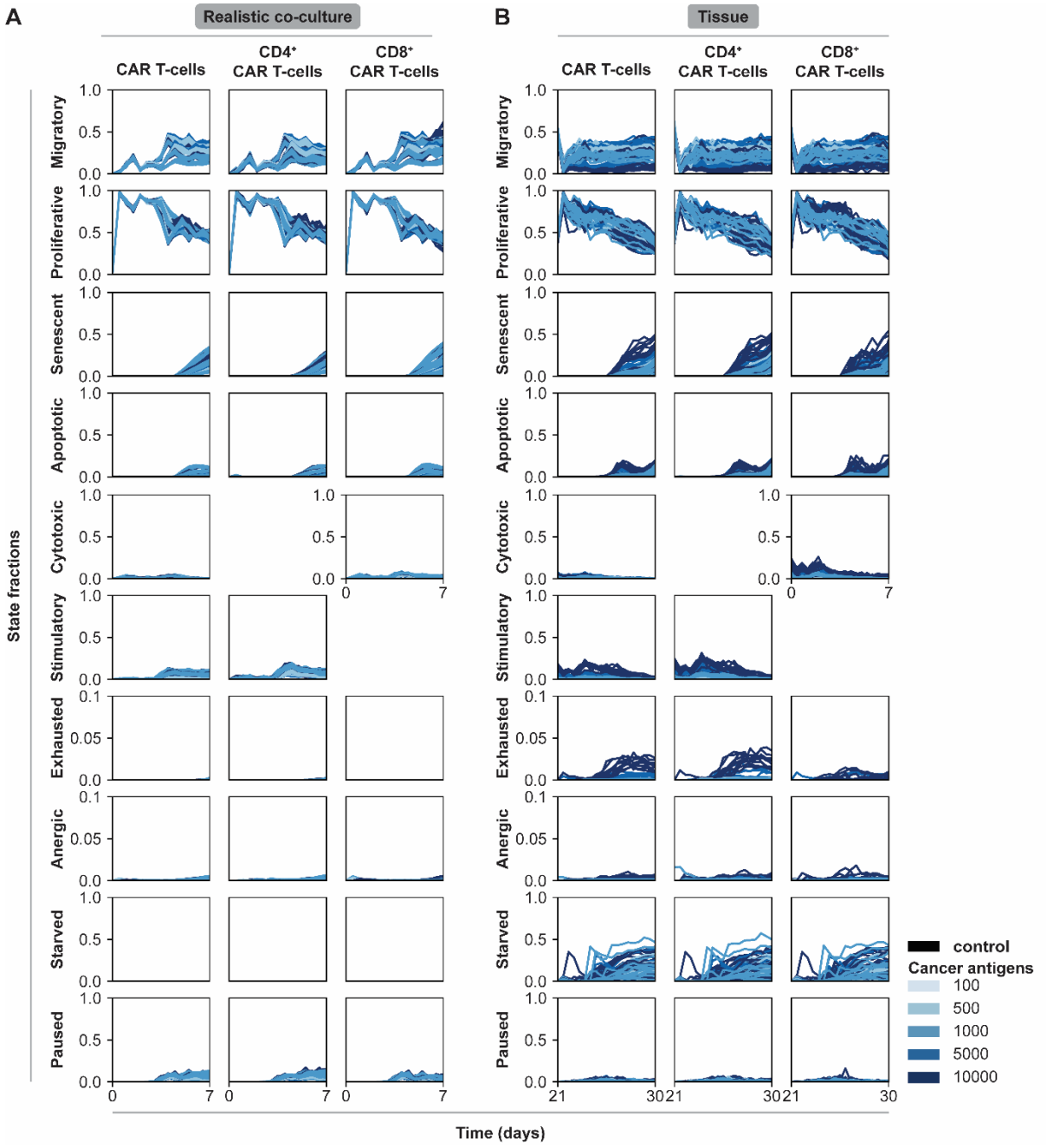

SUPPLEMENTARY FIGURE A.14. CAR T-cells that share locations with cancer cells show similar dynamics in realistic co-culture `dish` and `tissue`. CAR T-cell state fractions for CAR T-cells that share a location with at least one cancer cell in selected effective treatment conditions in both **(A)** realistic co-culture `dish` and **(B)** `tissue` (after treatment start) over time. Colors represent varying cancer antigen levels, which are reported in units of antigens/cell. Each column shows the cell type being plotted, while rows show the cell state fraction being plotted. Note: not all combinations of features were simulated, see Supplementary Table 6 for combinations tested. Also note the difference in axes scales for the exhausted and anergic states, which were used for increased visibility of these state fractions.

A.3.2 Supplementary Tables

SUPPLEMENTARY TABLE A.1. CARCADE parameter names, descriptions, values, and sources/derivations.

Parameter	Code	Value	Citation/Derivation
IL-2 Diffusivity in Blood	DIFFUSIVITY_IL2	10.0 um^2/s	1 x 10^{-7} cm^2/s [50] 36,000 um^2/hr [106] Both convert to 10 um^2/s
Initial IL-2 Concentration	CONCENTRATION_IL2	0 molecules/ cm^3	Assumption
Maximum damage value at which T-cells can spawn next to in source or pattern source	MAX_DAMAGE_SEED	1e7 (unitless)	Arbitrarily high value such that CAR T-cells can spawn at any vasculature point
Minimum radius value at which T-cells can spawn next to in graph source	MIN_RADIUS_SEED	2 um	Minimum diameter of vasculature edge is 4 um in ARCADE [49] so 2 um is minimum that the radius will ever be, so at this value CAR T-cells can spawn everywhere
CAR T-cell life span average	DEATH_AGE_AVG_T	6 weeks 60480 min	6 weeks [118]
CAR T-cell minimum age when T-cells are spawned	T_CELL_AGE_MIN	0 min	Assumption
CAR T-cell maximum age when T-cells are spawned	T_CELL_AGE_MIN	1 week 10080 min	Assumption
T-cell DNA synthesis time distribution average	SYNTHESIS_TIME_T	360 min 6 h	Same as tissue cell DNA synthesis time chosen in ARCADE [56] T-cell division time has been found to have a wide range of reported values, including 2 h [107]; 4-6 h [109]; and 13.4 +/- 5.4 and 14.3 +/- 4.4 h, but also slow cell cycle times of 24 h or can also be as low or less than as 600 min (10 h) [114] Additionally, a range of other values have been calculated by other models,

			such as 8 h for $CD8^+$s and 11 h for $CD4^+$s [102] and being capable of 4-5 divisions in 99 h with high IL-2 saturation giving 19-24 h per division [103]; or used in other models, such as 8 h [50]
T-cell DNA synthesis time distribution range	SYNTHESIS_TIME_T_RANGE	0 min	Same as tissue cell DNA synthesis time chosen in ARCADE [56]
Duration a CAR T-cell stays bound to a cell upon binding to antigen distribution average	BOUND_TIME	360 min 6 h	Assumption, chose 1/3rd of apoptosis time of cancer cells as dictated by ARCADE [56]
Duration a CAR T-cell stays bound to a cell upon binding to antigen distribution range	BOUND_TIME_RANGE	0 min	Assumption
CAR T-cell volume average	T_CELL_VOL_AVG	175 um^3	~140 fL (noting that activated T cells are larger) [105] 206 +/- 14.4 fl [98] Approximate average between two sources (fl = um^3)
CAR T-cell volume range	T_CELL_VOL_RANGE	10.0 um^3	~10% of T-cell volume (similar approach as tissue cell volume range in ARCADE)[56]
Energy requirement of an activated CAR T-cell to perform effector functions after antigen-induced activation	ACTIVE_ENERGY	0.002 fmol ATP/um^3 cell/min	Estimated
Increase in fraction of glucose used in cell mass production due to antigen-induced activation	FRAC_MASS_ACTIVE	0.25 (unitless)	Estimated; evidence of parameter existence [108]
Maximum increase in	META_PREF_IL2	0.1 (unitless)	Estimated; original parameter META_PREF in ARCADE [56]

overall metabolic preference for glycolysis due to IL-2 feedback			
Increase in overall metabolic preference for glycolysis due to antigen-induced activation	META_PREF_ACTIVE	0.3 (unitless)	Estimated; original parameter META_PREF in ARCADE [56]
Maximum increase in CAR T-cell glucose uptake rate due to impact of IL-2 on metabolism	GLUC_UPTAKE_RATE_IL2	0.56 fmol glucose/ um^2 cell/min/M glucose	Estimated; half of basal GLUCOSE_UPTAKE_RATE as defined by ARCADE [56]
Increase in CAR T-cell glucose uptake rate due to antigen-induced activation	GLUC_UPTAKE_RATE_ACTIVE	3.78 fmol glucose/ um^2 cell/min/M glucose	~5-fold increase in glucose uptake rate in activated T-cells (used 4.375-fold because Figure 3A of reference looks like it goes from 400 before activation and 1750 after) [101] 10-fold increase in glucose uptake rate in activated T-cells [105] Used first reference and original value of GLUCOSE_UPTAKE_RATE (1.12) to calculate full fold increase (which includes impact of antigen-induced activation and IL-2): 1.12 x 4.375 = 4.9 fmol glucose/um^2 cell/min/M glucose Subtract from total the increase from IL-2 independently to calculate increase from antigen-induced activation independently: 4.9 mol glucose/um^2 cell/min/M glucose – 0.56 fmol glucose/um^2 cell/min/M glucose = 3.78 fmol glucose/um^2 cell/min/M glucose
Time required for CAR T-cell to sustain antigen-induced activation before switching increasing metabolic preference (represents time	META_SWITCH_DELAY	60 min	Estimated; source noted “metabolic changes in T cells after activation occur extremely rapidly, as changes in calcium flux and lactate production can be observed only minutes after ligand binding” [109]

delay in protein production to alter metabolism)			
Distance above a cell that cells can sense molecules and proteins	SHELL_THICKNESS	2 um	[119]
Total IL-2 receptors per CAR T-cell (same both before and after IL-2Rα, as this is not limiting receptor part)	IL2_RECEPTORS	2 x 10^3 receptors/ cell	Reference pg. 30, 1993 [99]
IL-2 binding rate to IL-2Rβγc complex (k_{on})	IL2_BINDING_ON_RATE_MIN	3.8193 x 10^{-2} um^3 $molecules^{-1}$ min^{-1}	2.3 x 10^7 $M^{-1}min^{-1}$ Reference pg. 30, 1993 [99] 2.3 x 10^7 $M^{-1}min^{-1}$ = 2.3 x 10^7 L mol^{-1} min^{-1} = 2.3 x 10^{22} um^3 mol^{-1} min^{-1} Divide by Avogadro's number to get from moles to molecules: 2.3x10^{22} um^3 mol^{-1} min^{-1} / 6.022 x10^{22} molecules mol^{-1} = 0.038193 um^3 $molecules^{-1}$ min^{-1}
IL-2 binding rate to IL-2Rβγcα complex (k_{on})	IL2_BINDING_ON_RATE_MAX	3.155 um^3 $molecules^{-1}$ min^{-1}	1.9 x 10^9 $M^{-1}min^{-1}$ Reference pg. 30, 1993 [99] 111.6 $nM^{-1}h^{-1}$ (1.86 x 10^9 $M^{-1}min^{-1}$) [106] 1.9 x 10^9 $M^{-1}min^{-1}$ = 1.9 x 10^9 L mol^{-1} min^{-1} = 1.9 x 10^{24} um^3 mol^{-1} min^{-1} Divide by Avogadro's number to get from moles to molecules: 1.9 x 10^{24} um^3 mol^{-1} min^{-1} / 6.022 x10^{22} molecules mol^{-1} = 3.115 um^3 $molecules^{-1}$ min^{-1}
Binding off rate of IL-2 to IL-2Rβγc complex and IL-2Rβγcα complex (k_{off})	IL2_BINDING_OFF_RATE	0.015 min^{-1}	0.015 min^{-1} for heavy chain; 0.014 min^{-1} for heterodimer Reference pg. 30, 1993 [99] 0.83 hr^{-1} (0.01388 min^{-1}) [106]
Rate of conversion of IL-2Rβγc two-chain complex to IL-2Rβγcα, independent of if	K_CONVERT	1 x10^{-3} s^{-1}	Estimated

IL-2 bound to receptor complex (parameter found within Inflammation module class)			
Rate of recycling of any IL-2R complexes bound to IL-2 or IL-2Rβγ$_c$α complex back to IL-2Rβγ$_c$ (parameter found within Inflammation module class)	K_REC	1 x10^{-5} s^{-1}	Estimated
Maximum production rate of IL-2 by $CD4^+$ CAR T-cells due to IL-2 feedback	IL2_PROD_RATE_IL2	16.62 molecules IL-2/cell/min	1000 molecules/cell-min [106]
Maximum production rate of IL-2 by $CD4^+$ T-cells due to antigen-induced activation	IL2_PROD_RATE_ACTIVE	293.27 molecules IL-2/cell/min	4.87 x 10^{-16} umol/cell-min [106] 4.87 x 10^{-16} umol/cell-min * 1 mol/ 10^6 umol * 6.022 x 10^{23} molecules/mol = 293.27 molecules IL-2/cell/min Note: production rate is 0 molecules IL-2/cell/min for inactivated cells [33,105]
Maximum production rate of IL-2 by $CD4^+$ CAR T-cells due to antigen-induced activation and IL-2 feedback	Not a formal parameter; more for reference/note	N/A	10^{-5} ng/cell-day (calculated to be 1.79 fmol IL-2/cell-s Using IL-2 is 15.5kDa; winds up being 4.48 x 10^{-16} umol/cell-min) [110] Estimated 5.6 x 10^{-17} umol/min-cell (calculated from 1 ng IL-2/ml produced by 4.5 x 10^5 cells in a 48 well plate assumed to have at most 500 ul in it and MW of IL2 taken to be 15.5 kDa – but can be 1-40 ng/ml; this equates to 1.12 x 10^{-16} umol/cm^3-min-cell) (if you add together 4.87 x 10^{-16} and 2.76 x 10^{-17} you get 5.14 x 10^{-17} which is about this) [33] Calculated to be 4.87 x 10^{-16} umol/cell-min (from 17600 IL-2 molecules/cell-h in Gong ABM) [50]

			23400 molecules/cell-hr in first 8 h of antigen stimulation (6.47 x 10^{-16} umol/cell-min) and 6000 molecules/cell-hr (1.66 x 10^{-16} umol/cell-min) between 8 and 12 h [106] (noting that they estimated this from another study)
Time CAR T-cells must sustain antigen binding to produce IL-2 mRNA	IL2_SYNTHESIS_DELAY	180 min	2-4 h [104] (chose midpoint of 3 h = 180 min)
Time required for CAR T-cells to maintain bound contact with target antigen before activation signal induces granzyme production	GRANZ_SYNTHESIS_DELAY	15 min	Estimated
Moles of granzyme produced by $CD8^+$ CAR T-cells per mol IL-2 bound (parameter found within InflammationCD8 module class)	GRANZ_PER_IL2	0.005 mol granzyme/ mol IL-2	Estimated
Moles granzyme required by $CD8^+$ CAR T-cells to kill target cell (parameter found indirectly KillerCARTHelper helper)		1 mole	Estimated
CAR T-cell division potential	DIVISION_POTENTIAL_T	10 divisions/cell	9 divisions/cell [114] Average of 7 divisions/cell with range 4-10 divisons/cell for $CD4^+$ T-cells; Range of 15-19 divisions/cell for $CD8^+$ T-cells[115] (note: used 17 as middle of 15-19 range given for $CD8^+$ T-cells from provided citation) 8 divisions per T-cell [50]

			Average of 9, 7, 17, and 8 = 10.25, rounded down to 10
CAR T-cell fraction that becomes proliferative (as opposed to migratory) if not activated via antigen-induced activation	PROLI_FRAC	0.5 (unitless)	Estimated
CAR T-cell fraction that becomes exhausted vs apoptotic	EXHAU_FRAC	0.5 (unitless)	Estimated
CAR T-cell fraction that becomes anergic vs apoptotic	ANERG_FRAC	0.5 (unitless)	Estimated
Maximum number of cells a CAR T-cell could attempt to make contact with per time step	SEARCH_ABILITY	1 cell	Estimated
Number of times a CAR T-cell can bind to a target before becoming exhausted	MAX_ANTIGEN_BINDING	10 binding events	Estimated
Average number of CARs on a CAR T-cell's surface	CARS	50000 receptors/cell	>50000 but varies receptors/cell [116] Noted that value is the same on both 41BB and CD28 CAR T-cells [120]
Average number of CAR antigens on a healthy tissue cell	CAR_ANTIGENS_HEALTHY	100 antigens/cell	minimum of 100 antigens/cell [116] 1000 antigens/cell [24,100,111,116] 10000 (maximum 1 million) antigens/cell [24,100,111] 1000-7500 antigens/cell [117]
Average number of CAR antigens on a cancerous tissue cell (Should be higher on cancer	CAR_ANTIGENS_CANCER	1000 antigens/cell	minimum of 100 antigens/cell [116] 1000 antigens/cell [24,100,111,116] 10000 (maximum 1 million) antigens/cell [24,100,111]

cells than healthy cells)			1000-7500 antigens/cell [117]
Average number of self-receptors (PD1s) on a CAR T-cell	SELF_RECEPTORS	150 surface ligands/cell	150 surface ligands/cell before antigen-induced activation, 9000 after antigen-induced activation [112]
Average number of self-receptors (PDL1s) on a tissue cell	SELF_TARGETS	3,600 surface ligands/cell	MDA-MB-231 breast cancer cells: 47,700 +/- 2,900 (89.4% PDL1^{+}) [113] SK-Br-3 breast cancer cells: 2,000 +/- 100 (2.9% PDL1^{+}) [113] SUM149 breast cancer cells: 3,600 +/- 400 for (8.9% PDL1^{+}) [113]
Affinity of CAR for target antigen	CAR_AFFINITY	1 x 10^{-7} M	Weak = 1000 nmol/L (10^{-6} M) [25,26,116] Strong = 0.1 nmol/L (10^{-10} M) [25,26,116]
Fitting factor α in CAR binding function	CAR_ALPHA	3 (unitless)	Estimated
Fitting factor β in CAR binding function	CAR_BETA	0.01 antigens/M	Estimated
Affinity of self-receptor for self (based on PD1 for PDL1)	SELF_RECEPTOR_AFFINITY	7.8 x 10^{-6} M	7.8 uM (at 37°C) [112] Converted to 7.8 x 10^{-6} M
Fitting factor α in self-receptor (PD1) binding function	SELF_ALPHA	3 (unitless)	Estimated
Fitting factor β in self-receptor (PD1) binding function	SELF_BETA	0.02 antigens/M	Estimated
Fraction of cell surface contacting a bound cell during a binding event (γ)	CONTACT_FRAC	0.2 (unitless)	Estimated

SUPPLEMENTARY TABLE A.2. Tuned feature values for monoculture `dish` simulations.

Modified Features	Simulated Values
Dose of CAR T-Cells (CAR T-cell dose)	250, 500, 1000
$CD4^+$:$CD8^+$ CAR T-Cell Ratio ($CD4^+$:$CD8^+$ratio)	100:0, 75:25, 50:50, 25:75, 0:100
CAR-Antigen Affinity (CAR affinity, units: M)	$1x10^{-6}$, $1x10^{-7}$, $1x10^{-8}$, $1x10^{-9}$
Antigens Per Cancer Cell (cancer antigens)	100, 500, 1000, 5000, 10000
Total combinations	300
Total simulations	3000

SUPPLEMENTARY TABLE A.3. Tuned feature values for co-culture `dish` simulations.

Modified Parameters	Simulated Values
Dose of CAR T-Cells (CAR T-cell dose)	250, 500, 1000
$CD4^+$:$CD8^+$ CAR T-Cell Ratio ($CD4^+$:$CD8^+$ratio)	100:0, 75:25, 50:50, 25:75, 0:100
CAR-Antigen Affinity (CAR affinity, units: M)	$1x10^{-6}$, $1x10^{-7}$, $1x10^{-8}$, $1x10^{-9}$
Antigens Per Cancer Cell (cancer antigens)	100, 500, 1000, 5000, 10000
Antigens Per Healthy Cell (healthy antigens)	0 (ideal), 100 (realistic)
Total combinations	600
Total simulations	6000

SUPPLEMENTARY TABLE 4. Input options used to run monoculture `dish` simulations. For clarity, wrapping `<set>` tags, `<series>` name attributes, `<profilers>` simulation tags, `<globals>` environment tags are not shown. All sets use growth, parameter, and lysis profilers, each using interval 720. All cancer and healthy cells use default modules. For each set, simulations were run for every combination of bold options grouped by square brackets and separated by pipes.

Set	Input

Untreated	`<series start="0" end="10" days="7">`
	`  <simulation type="growth">`
	`  </simulation>`
	`  <agents initialization="2000" plate="dish">`
	`  <populations>`
	`  <population type="C" fraction="1.0">`
	`  <variables>`
	`  <variable id="CAR_ANTIGENS_CANCER" value="1000"/>`
	`  </variables>`
	`  </population>`
	`  <population type="H" fraction="0">`
	`  <variables>`
	`  <variable id="CAR_ANTIGENS_HEALTHY" value="0"/>`
	`  </variables>`
	`  </population>`
	`  <population type="4" fraction="0.0">`
	`  </population>`
	`  <population type="8" fraction="0.0">`
	`  </population>`
	`  </populations>`
	`  <helpers>`
	`  <helper type="treat" delay="10" dose="0"/>`
	`  </helpers>`
	`  </agents>`
	`  <environment coordinate="hex">`
	`  <components>`
	`  <component type="sites" class="source">`
	`  <specifications>`
	`  <specification id="X_SPACING" value="*" />`
	`  <specification id="Y_SPACING" value="*" />`
	`  <specification id="SOURCE_DAMAGE" value="0.0" />`
	`  </specifications>`
	`  </component>`
	`  </components>`
	`  </environment>`
	`</series>`

Treated	`<series start="0" end="10" days="7">`
	`  <simulation type="growth">`
	`  </simulation>`
	`  <agents initialization="2000" plate="dish">`
	`  <populations>`
	`  <population type="C" fraction="1.0">`
	`  <variables>`
	`  <variable id="CAR_ANTIGENS_CANCER"`
	`  value="[**100**|**500**|**1000**|**5000**|**10000**]"/>`
	`  </variables>`
	`  </population>`
	` <population type="H" fraction="0">

```
                  <variables>
                     <variable id="CAR_ANTIGENS_HEALTHY" value="0" />
                  </variables>
               </population>
               <population type="4" fraction="0.0">
                  <variables>
                     <variable id="CAR_AFFINITY" value="[1e-6|1e-7|
                     1e-8|1e-9]" />
                  </variables>
               </population>
               <population type="8" fraction="0.0">
                  <variables>
                     <variable id="CAR_AFFINITY" value="[1e-6|1e-7|
                     1e-8|1e-9]" />
                  </variables>
               </population>
            </populations>
            <helpers>
               <helper type="treat" delay="10" dose="[250|500|1000]"
                  ratio="[1:0|0.75:0.25|0.5:0.5|0.25:0.75|0:1]" />
            </helpers>
         </agents>
         <environment coordinate="hex">
            <components>
               <component type="sites" class="source">
                  <specifications>
                     <specification id="X_SPACING" value="*" />
                     <specification id="Y_SPACING" value="*" />
                      <specification id="SOURCE_DAMAGE" value="0.0" />
                  </specifications>
               </component>
            </components>
         </environment>
      </series>
```

SUPPLEMENTARY TABLE 5. Input options used to run co-coculture dish simulations. For clarity, wrapping <set> tags, <series> name attributes, <profilers> simulation tags, <globals> environment tags are not shown. All sets use growth, parameter, and lysis profilers, each using interval 720. All cancer and healthy cells use default modules. For each set, simulations were run for every combination of bold options grouped by square brackets and separated by pipes. Simulations that where the healthy population had a value of 0 for CAR_ANTIGENS_HEALTHY are part of the ideal co-culture data, while simulations that where the healthy population had a value of 0 for CAR_ANTIGENS_HEALTHY are part of the realistic co-culture data.

Set	Input

Untreated	`<series start="0" end="10" days="7">`
	`  <simulation type="growth">`
	`  </simulation>`
	`  <agents initialization="2000" plate="dish">`
	`  <populations>`
	`  <population type="C" fraction="0.5">`
	`  <variables>`
	`  <variable id="CAR_ANTIGENS_CANCER" value="1000"/>`
	`  </variables>`
	`  </population>`
	`  <population type="H" fraction="0.5">`
	`  <variables>`
	`  <variable id="CAR_ANTIGENS_HEALTHY" value="100"/>`
	`  </variables>`
	`  </population>`
	`  <population type="4" fraction="0.0">`
	`  <variables>`
	`  <variable id="CAR_AFFINITY" />`
	`  </variables>`
	`  </population>`
	`  <population type="8" fraction="0.0">`
	`  <variables>`
	`  <variable id="CAR_AFFINITY" />`
	`  </variables>`
	`  </population>`
	`  </populations>`
	`  <helpers>`
	`  <helper type="treat" delay="10" dose="0"/>`
	`  </helpers>`
	`  </agents>`
	`  <environment coordinate="hex">`
	`  <components>`
	`  <component type="sites" class="source">`
	`  <specifications>`
	`  <specification id="X_SPACING" value="*" />`
	`  <specification id="Y_SPACING" value="*" />`
	`  <specification id="SOURCE_DAMAGE" value="0.0" />`
	`  </specifications>`
	`  </component>`
	`  </components>`
	`  </environment>`
	`</series>`

Treated	`<series start="0" end="10" days="7">`
	`  <simulation type="growth">`
	`  </simulation>`
	`  <agents initialization="2000" plate="dish">`

```
                <populations>
                   <population type="C" fraction="0.5">
                      <variables>
                         <variable id="CAR_ANTIGENS_CANCER"
                              value="[100|500|1000|5000|10000]"/>
                      </variables>
                   </population>
                   <population type="H" fraction="0.5">
                      <variables>
                         <variable id="CAR_ANTIGENS_HEALTHY" value="[0|100]"
          />
                      </variables>
                   </population>
                   <population type="4" fraction="0.0">
                      <variables>
                         <variable id="CAR_AFFINITY" value="[1e-6|1e-7|
                         1e-8|1e-9]" />
                      </variables>
                   </population>
                   <population type="8" fraction="0.0">
                      <variables>
                         <variable id="CAR_AFFINITY" value="[1e-6|1e-7|
                         1e-8|1e-9]" />
                      </variables>
                   </population>
                </populations>
                <helpers>
                   <helper type="treat" delay="10" dose="[250|500|1000]"
                      ratio="[1:0|0.75:0.25|0.5:0.5|0.25:0.75|0:1]" />
                </helpers>
             </agents>
             <environment coordinate="hex">
                <components>
                   <component type="sites" class="source">
                      <specifications>
                         <specification id="X_SPACING" value="*" />
                         <specification id="Y_SPACING" value="*" />
                          <specification id="SOURCE_DAMAGE" value="0.0" />
                      </specifications>
                   </component>
                </components>
             </environment>
          </series>
```

SUPPLEMENTARY TABLE A.6. Reference information from cited papers' in vitro experiments shown in Figure 2.2B.

Citation	Reference Figure Containing Data	CAR Construct Used in Study	E:T Ratio	Notes
Arcangeli 2017	Figure 4	CD123-CD28-OX40-CD3ζ	5:1	Short-Term Assay (4 h); co-culture with low antigen expressing cells
Caruso 2015	Figure 1 for 1e6 and 0, other data from Figure 4	EGFR-CD28-CD3ζ	5:1	
Chmielewski 2004	Figure 4	ErbB2-Fc-CD3ζ	1:1	Antigen levels are MFI; They provided viability data so convereted to % lysis by using: % Kill = 1-Viability %; Used E:T ratio closed to 1:1
Ghorashian 2019	Figure 1	CD19-41BB-CD3ζ	6.4:1	
Hernandez-Lopez	Figure 2A upper plot	HER2-41BB-CD3ζ	not found	
Liu 2015	Figure 2	ErbB2-41BB-CD3ζ	1:1	Antigen level = ErbB2 RNA ug
Watanabe 2014	Figure 2C	CD20-CD28-CD3ζ	1:1	

SUPPLEMENTARY TABLE A.7. Effective treatments identified in co-culture `dish` simulations. Simulations were averaged across replicates and ordered from highest to lowest difference metric.

CAR T-Cell Dose	$CD4^+$:$CD8^+$ T-Cell Ratio	CAR Affinity (M)	Antigens Cancer	Antigens Healthy	Normalized Cancer Cell Count	Normalized Healthy Cell Count	Normalized T-cell Count	Difference Metric Value
1000	0.25	1E-06	10000	100	0.03	0.75	73.09	0.72
500	0.25	1E-06	10000	100	0.13	0.83	141.33	0.69
1000	0.5	1E-06	10000	100	0.12	0.80	70.68	0.68
1000	0.25	1E-06	5000	100	0.36	0.83	65.38	0.48
500	0.5	1E-06	10000	100	0.40	0.86	131.76	0.46
1000	0.75	1E-06	10000	100	0.61	0.86	61.97	0.25
250	0.25	1E-06	10000	100	0.80	0.92	231.88	0.12
1000	0.5	1E-06	5000	100	0.75	0.87	59.82	0.12
500	0.25	1E-06	5000	100	0.78	0.88	118.79	0.10
500	0.5	1E-07	1000	100	0.42	0.50	137.30	0.09
1000	0.75	1E-07	1000	100	0.59	0.56	64.57	-0.03
1000	0.5	1E-07	500	100	0.68	0.52	63.45	-0.16
250	0.25	1E-07	1000	100	0.83	0.63	240.64	-0.20
500	0.25	1E-07	500	100	0.75	0.54	126.98	-0.21

SUPPLEMENTARY TABLE A.8. Input options used to run tissue simulations. For clarity, wrapping <set> tags, `<series>` name attributes, `<checkpoint>` name and path attributes, `<profilers>` simulation tags, and `<globals>` environment tags are not shown. All untreated and treated sets use growth, parameter, and lysis profilers, each using interval 720, except the untreated set used to produce the graph in which a graph profiler was used instead of a parameter profiler. All cancer and healthy cells use default modules. For the treated set, simulations were run for each of the 14 treatment conditions shown in Supplementary Table 5. Variable values shown are chosen in the listed order of the values in square brackets and separated by pipes, where a single simulation uses one value from each variable list such that all values are at the same list position. For example, if parameter A has list [**a1** | **a2**] and parameter B has list [**b1** | **b2**], then the first simulation would use parameter values **a1** and **b1**, while the second simulation would use parameter values **a2** and **b2**.

Set	Input

Graph	`<series start="0" end="1" days="1">`
	`  <simulation type="growth">`
	`  <checkpoints>`
	`  <checkpoint type="graph" class="save" day="0" />`
	`  </checkpoints>`
	`  </simulation>`
	`  <agents initialization="0" />`
	`  <environment coordinate="hex">`
	`  <components>`
	`  <component type="sites" class="graph" complexity="simple">`
	`  <specifications>`
	`  <specification id="GRAPH_LAYOUT" value="S" />`
	`  <specification id="ROOTS_LEFT" value="50A" />`
	`  <specification id="ROOTS_RIGHT" value="50A" />`
	`  <specification id="ROOTS_TOP" value="50V" />`
	`  <specification id="ROOTS_BOTTOM" value="50V" />`
	`  </specifications>`
	`  </component>`
	`  </components>`
	`  </environment>`
	`</series>`

Untreated	`<series start="0" end="10" days="31">`
	`  <simulation type="growth">`
	`  <checkpoints>`
	`  <checkpoint type="graph" class="load" day="0" />`
	`  </checkpoints>`
	`  </simulation>`
	`  <agents initialization="FULL">`
	`  <populations>`
	`  <population type="C" fraction="0.0">`
	`  <variables>`
	`  <variable id="CAR_ANTIGENS_CANCER" value="1000"/>`
	`  </variables>`
	`  </population>`
	`  <population type="H" fraction="1.0">`
	`  <variables>`
	`  <variable id="CAR_ANTIGENS_HEALTHY" value="100" />`
	`  </variables>`
	`  </population>`
	`  <population type="4" fraction="0.0">`
	`  <variables>`
	`  <variable id="CAR_AFFINITY" />`

```
                  </variables>
               </population>
               <population type="8" fraction="0.0">
                  <variables>
                     <variable id="CAR_AFFINITY" />
                  </variables>
               </population>
            </populations>
            <helpers>
               <helper type="insert" delay="1440" populations="0"
               bounds="0.05" />
               <helper type="treat" delay="31680" dose="0" />
            </helpers>
         </agents>
         <environment coordinate="hex">
            <components>
               <component type="sites" class="graph" layout="(S)"
               left="(50A)" right="(50A)" top="(50V)" bottom="(50V)" />
               <component type="remodel" interval="60" />
               <component type="degrade" interval="1" />
            </components>
         </environment>
      </series>
      <series start="0" end="10" days="31">
         <simulation type="growth">
            <checkpoints>
               <checkpoint type="graph" class="load" day="0" />
            </checkpoints>
          </simulation>
          <agents initialization="FULL">
             <populations>
                <population type="C" fraction="0.0">
                   <variables>
                      <variable id="CAR_ANTIGENS_CANCER" value="1000"/>
                   </variables>
                </population>
                <population type="H" fraction="1.0">
                   <variables>
                      <variable id="CAR_ANTIGENS_HEALTHY" value="100" />
                   </variables>
                </population>
                <population type="4" fraction="0.0">
                   <variables>
                      <variable id="CAR_AFFINITY" />
                   </variables>
                </population>
                <population type="8" fraction="0.0">
                   <variables>
                      <variable id="CAR_AFFINITY" />
                   </variables>
                </population>
             </populations>
             <helpers>
                <helper type="insert" delay="1440" populations="0"
                bounds="0.05" />
                <helper type="treat" delay="31680" dose="0" />
```

Untreated (generate graph images for Figure 1)

```
            </helpers>
         </agents>
         <environment coordinate="hex">
            <components>
               <component type="sites" class="graph" layout="(S)"
               left="(50A)" right="(50A)" top="(50V)" bottom="(50V)" />
               <component type="remodel" interval="60" />
               <component type="degrade" interval="1" />
            </components>
         </environment>
      </series>
      <series start="0" end="10" days="31">
         <simulation type="growth">
            <checkpoints>
               <checkpoint type="graph" class="load" day="0" />
                  </checkpoints>
              </simulation>
         <agents initialization="FULL">
            <populations>
               <population type="C" fraction="0.0">
                  <variables>
                     <variable id="CAR_ANTIGENS_CANCER"
                     value="[10000|10000|10000|5000|10000|10000|10000|
                     5000|5000|1000|1000|500|1000|500]"/>
                  </variables>
               </population>
               <population type="H" fraction="1.0">
                  <variables>
                     <variable id="CAR_ANTIGENS_HEALTHY" value="100" />
                  </variables>
               </population>
               <population type="4" fraction="0.0">
                  <variables>
Treated              <variable id="CAR_AFFINITY" value="[1e-6|1e-6|1e-6|
                     1e-6|1e-6|1e-6|1e-6|1e-6|1e-6|1e-7|1e-7|1e-7|1e-7|
                     1e-7]" />
                  </variables>
               </population>
               <population type="8" fraction="0.0">
                  <variables>
                     <variable id="CAR_AFFINITY" value="[1e-6|1e-6|1e-6|
                     1e-6|1e-6|1e-6|1e-6|1e-6|1e-6|1e-7|1e-7|1e-7|1e-7|
                     1e-7]" />
                  </variables>
               </population>
            </populations>
            <helpers>
               <helper type="insert" delay="1440" populations="0"
               bounds="0.05" />
               <helper type="treat" delay="31680" dose="[1000|500|1000|
               1000|500|1000|250|1000|500|500|1000|1000|250|500]"
               ratio="[0.25:0.75|0.25:0.75|0.5:0.5|0.25:0.75|0.5:0.5|
               0.75:0.25|0.25:0.75|0.5:0.5| 0.25:0.75|0.5:0.5|0.75:0.25|
               0.5:0.5|0.25:0.75|0.25:0.75]" />
            </helpers>
         </agents>
```

```
            <environment coordinate="hex">
               <components>
                  <component type="sites" class="graph" layout="(S)"
                  left="(50A)"
                     right="(50A)" top="(50V)" bottom="(50V)" />
                  <component type="remodel" interval="60" />
                  <component type="degrade" interval="1" />
               </components>
            </environment>
         </series>
```

SUPPLEMENTARY TABLE 9. Difference metric for `tissue` simulations. Simulations were averaged across replicates, ranked by difference metric in `tissue` simulations, but are shown with rank in `dish` simulations.

CAR T-cell Dose	$CD4^+$:$CD8^+$ T-Cell Ratio	CAR Affinity (M)	Antigens Cancer	Antigens Healthy	Normalized Cancer Cell Count	Normalized Healthy Cell Count	Normalized T-cell Count	Difference Metric Value	Rank in `dish`	Rank in `tissue`
1000	0.25	1E-06	10000	100	0.15	0.90	39.20	0.04	1	1
1000	0.5	1E-06	10000	100	0.17	0.91	39.27	0.02	3	2
1000	0.25	1E-06	5000	100	0.21	0.91	39.01	-0.02	4	3
500	0.25	1E-06	10000	100	0.23	0.91	58.23	-0.03	2	4
1000	0.75	1E-07	1000	100	0.22	0.84	39.65	-0.04	11	5
1000	0.75	1E-06	10000	100	0.24	0.92	38.46	-0.05	6	6
1000	0.5	1E-06	5000	100	0.27	0.92	38.50	-0.07	8	7
1000	0.5	1E-07	500	100	0.25	0.82	40.36	-0.08	12	8
500	0.5	1E-06	10000	100	0.28	0.92	56.74	-0.08	5	9
500	0.5	1E-07	1000	100	0.26	0.82	56.78	-0.09	10	10
500	0.25	1E-06	5000	100	0.33	0.93	56.29	-0.13	9	11
500	0.25	1E-07	500	100	0.31	0.82	59.52	-0.13	14	12
250	0.25	1E-06	10000	100	0.33	0.92	88.55	-0.13	7	13
250	0.25	1E-07	1000	100	0.33	0.84	96.43	-0.15	13	14

A.4 Supplementary Methods Details

A.4.1 Model framework

The model integrates CAR T-cell agents into the agent-based modeling framework ARCADE [49,56]. The ARCADE framework utilizes interfaces to enable modular model composition. CARCADE implements the Cell interface for CAR T-cells. This CAR T-cell class extends into two subclasses representing $CD4^+$ and $CD8^+$ CAR T-cells. Each subclass contains two modules controlling metabolism and inflammation. All existing parameters are kept at default values [49,56]. All new parameters specific to CARCADE are listed in **Supplementary Table A.1** and described below.

A.4.2 Tissue cell agents

Tissue cell agents, which represent cancer and healthy tissue cells, can enter any one of seven cell states: quiescent, migratory, proliferative, apoptotic, necrotic, senescent, and uncommitted by following a specific set of rules [56]. Tissue cells in this study use the default metabolism and signaling modules. Cancer cell agents are identical to healthy cells except that they can escape quiescence, are more amenable to cell crowding upon looking for new locations while migrating or proliferating, and they differ in parameter name for antigen expression level. To interact with CAR T-cell agents, two parameters were added to tissue cell agents: the number of antigens (`CAR_ANTIGENS_CANCER` for cancer cells and `CAR_ANTIGENS_HEALTHY` for healthy cells) and the number of PD-1 ligand "self targets"expressed on the cell surface (`SELF_TARGETS`).

A.4.3 CAR T-cell agents

A.4.3.1 Initialization

All CAR T-cells are initialized with an age pulled from a uniform distribution with a specified minimum (`T_CELL_AGE_MIN`) and maximum (`T_CELL_AGE_MAX`) age, a volume pulled from a normal distribution with a specified average (`T_CELL_VOL_AVG`) and range (`T_CELL_VOL_RANGE`), and an approximate age at which death is more likely to occur from a normal distribution with specified average (`DEATH_AGE_AVG_T`) and range (`DEATH_AGE_RANGE`, parameter as in ARCADE) [56]. To account for the

Hayflick limit, each CAR T-cell is also initiated with a maximum division potential (`DIVISION_POTENTIAL_T`). Additionally, CAR T-cells are initiated with a number of surface CAR receptors (CARS) and surface self (PD1) receptors (`SELF_RECEPTORS`).

A.4.3.2 States and rules

Though it is difficult to directly observe transitions between states in individual cells, discrete CAR T-cells states are generally agreed to exist and mechanisms are hypothesized for state transitions [140,167,168]. When needed, we rely on more general T-cell studies to define parameters and state transitions. CAR T-cells can enter one of eleven states: migratory, proliferative, cytotoxic, stimulatory, paused, senescent, apoptotic, exhausted, anergic, starved, and uncommitted.

CAR T-cell agents move through the state diagram shown in **Supplementary Figure A.1** at each time point as a function of their state at the start of the time point.

A.4.3.2.1 Migratory state

Migratory is the default state for a healthy, activated or yet-to-be activated T-cell agent as it travels around looking for potential threats. Upon entering the migratory state, the time it takes a cell to migrate is determined as a function of the distance the cell is moving and the speed at which the cell is moving. Cells assess their current and surrounding locations to determine valid locations to which they can move. To be a valid location, a location must meet the following checks: (i) adding the cell to the location must not increase the total volume of all cells in that location to be greater than the volume of that location, and (ii) adding the cell to the location cannot increase the number of agents in that location beyond the max number of allowed agents. CAR T-cells assign a score to each location meeting the above criteria, where the score is a function of the amount of free glucose and the number of cancer cells in the location. CAR T-cells move towards the location with the highest score, though there is a level of inaccuracy introduced in assessing the amount of glucose in each location. The score (S_{loc}) is given by:

$$S_{loc} = \left[\beta \frac{G_i}{G^{\circ}} + (1-\beta)u\right] + C_i$$

where

- β is the accuracy (ACCURACY)
- $G°$ is the source concentration of glucose (CONC_GLUC)
- G_i is the amount of glucose in the location being assessed
- u is a random number drawn from a uniform distribution *U(*[0,1])
- C_i is the number of cancer cells in the location

Accounting for the number of cancer cells in each location within the score serves as a proxy for the bias of T-cells to move towards cytokines and chemokines indicating necessary immune activity. If there are no locations available, the cell becomes paused.

A.4.3.2.2 Proliferative state

Proliferative CAR T-cell agents, like typical T-cells, asymmetrically divide, splitting their volume unevenly, to produce daughter cell agents [145]. Upon entering the proliferative state, cells either divide or exit the proliferative state if the cell becomes no longer able to proliferate. Specifically, at each time step, the cell checks whether it has entered a state, such as apoptotic, such that it is no longer able to proliferate and checks if there are no locations into which the cell can divide. If there are no available locations for the daughter cell, the dividing cell becomes paused. To successfully proliferate, the cell must double in volume, where the rate at which this occurs is dictated by the metabolism module. Once this check has passed, the cell checks if the time since entering the proliferative state has exceeded the required DNA replication time, which is calculated as the average DNA synthesis time (SYNTHESIS_TIME_T) plus or minus a randomly drawn value within the DNA synthesis time range (SYNTHESIS_TIME_T_RANGE). If both checks are met, the cell divides, creating a daughter cell with 50% plus or minus up to 5% of the volume, bound IL-2, and granzyme (if $CD8^+$). The division count for both the parent and daughter cell is decreased. The daughter cell inherits the number of “self” (PD1) receptors, number of times the parent cell bound to antigen, the number of times the parent cell bound to “self” (PD1) ligands, and the activation condition. The duration of time spent in the proliferative state is defined as a cell cycle length, which is recorded each time a cell divides. The new daughter cell’s location is determined in the same way as described for migratory cells.

A.4.3.2.3 Paused state

Cell agents become paused when they are unable to migrate or proliferate. Paused agents have no active cell behavior, but they will remain paused until they enter a different state. Agents may accumulate in the paused state over time, as this behavior represents a biological phenomenon.

A.4.3.2.4 Stimulatory and cytotoxic states

Stimulatory and cytotoxic states represent the effector functions of $CD4^+$ and $CD8^+$ CAR T-cells, respectively. Stimulatory CAR T-cell agents produce IL-2, while cytotoxic CAR T-cell agents produce granzyme and, once bound to a target, kill the target cell, which becomes apoptotic. Effector cells enter the uncommitted state after a time delay to represent how long a T-cell stays bound to a target. This time delay is calculated as the average time bound to a target (`BOUND_TIME`) plus or minus a randomly drawn value from within the bound time range (`BOUND_TIME_RANGE`). Once a cell is activated it remains activated until it (i) becomes deactivated over time by not interacting with antigen for 7 days [38], (ii) enters the anergic or exhausted states, as these cause cells to lose effector function, or (iii) dies. Activation biases previously activated cells towards proliferation over migration when the agent has not bound to a surrounding target in subsequent time steps. Additionally, activation strongly influences cell effector function and metabolism.

A.4.3.2.5 Anergic state

Anergy is a non-functional, undesired T-cell state induced from either (i) T-cell stimulation via antigen interaction in the absence of proper co-stimulation [138,140,142,147,148] or by (ii) simultaneous T-cell stimulation with antigen and co-inhibitory signals, such as self-identification signals [138,140]. Proper co-stimulation is often conferred by co-stimulatory receptors such as CD28 [138,143]. Since second-generation CARs and beyond contain these co-receptors, anergy induction caused by T-cell stimulation via antigen interaction in the absence of proper co-stimulation is less likely. Only the latter possible mechanism is considered in the model, as we assume CARs in the model are at least second generation, as these are the only FDA approved and studied CARs in current research. CARCADE CAR T-cell agents enter the anergic state when they receive mixed signals, binding to both the antigen and the “self” receptors. Upon

binding to both signals, cells have some probability (ANERG_FRAC) of undergoing apoptosis or otherwise become anergic. Though most anergy studies come from work on $CD4^+$ T-cells [147], some studies show $CD8^+$ T-cells can enter this state [144]. In the model, both $CD4^+$ and $CD8^+$ T-cell agents can become anergic.

Anergic cells characteristically exhibit little to no effector function [148], proliferative potential [142,148], no IL-2 production [142,144], and an inability to respond to subsequent proper stimulation [142,147]. Thus, agents in the anergic state de-activate if previously activated, turning off all effector function, and they can only escape from the anergic state through eventual cell death.

Anergic T-cells escape this state either by eventual induction of apoptosis or, if induced due to lack of proper co-stimulation, by sufficient uptake of IL-2 to recover proper cell function [142,144]. Anergy occurs within the time frame of a few days [148], making it particularly relevant for this model, which can simulate tumor growth for up to a few months, and for understanding CAR T-cell dynamics. Since IL-2 only recovers cells induced into anergy by lack of proper co-stimulation, and this is less likely to be an issue in CAR T-cells, IL-2 recovery from anergy is not included in CARCADE and anergy is an irreversible state in the model.

A.4.3.2.6 Exhausted state

Similar to anergy, exhaustion is a distinct, non-functional T-cell state induced by repeated activation [138,140]. Though exhaustion occurs on the time scale of weeks [148], this state is highly prevalent in CAR T-cell work and is one attributed cause of low therapeutic efficacy [141]. Including exhaustion as a state in the model is therefore relevant for understanding and improving CAR T-cell dynamics.

Most research on exhaustion focuses on $CD8^+$ T-cells [137], but exhaustion also occurs in $CD4^+$ T-cells [137,148]. Exhausted $CD8^+$ T-cells lose cytotoxic activity [137], while exhausted $CD4^+$ T-cells express significantly decreased levels of effector cytokines [148]. In the model, both subtypes of CAR T-cell agents can become exhausted.

To capture the dynamics that induce exhaustion over time, CAR T-cells count of the number of times they have bound to antigen. If a cell goes 24 h without binding antigen, the count decreases by one. If this count exceeds a set maximum (MAX_ANTIGEN_BINDING), the next binding event will cause them to become exhausted. Upon exceeding the maximum antigen binding count, cells have some probability (EXHAU_FRAC) of undergoing apoptosis but otherwise become exhausted. Exhausted T-cells characteristically exhibit little to no proliferative potential [137,147,148], high expression of PD-1 [137,138,140,148], and higher rates of apoptosis [141]. Though not fully inert [148], exhausted T-cells lose some effector functions before others [137]. For simplicity, CAR T-cell agents in the model lose all effector function simultaneously upon entering the exhausted state. Exhausted agents de-activate if previously activated, turning off all effector function, and can only escape from the exhausted state through eventual cell death.

Exhaustion was thought to be reversible with PD-1 blockades [137,147,148], but new data suggest that PD-1 blockades promote expansion of T-cell populations outside of those exhausted within the tumor [149]. Both hypotheses motivate combining CAR T-cell therapy with either internally-engineered or intravenously injected PD-1 blockades [16,18-20]. However, PD-1 blockades are not included in the model at present, and exhaustion is an irreversible state in the model.

A.4.3.2.7 Senescent state

Due to the natural ageing process, all cells can become senescent, which is a non-reversible state causing cells to undergo cell cycle arrest and stop proliferating [137,138,140]. Upon hitting their division limit (DIVISION_POTENTIAL_T), cells have some probability (SENES_FRAC) of becoming senescent or apoptotic. Senescent cells remain in this state until they are eventually removed from the simulation due to age-induced apoptotic cell death.

A.4.3.2.8 Starved state

Cells require sufficient nutrients to sustain normal cellular function. Cells that do not meet their energy needs, as dictated by the metabolism module, become starved. Cells can escape the starved state upon

recovering from the energy deficient by accumulation of energy. Recovered cells are set to the uncommitted state to then continue in the decision sequence.

A.4.3.2.9 Apoptotic state

Cells can enter the apoptotic state due to age or sustained lack of nutrients or energy. Cells have an increased probability of entering the apoptotic state once they exceed their average life span (`DEATH_AGE_AVG_T`) as defined by a cumulative normal distribution where the mean is set to the `DEATH_AGE_AVG_T` and the standard deviation is set to the `DEATH_AGE_RANGE`. Cells can also become apoptotic under conditions of sustained energy deficiency, meaning their energy goes below a set threshold (`ENERGY_THRESHOLD`). Upon entering the apoptotic state, the cell is removed from the simulation after a time delay (`DEATH_TIME`) representing the time it takes a cell to die by apoptosis.

A.4.3.3 Antigen-induced activation process

Upon antigen-induced activation, CAR T-cells enter an effector state based on subtype, entering either the cytotoxic state to cytotoxically kill target agents or the stimulatory state to stimulate other T-cells by releasing cytokines [38]. While there is evidence that both T-cell subtypes can become cytotoxic and stimulatory, $CD8^+$ T-cells primarily provide cytotoxic functions, while $CD4^+$ T-cells primarily provide stimulatory functions [31,96,97]. For simplicity, the model assumes only $CD8^+$ CAR T-cell agents can enter the cytotoxic state and only $CD4^+$ CAR T-cell agents can enter the stimulatory state to perform associated functions. As the time required for CAR T-cells to form stable and functional immune synapses is shorter than two min [146], we assume signal binding and activation occur within a single time step within the model, which equates to one min.

The probability of an antigen binding or “self” (PD1) binding events occurring are a function of affinity of a receptor for its ligand, the number of ligands on the target cell surface, the number of receptors on the CAR T-cell surface, distance from and contact with a target cell, and probability of receptors making contact. We developed a sequence of events and a binding probability heuristic that captures these general trends. After stepping their metabolism module, CAR T-cell agents in the paused or uncommitted states assess

their surroundings and randomly select one neighboring agent. If that agent is a CAR T-cell agent, nothing happens and the searching CAR T-cell agent goes on to assess another target as until it hits the max number of neighbors assessable in a given time point (`SEARCH_ABILITY`). If the found agent is a tissue cell, the probability of binding and killing $P(binding\ and\ killing)$ is calculated according to a heuristic equation:

$$P(binding\ and\ killing) = 2\left(\frac{1}{1+e^{-x}}\right) - 1$$

where

$$x = \left(\frac{\gamma L_{target}}{\beta K_D V_{loc} N_A + \gamma L_{target}}\right)\left(\frac{R}{R_{avg}}\right)\alpha$$

where:

- L_{target} is the number of ligands on the target cell (`CAR_CANCER_ANTIGENS` or `CAR_HEALTHY_ANTIGENS` for cancer and healthy cells, respectively, for CAR-antigen binding events and `SELF_LIGANDS` for self-receptor binding events)
- R is the number of CARs for CAR-antigen binding events or number of self-receptors for self-receptor binding events on the CAR T-cell
- R_{avg} is the average number of receptors on the CAR T-cell (`CARS`) for CAR-antigen binding events and is the number of self-receptors (`SELF_RECEPTORS`) a cell starts with for self-receptor binding events
- K_D is the affinity of the receptor for the antigen in M (`CAR_AFFINITY` for CAR-antigen binding events and `SELF_AFFINITY` for self-receptor binding events)
- V_{loc} is the volume of the location in L
- N_A is Avogadro's Number
- γ is the contact fraction (`CONTACT_FRAC`)
- α (`CAR_ALPHA` for CAR-antigen binding events and `SELF_ALPHA` for self-receptor binding events) and β (`CAR_BETA` for CAR-antigen binding events and `SELF_BETA` for self-receptor binding events) are fitting factors

Overall, this function produces trends fitting with the expected outcomes where increasing antigen/ligand number, receptor number, and K_D will result in a higher probability if binding (for self-receptor binding events) and/or killing (for CAR binding events), as shown in **Supplementary Figure A.2**, which matches previously determined T-cell activation curves [135]. This calculation is done for both the CAR-antigen binding event and the PD1-PDL1 binding event. If the CAR T-cell binds to antigen and not to "self", the agent will become activated, enter its effector state, and increase the antigen-binding counter. If the CAR

T-cell binds to both antigen and “self”, the agent will become anergic (more detail described below) and increase the antigen-binding counter. If the CAR T-cell binds to neither antigen nor “self” or only to “self”, the agent becomes either migratory or proliferative, biasing towards proliferative if the CAR T-cell agent is activated. If the cell is not activated, cells become proliferative with a given probability (`PROLI_FRAC`); otherwise, it becomes migratory.

Additionally, upon each binding event in which cells bind to antigen, independent of binding to “self” receptor, CAR T-cells increase the amount of “self” receptors on their surface according to the following equation:

$$R_{i+1} = R_i + uR_0$$

where:

- R_0 is the initial number of “self” receptors on the cell
- u is a random number drawn from a uniform distribution *U(*[0.95,1.05])
- R_i is the number of “self” receptors on the cell after i binding events
- R_{i+1} is the number of “self” receptors on the cell after the new binding event

Thus, after each binding event, the number of “self” receptors on the cell surface will increase by 95-105% of the original number of receptors (`SELF_RECEPTORS` for initialized cells) after each binding event. This increase serves as both a marker for exhaustion (described in more detail below) and can increase the probability of a cell becoming anergic (described in more detail below) over time.

A.4.3.4 Subcellular modules

A.4.3.4.1 Inflammation module

T-cell cytokine signaling is dynamic and provides self-feedback. Additionally, cytokines influence effector function, metabolism, growth, and proliferation [17]. Though many important cytokines exist, the model only utilizes IL-2, which is a well-studied driver of immune response and is FDA approved as an intravenously administered immunotherapy treatment [125,126].

Unstimulated T-cells do not express IL-2Rα until after antigen-induced activation or stimulation with IL-2, making cells more sensitive to IL-2 after activation to amplify the immune response [123,124,135]. Upon

stimulation, IL-2 (i) promotes T-cell growth and proliferation by upregulating glycolysis and glucose uptake and (ii) induces effector function by activating relevant genes [123,124]. Effector function varies for T-cell subtypes; $CD4^+$ T-cells primarily secrete cytokines, such as IL-2, while $CD8^+$ T-cells produce cytolytic material, such as granzymes, that kills bound target cells when secreted [124].

All CAR T-cells are equipped with inflammation modules specific to their cell type. Broadly, the $CD4^+$ Inflammation module produces IL-2, while the $CD8^+$ Inflammation module produces granzyme that is used to kill target cells. Both T-cell subtypes bind IL-2 using a receptor complex composed of three receptor chains: IL-2Rα, IL-2Rβ, and IL-2Rγ_c. IL-2 binds to IL-2Rα weakly, the two-chain receptor complex IL-2R$\beta\gamma_c$ with intermediate affinity, and the full three-part complex with high affinity [123,124,126]. Both cell agents use the same set of ordinary differential equations (ODEs) to determine the amount of IL-2 bound to their surface. All species and parameters within the ODEs are detailed in the table below.

Species

Name	Description	Symbol
External IL-2	IL-2 in the environment accessible to the cell	X_1
IL-2R$\beta\gamma_c$	lower affinity two-chain IL-2 receptor complex	X_2
IL-2R$\beta\gamma_c\alpha$	higher affinity three-chain receptor complex	X_3
IL-2R$\beta\gamma_c$:IL-2	IL-2 bound two-chain IL-2 receptor complex	X_4
IL-2R$\beta\gamma_c\alpha$:IL-2	IL-2 bound three-chain IL-2 receptor complex	X_5
Total unbound IL-2 receptors	Total receptors (two- and three-chain) on cell surface not bound to IL-2	X_6
Total bound IL-2	Total receptors (two- and three-chain) on cell surface bound to IL-2	X_7

Parameters

Name	Description	Parameter Name	Symbol
Two-chain complex IL-2 binding on rate	Rate of IL-2 binding to IL-2R$\beta\gamma_c$	`IL2_BINDING_ON_RATE_MIN`	$k_{on,2}$
Three-chain complex IL-2 binding on rate	Rate of IL-2 binding to IL-2R$\beta\gamma_c\alpha$	`IL2_BINDING_ON_RATE_MAX`	$k_{on,3}$
IL-2 binding off rate	Rate of IL-2 unbinding from IL-2R$\beta\gamma_c$ or IL-2R$\beta\gamma_c\alpha$	`IL2_BINDING_OFF_RATE`	k_{off}
Three-chain receptor conversion rate	Captures rate of conversion of the two-chain complex IL-2R$\beta\gamma_c$, whether bound or unbound, into the three-chain complex IL-2R$\beta\gamma\alpha$ though positive feedback	`K_CONVERT`	$k_{convert}$
IL-2 receptor recycle rate	Rate at which IL-2R$\beta\gamma_c$:IL-2, IL-2R$\beta\gamma_c\alpha$:IL-2, or IL-2R$\beta\gamma_c\alpha$ are internalized be converted via recycle back into unbound IL-2R$\beta\gamma_c$ chains.	`K_REC`	k_{rec}

External IL-2 (X_1) binds reversibly to unbound receptor complexes X_2 and X_3 with on rate $k_{on,2}$ and $k_{on,3}$, respectively, to from the bound receptor complexes X_4 and X_5, respectively. The high affinity and lower affinity receptors bind with the same off rate k_{off} but different on rates [99]. The equation describing X_1 kinetics are as follows:

$$\frac{dX_1}{dt} = k_{off}X_4 + k_{off}X_5 - k_{on,2}X_1X_2 - k_{on,3}X_1X_3$$

The IL-2Rα subunit, which converts two-chain complexes into three-chain complexes with higher IL-2 affinity, is only produced after initial binding of IL-2 to the two-chain complex. To reduce the model complexity and the number of species tracked, the production of the IL-2Rα chain alone is not explicitly modeled. However, the impact of IL-2 binding on conversion of the two-chain complex IL-2Rβγc, whether bound or unbound, into the three-chain complex IL-2Rβγα though positive feedback is captured through the parameter $k_{convert}$, where the summed number of bound IL-2 complexes is meant to represent the magnitude of signal that produces the IL-2Rα chain [106]. Unbound and bound receptors without the IL-2Rα chain, X_2 and X_4, can be converted to three-chain receptor complexes X_3 and X_5, respectively, through the convert mechanism. Additionally, since the X_2 is constitutively expressed [123], we capture this process by having any IL-2 bound chains X_4 and X_5 or unbound chain X_3 that are internalized be converted via recycle, represented by k_{rec}, back into unbound X_2. This recycling process enables the response of the production of the IL-2Rα chain to be pulsatory and will eventually stop in the prolonged absence of IL-2. The equation describing X_2, X_3, X_4, and X_5 kinetics are as follows:

$$\frac{dX_2}{dt} = k_{off}X_4 - k_{on,2}X_1X_2 - k_{convert}(X_4 + X_5)X_2 + k_{rec}(X_3 + X_4 + X_5)$$

$$\frac{dX_3}{dt} = k_{off}X_5 - k_{on,3}X_1X_3 + k_{convert}(X_4 + X_5)X_2 - k_{rec}X_3$$

$$\frac{dX_4}{dt} = k_{on,2}X_1X_2 - k_{off}X_4 - k_{convert}(X_4 + X_5)X_4 - k_{rec}X_4$$

$$\frac{dX_5}{dt} = k_{on,3}X_1X_3 - k_{off}X_5 + k_{convert}(X_4 + X_5)X_4 - k_{rec}X_5$$

For convenience, we also track X_6 and X_7.

$$\frac{dX_6}{dt} = \frac{dX_2}{dt} + \frac{X_3}{dt}$$

$$\frac{dX_7}{dt} = \frac{dX_4}{dt} + \frac{dX_5}{dt}$$

Each species is in units of molecules of IL-2 in ODEs, but the environment keeps track of the concentration of IL-2 in units of molecules/cm^3. The ODEs are run within each individual cell at each model step (one minute), using a Runge-Kutta solver, with a time step of 1/3rd of a second. This set of reduced equations captures a few key aspects of IL-2 signaling with the brevity necessary to run the model without excess delay, as these ODEs are run in all CAR T-cells and on a large scale are very computationally expensive.

The amount of external IL-2 is determined based on both the cell's location within the environment and the distance from the cell surface a cell can sense (d_{shell}, `SHELL_THICKNESS`). T-cells are relatively small compared to the volume of a location in the model, and they have access to all the IL-2 present in the environment. A shell thickness value was set such that cells can sense a few microns out from their external surfaces [119]. The cell's volume (V_{cell}) is known for each agent, and thus, assuming the cell to be a sphere, the cell radius (r_{cell}) can be calculated as follows:

$$r_{cell} = \sqrt[3]{\frac{3}{4\pi} V_{cell}}$$

Subsequently, the shell radius (r_{shell}), which is the distance of the cell radius and the distance from the cell surface that a cell can sense (d_{shell}, `SHELL_THICKNESS`), can be calculated as follows:

$$r_{shell} = r_{cell} + d_{shell}$$

Thus, the volume within the shell (V_{shell}) that exists between the external surface of the cell, assuming the cell to be a sphere, and the distance from the cell defined by this shell's thickness is calculated as follows:

$$V_{shell} = V_{r_{shell}} - V_{cell} = V_{cell}\left(\frac{r_{shell}^3}{r_{cell}^3} - 1\right)$$

The fraction of total volume in the environment that makes up this shell volume (f_{shell}) is the calculated as follows:

$$f_{shell} = \frac{V_{shell}}{V_{loc}}$$

The amount of external IL-2 (X_1) a cell as access to at each time point is calculated as follows:

$$X_1 = f_{shell} n_{IL2}$$

where n_{IL2} is the total number of molecules of IL-2 in the environment at the cell's location.

The inflammation module includes a memory of the total amount of IL-2 bound on the surface to capture a time delay in various cellular processes that are a function of IL-2 binding, as no process is instantaneous and must first undergo internal signaling networks to initiate cellular responses.

When a CAR T-cell divides, the amount of each species, with the exception of IL-2Rβγ$_c$ but including granzyme in the CD8$^+$ CAR T-cells, is divided between the two daughter cells, splitting according to the same fraction described in the proliferative state section. Since IL-2Rβγ$_c$ is assumed to be constitutively expressed, the amount in the daughter cell is the steady state value of IL-2 receptors total (`IL2_RECEPTORS`) minus the amount of receptors that are already bound to IL-2.

Each CAR T-cell subtype has specific functions corresponding to the typical functions of T-cell subtypes. While IL-2 is secreted primarily by CD4$^+$ T-cells after antigen-induced activation, the model assumes IL-2 is exclusively secreted by this cell subtype [123-125]. Upon antigen-induced activation, IL-2 drives the production of granzyme and other cytotoxins in CD8$^+$ T-cells [124]. Though CD4$^+$ CAR T-cells have been found to be capable of killing, it is at a much slower rate and most killing is done by CD8$^+$ CAR T-cells [96]. For simplicity, the model assumes all granzyme production and cytotoxic killing is done exclusively by CD8$^+$ CAR T-cells.

A.4.3.4.1.1 CD4+ CAR T-cell agent IL-2 production

CD4⁺ CAR T-cell agents produce IL-2 in both an antigen-induced independent and dependent manner [106]. Independent of antigen-induced activation, CD4⁺ T-cells produce IL-2 as a function of the amount of IL-2 bound on their surface due to positive feedback [106]. The maximum amount of IL-2 produced due to IL-2 feedback (`IL2_PROD_RATE_IL2`) is scaled by the amount of IL-2 bound at a previous time point corresponding to the delay necessary to turn on IL-2 production (`IL2_SYNTHESIS_DELAY`) [104]. The rate of IL-2 production as a function of IL-2 feedback at time step t (r_{IL2}^{t}) in units of molecules/cell/min is calculated as follows:

$$r_{IL2}^{t} = R_{IL2,}\left(\frac{n_{IL2}^{t-\tau_{IL2}}}{N_{IL2}}\right)$$

where:

- R_{IL2} is the maximum rate of production of IL-2 per time step due to IL-2 feedback in units of molecules/cell/min
- $n_{IL2}^{t-\tau_{IL2}}$ is the total amount of IL-2 bound to the cell surface at the previous time point corresponding to delay in IL-2 synthesis (`IL2_SYNTHESIS_DELAY`)
- N_{IL2} is the maximum amount of IL-2 that can be bound to a cell, which corresponds to the total number of IL-2 receptors (`IL2_RECEPTORS`)

Upon antigen-induced activation and after a time delay (`IL2_SYNTHESIS_DELAY`), CD4⁺ CAR T-cells begin to produce additional IL-2 at a constant rate (`IL2_PROD_RATE_ACTIVE`) that is added to the rate of production of IL-2 per time step due to IL-2 feedback. The equation for the total amount of IL-2 produced by the cell in a given (r) in units of molecules/cell/min is as follows:

$$r = \begin{cases} r_{IL2} + r_{active}, & if\ active\ and\ t_{active} > \tau_{IL2} \\ r_{IL2}, & else \end{cases}$$

where:

- r_{active} is the rate of IL-2 production due to antigen-induced activation (`IL2_PROD_RATE_ACTIVE`) in units of molecules/cell/min
- t_{active} is the length of time since the T-cell was activated
- τ_{IL2} is the time delay required to synthesized IL-2 (`IL2_SYNTHESIS_DELAY`)

The IL-2 produced during this time step is then added to the IL-2 in the local environment.

A.4.3.4.1.2 CD8+ CAR T-cell agent granzyme production

CD8⁺ CAR T-cell agents produce granzyme upon antigen-induced activation as a function of IL-2 [139]. Granzyme increases linearly as a function of IL-2 until it eventually plateaus [139]. Additionally, granzyme builds up in a cell over time. In the model, to account for delay in granzyme production after antigen-induced activation due to internal signal transduction, granzyme production begins after a time delay (`GRANZ_SYNTHESIS_DELAY`). The amount of IL-2 sensed by the cell is used to scale the maximum rate of granzyme production and is calculated using the same time delay. Overall, the amount of granzyme in a CD8⁺ CAR T-cell each time step (n_g^t) in arbitrary units is calculated as follows:

$$n_g^t = n_g^{t-1} + G\left(\frac{n_{IL2}^{t-\tau_g}}{N_{IL2}}\right)$$

where:

- n_g^{t-1} is the amount of granzyme in the cell in the previous time step in arbitrary units
- G is the moles of granzyme produced per moles of IL-2 (`GRANZ_PER_IL2`)
- $n_{IL2}^{t-\tau_g}$ is the total amount of IL-2 bound to cell surface at the previous time point corresponding to the delay in granzyme synthesis (τ_g, `GRANZ_SYNTHESIS_DELAY`)
- N_{IL2} is the maximum amount of IL-2 that can be bound to a cell, which corresponds to the total number of IL-2 receptors (`IL2_RECEPTORS`)

As described in the cytotoxic state section, one unit of granzyme in arbitrary units is lost when a target cell is killed.

A.4.3.4.2 Metabolism module

T-cell metabolism is complex, as it is a function of both antigen-induced activation and IL-2. Naïve, inactivated T-cells are metabolically quiescent, require less oxygen and glucose consumption, and primarily utilize oxidative phosphorylation (OXPHOS) and fatty acid oxidation (FAO) for energy [36-38,97]. Antigen-induced activation causes T-cells to shift their metabolism by upregulating glycolysis [36,38-40,101,109,121,122], increasing glucose uptake [38-40,97,101,105,109,121], and downregulating mitochondrial metabolism [36,39]. This process is co-stimulation dependent, requiring signals like CD28,

which is part of the CAR construct, to further activate the PI3K/Akt/mTOR pathway to increase Glut1 expression and thus increase glucose uptake and glycolysis [38-40,97,101]. IL-2 enhances this process, promoting glycolysis by further activating mTOR [37,97,124]. Thus, both activation and IL-2 influence CAR T-cell metabolism in the model.

The metabolism module used for CAR T-cell agents uses IL-2 and antigen-induced activation to regulate T-cell energy requirements, nutrient uptake, metabolic preference for glycolysis, and cell mass production by building the default metabolism module used for tissue cells. The metabolism module calculates energy required to maintain antigen-induced activation (`ACTIVE_ENERGY`) in addition to basal, proliferative, and migratory energy requirements. Three parameters are altered as a function of antigen-induced activation and/or IL-2: (i) the metabolic preference for glycolysis over OXPHOS, (ii) the glucose uptake rate, and (iii) the fraction of internal nutrients converted to mass.

The metabolic preference for glycolysis over OXPHOS (`META_PREF`) is such that higher value dictates that a cell is getting more of its energy from glycolysis. This parameter changes as a function of both IL-2 bound to the cell agent as well as antigen induced activation independently. To account for delays in metabolic shifts due to intracellular signaling, a time delay is implemented much in the same way as for IL-2 and granzyme synthesis in the inflammation modules. The maximum possible influence of IL-2 on the metabolic preference (`META_PREF_IL2`) is scaled by the amount of IL-2 bound to the cell at the previous time point dictated by the time delay (`META_SWITCH_DELAY`) to calculate influence of IL-2 on the metabolic preference during time step t (m_{IL2}^{t}) as follows:

$$m_{IL2}^{t} = M_{IL2}\left(\frac{n_{IL2}^{t-\tau_m}}{N_{IL2}}\right)$$

where:

- M_{IL2} is the maximum possible influence of IL-2 on the metabolic preference (`META_PREF_IL2`)
- $N_{IL2}^{t-\tau_m}$ is the total amount of IL-2 bound to the cell surface at the previous time point corresponding to delay metabolic switching (τ_m, `META_SWITCH_DELAY`)
- N_{IL2} is the maximum amount of IL-2 that can be bound to a cell, which corresponds to the total number of IL-2 receptors (`IL2_RECEPTORS`).

This influence of IL-2 is added to the base metabolic preference value (`META_PREF`). Upon antigen-induced activation and after a time delay (`META_SWITCH_DELAY`), the influence of antigen-induced activation on the metabolic preference (`META_PREF_ACTIVE`) is also added to the base value. The total metabolic preference (m) during any given time step is calculated as:

$$m = \begin{cases} m_{base} + m_{IL2} + m_{active}, & if\ active\ and\ t_{active} > \tau_m \\ m_{base} + m_{IL2}, & else \end{cases}$$

where

- m_{base} is the base value of the metabolic preference (`META_PREF`)
- m_{IL2} is the calculated influence of IL-2 on metabolic preference
- m_{active} is the influence of antigen-induced activation on metabolic preference (`META_PREF_ACTIVE`)
- t_{active} is the length of time since the T-cell became activated
- τ_m is the time delay required to synthesize IL-2 (`META_SWITCH_DELAY`).

The glucose uptake rate parameter, like the metabolic preference, is a function of both IL-2 and antigen-induced activation, and follows the same formulation as the above parameter where the influence of IL-2 on glucose uptake rate during time step t (u_{IL2}^t) is calculated as follows:

$$u_{IL2}^t = U_{IL2}\left(\frac{n_{IL2}^{t-\tau_m}}{N_{IL2}}\right)$$

where

- U_{IL2} is the maximum possible influence of IL-2 on the glucose uptake rate (`GLUC_UPTAKE_RATE_IL2`)
- $n_{IL2}^{t-\tau_m}$ is the total amount of IL-2 bound to the cell surface at the previous time point corresponding to delay metabolic switching (τ_m, `META_SWITCH_DELAY`)
- N_{IL2} is the maximum amount of IL-2 that can be bound to a cell, which corresponds to the total number of IL-2 receptors (`IL2_RECEPTORS`).

This influence of IL-2 is added to the base glucose uptake rate (`GLUC_UPTAKE_RATE`). Upon antigen-induced activation and after a time delay (τ_m, `META_SWITCH_DELAY`), the influence of antigen-induced activation on the metabolic preference (`GLUC_UPTAKE_RATE_ACTIVE`) is also added to the base value. The total glucose uptake rate (u) during any given time step is calculated as:

$$u = \begin{cases} u_{base} + u_{IL2} + u_{active}, & if\ active\ and\ t_{active} > \tau_m \\ u_{base} + u_{IL2}, & else \end{cases}$$

where:

- u_{base} is the base value of the glucose uptake rate (`GLUC_UPTAKE_RATE`)
- u_{IL2} is the calculated influence of IL-2 on glucose uptake rate
- u_{active} is the influence of antigen-induced activation on glucose uptake rate (`GLUC_UPTAKE_RATE_ACTIVE`)
- t_{active} is the length of time since the T-cell became activated
- τ_m is the time delay required to synthesized IL-2 (`META_SWITCH_DELAY`)

Using anabolic metabolism, which produces more growth-related intermediates than energy, enables effector T-cells to undergo rapid growth and proliferation, a necessary component of immune response [38,122]. Additionally, through the support of upregulated glycolysis, T-cells upregulate biosynthesis pathways such as lipid, protein, and nucleic acid production [121,122]. Thus, the fraction of internal nutrients converted to mass is also increased as function of antigen-induced activation. The total fraction of internal nutrients converted to mass (f) is calculated as follows:

$$f = \begin{cases} f_{base} + f_{active}, & if\ active\ and\ t_{active} > \tau_m \\ f_{base}, & else \end{cases}$$

where:

- f_{base} is the base value of the fraction of nutrients converted to mass (`FRAC_MASS`)
- f_{active} is the increase in the fraction of nutrients converted to mass as a function due to antigen-induced activation (`FRAC_MASS_ACTIVE`)
- t_{active} is the length of time since the T-cell became activated
- τ_m is the time delay required to synthesized IL-2 (`META_SWITCH_DELAY`)

A.4.4 Model environment

A.4.4.1 Molecule diffusion

The model includes diffusion of IL-2 in addition to the default species (oxygen, glucose, and TGFα). The environment is initiated with a specified concentration of IL-2 (`CONCENTRATION_IL2`), which for this study was always zero. The diffusion of IL-2 is handled the same as the other species using a reaction-diffusion

equation, where the diffusion rate of IL-2 is specified (`DIFFUSIVITY_IL2`). Parameters for oxygen, glucose, and TGFα are left at default values.

A.4.4.2 Nutrient sources

The design of the nutrient (glucose and oxygen) sources in the simulation can be used to emulate specific contexts. `Dish` simulations utilize a constant source environment to replicate the evenly mixed nature of a well-mixed *in vitro* experiment [56]. `Tissue` simulations utilize vasculature comprising two arteries and two veins that simulate realistic hemodynamics where vasculature can become increasingly damaged over time by cell crowding and movement [49].

A.4.5 Cell placement and treatment

A.4.5.1 Tissue cell placement

A.4.5.1.1 Simulations in `dish`

For `dish` simulations, a specified total number of cells, with defined fractions of each population present, are plated randomly across the entire simulation environment. This plating aims to replicate an *in vitro* experiment where cells are plated in a monolayer in a cell culture dish with media.

A.4.5.1.2 Simulations in `tissue`

For `tissue` simulations, a bed of healthy cells is placed throughout the simulation environment and a population of cancer cells is introduced to the center of the environment after a specified time delay. This tumor is then allowed to grow for 21 days before treatment with CAR T-cells. This setup aims to replicate a tumor growing within a bed of healthy, vascularized tissue that may present resource limitations in high cell density areas.

A.4.6 CAR T-cell treatment

CAR T-cells are added at a specified time delay, with a specific CAR T-cell dose and $CD4^+$:$CD8^+$ ratio. Parameters for CAR T-cell populations, such as the affinity of the CAR for its antigen (`CAR_AFFINITY`),

are specified in the population tags. CAR T-cell agents are biased toward spawning in locations with higher numbers of cancer cells to serve as a proxy for trafficking to tumors, which is not explicitly captured by the model. While placing CAR T-cells, each location is checked to ensure adding the agent will not (i) make the total cell volume exceed the volume of the location and (ii) cause tissue cells to exist beyond their tolerable heights (`MAX_HEIGHT`), which is described in ARCADE [56].

A.4.6.1 Simulations in `dish`

CAR T-cells plated when sources or patterns are used for the nutrient environment, such as in `dish` simulations, can be placed in any location that does not exceed a maximum level of damage (`MAX_DAMAGE_SEED`). For simulations in this paper, source locations could not take damage.

A.4.6.2 Simulations in `tissue`

When a dynamic graph vasculature is used for the nutrient environment, such as in `tissue` simulations, CAR T-cells can spawn in any location next to a vasculature graph edge where the radius of the vein is greater than or equal to the specified minimum value (`MIN_RADIUS_SEED`), representing CAR T-cell trafficking through vasculature and preventing cells from spawning at locations with excessive damage. Cells cannot spawn where there is no vasculature edge or there the radius is too small. This spawning setup aims to replicate CAR T-cell trafficking to tumors through vasculature without explicitly modeling transfer of the CAR T-cell from vasculature into the tissue.

A.4.7 Simulated experiments

A.4.7.1 Simulations of monoculture `dish`

We simulate *in vitro* monoculture experiments of cancer cells. Four different features (CAR T-cell dose, $CD4^+$:$CD8^+$ ratio, CAR affinity, and cancer antigens) were changed in this dataset, with 10 replicates for each possible combination of parameter choices, one in each category. **Supplementary Table A.2** shows the set of simulated values per modified parameter. Simulated untreated cancer cells in `dish` (10 replicates) served as a negative control.

At the start of each simulation, 2000 cancer cells are plated randomly across a simulation environment with radius 34 and margin 6. Each cancer cell has the specified level of antigens (CANCER ANTIGENS, `CAR_ANTIGENS_CANCER`) for that combination of parameters. If treated, after a time delay of t = 10 min, a specified CAR T-cell dose (CAR T-CELL DOSE) with a specified $CD4^+$:$CD8^+$ ratio ($CD4^+$:$CD8^+$ RATIO) and CAR-antigen affinity (CAR AFFINITY) is added into the simulation. Data were collected every half day (720 time steps). In both treated and untreated simulations, the simulations lasted 7 days (10,080 time steps). Input files to create the simulations are shown in **Supplementary Table A.7**.

A.4.7.2 Simulations of ideal and realistic co-culture `dish`

This simulation setup aims to most closely replicate *in vitro* co-culture experiments with a mix of cancer and healthy cells. Four different axes (CAR T-cell dose, $CD4^+$:$CD8^+$ ratio, CAR affinity, cancer antigens) were changed to create both the ideal (antigen-negative healthy cells) and realistic (antigen-expressing healthy cells), with 10 replicates for each possible combination of parameter choices, one in each category. **Supplementary Table A.3** shows the set of simulated values per modified parameter. Simulated untreated cancer cells in `dish` (10 replicates) served as a negative control.

At the start of each simulation, 2000 total cells (1000 cancer cells and 1000 healthy cells) are plated randomly across a 2D simulation with radius 34 and margin 6. Each cancer and healthy cell have the specified level of antigens (CANCER ANTIGENS/`CAR_ANTIGENS_CANCER` and HEALTHY ANTIGENS/`CAR_ANTIGENS_HEALTHY`, respectively) for that combination of parameters. If treated, after a time delay of t = 10 min, a specified CAR T-cell dose (CAR T-CELL DOSE) with a specified $CD4^+$:$CD8^+$ ratio ($CD4^+$:$CD8^+$ RATIO) and CAR-antigen affinity (CAR AFFINITY) is added into the simulation. Data were collected every half day (720 time steps). In both treated and untreated simulations, the simulations lasted 7 days (10,080 time steps). Input files to create the simulations are shown in **Supplementary Table 8**.

A.4.7.3 Simulations of `tissue` with cancer and healthy cells

This simulation setup aims to most closely replicate *in vivo* experiments in which a tumor exists in a bed of healthy cells amongst a dynamic vasculature. We simulated the set of conditions described in **Supplementary Table 5**, co-culture `dish` conditions deemed as effective treatment conditions, in `tissue`. A set of 10 replicates of untreated cancer cells within a bed of healthy cells served as the control experiment.

At the start of each simulation, healthy cells are plated at one cell per location across the entire simulation with radius 34 and margin 6. The simulation environment uses the S_{22} vasculature setup, where there are two arteries and two veins total, each one starting from a different side of the simulation and alternating between veins and arteries, described in the ARCADE vasculature study [49]. A population of cancer cells is then inoculated into the model t = 1 d (1,440 time steps) into the simulation at the center out to a radius bounds of 0.05 (radii 1 and 2). Each cancer and healthy cell have the specified level of antigens (`CAR_ANTIGENS_CANCER` and `CAR_ANTIGENS_HEALTHY`, respectively) for that combination of parameters. The tumor is then allowed to grow until t = 31 d (44,640 time steps). If treated, the treatment begins at t = 22 d (31,680 time steps). A specified CAR T-cell dose (CAR T-CELL DOSE) with a specified $CD4^+$:$CD8^+$ ratio ($CD4^+$:$CD8^+$ RATIO) and CAR-antigen affinity (CAR AFFINITY) is added into the simulation. Data were collected every half day (720 time steps). To minimize variation as a result of the vasculature, all simulations use the same vasculature structure. Input files to create the simulations are shown in **Supplementary Table 9**.

A.4.8 Data analysis

A.4.8.1 Analysis of experimental data

Data from published studies of percent lysis at given antigen densities from various CARs, detailed in **Supplementary Table A.4** and **Supplementary Data A.1**, were estimated from plots included within each paper's results and processed for use in **Figure 2.2F** for the purpose of model validation. To ensure all the data could be viewed on plots with the same scaling, each percent lysis value was normalized to the maximum percent lysis for that CAR, and antigen values were normalized to the maximum value tested

within a given dataset. The normalized values of the percent lysis or antigen values (N_x) plotted in **Figure 2.2B** were calculated as follows:

$$N_x = \frac{x}{X}$$

where:

- x is the percent lysis or antigen value for a given data point within a dataset
- X is the maximum percent lysis or antigen value within that given dataset

The error bars for both percent lysis and antigen value were also used, but they were normalized using the following error propagation formula using standard deviation for divided values (such as our normalized values) to calculate the error of the normalized percent lysis or normalized antigen value (N_{σ_x}):

$$N_{\sigma_x} = N_x \sqrt{\left(\frac{\sigma_x}{x}\right)^2 + \left(\frac{\Sigma_x}{X}\right)^2}$$

where

- N_{σ_x} is the error of the normalized percent lysis or normalized antigen value
- x is the percent lysis or antigen value for a given data point within a dataset
- σ_x is the error for the percent lysis or antigen value for that given data point within a dataset
- X is the maximum percent lysis or antigen value within that given data set
- Σ_x is the error for the maximum percent lysis or maximum antigen value for that given data point within that dataset

When estimating data values from published plots, not all of the papers provided equivalent data, and some assumptions had to be made. Chmielewski et. al. recorded antigen levels in MFI and provided viability data rather than percent lysis [128], so the data were converted to percent lysis (P_{lysis}) using the following formula:

$$P_{lysis} = 1 - P_{viability}$$

where $P_{viability}$ is the percent viability. Liu et. al. recorded antigen level in terms of ErbB2 RNA µg [24]. Given that values were all normalized, this RNA quantity was used as a proxy for antigen expression level. Each of calculated value, assumptions, and notes associated with each published study are listed in **Supplementary Table A.4** and **Supplementary Data A.1**.

A.4.8.2 Normalized cell counts

To compare outcomes between *in silico* experiments, we used normalized values of live cancer and healthy counts. Each normalized live cell metric (N_P) is calculated as follows:

$$N_P = \frac{n_F}{n_T}$$

where

- n_F is the total number of live and cancer cell counts at the final time point (t = 7 d for `dish` and t = 30 d for `tissue`)
- n_T is the total number of live cancer or healthy cells at the start of treatment timepoint (t = 0 d for `dish` and t = 21 for `tissue`)

To make a comparable metric to compare simulated monoculture `dish` outcomes to percent lysis values from experimental studies for use in **Figure 2.2B**, we calculated the percent lysis of simulated experiments (P_{lysis}) as follows:

$$P_{lysis} = 1 - N_C$$

where

- N_C is the normalized live cancer cell metric

A.4.8.3 Difference metric

To compare the outcomes of simulations with both cancer and healthy cells in a way that accounts for the tradeoff of cancer cell killing with healthy cell killing, we used a difference metric. The difference metric (D) is as follows:

$$D = N_H \left(\frac{c_\mathrm{T}}{h_\mathrm{T}}\right) - N_C$$

where

- N_H is the normalized live healthy cell metric
- N_C is the normalized live cancer cell metric
- c_T is the number of live cancer cells at the start of treatment (t = 0 d for `dish` and t = 21 d for `tissue`)

- h_T is the number of live healthy cells at the start of the treatment (t = 0 d for `dish` and t = 21 d for `tissue`)

The normalized live healthy cell metric is normalized by the ratio of initial live cancer to healthy cells at treatment start to account for differences in initial cell counts and ensure ratio components are equally weighted.

B Supplementary Information for Chapter 3

B.1 Supplementary Workshop Content

The content presented constitutes the information, provided in order, of the asynchronous pre-work portion of the ARDEI-Question Writing Workshop for Faculty. While videos were also made to accompany each section, these videos are not included here. All of this content was developed by ChBE ARDEI Committee Undergraduate Education Subcommittee: Dr. Jennifer Cole, Ayinoluwa Abegunde, Lauren Simitz, Kenzie Sanroman Gutierrez, Alex Prybutok, and Chloé Archuleta.

B.1.1 Definitions and establishing community guidelines

B.1.1.1 Definitions

In order to bring everyone to the same level of understanding, we are providing a series of definitions core to understanding anti-racism, diversity, equity, and inclusion (ARDEI) broadly and in the context of education.

- **BIPOC:** Black, Indigenous, and People of Color, meant to unite all POC in the work for liberation while acknowledging that not all POC face the same levels of injustice
- **White privilege:** the implicit or systemic advantages that people who are perceived as white have relative to people who are not deemed white
- **Racism:** Discrimination based on race, racial prejudice, and oppression of racial groups
- **Individual racism:** the beliefs, attitudes, and actions of individuals that support or perpetuate racism in conscious and unconscious ways
- **Systemic racism:** the ways in which policies and practices of organizations or parts of systems create different outcomes for different racial groups
- **Ableism:** discrimination of and social prejudice against people with disabilities and chronic conditions, which includes the full spectrum of disability from physical to cognitive disabilities and mental illnesses, based on the belief that typical abilities are superior

- **Bias:** a particular tendency, trend, inclination, feeling, or opinion, especially one that is preconceived or unreasoned
- **Unconscious bias:** having and/or acting on biases without realizing they exist or acknowledging how they might be affecting others
- **Allyship:** the practice of emphasizing social justice, inclusion, anti-racism, and human rights to advance the interests of an oppressed or marginalized out-group
- **Positionality:** the social and political context that creates your identity in terms of race, class, gender, sexuality, and ability status. Positionality also describes how your identity influences, and potentially biases, your understanding of and outlook on the world.
- **Anti-racism:** an active and conscious effort to work against multidimensional aspects of racism
- **Diversity:** having a people of different backgrounds, ethnicities/races, genders, sexualities, perspectives, and mental and physical ability present; note that the presence of a diverse group does not necessarily mean each member is being treated equitably or being supported as needed
- **Equity:** providing support to people on an individual basis to ensure that each member of a group or community can participate equally
- **Inclusion:** the active, intentional, and ongoing engagement with diversity (in the classroom or broader communities) in ways that increase awareness, knowledge, and understanding of the complex ways individuals interact within systems and institutions.

  **This is a more traditional definition of inclusion, but we want to incorporate the idea that we are trying to create an environment and culture where members who have historically been excluded or marginalized are welcomed and accommodated within an organization or group.
- **Inclusive teaching:** teaching in such a way that all students are able to succeed and learn; this is often accomplished by including active learning, diverse ways of communicating and assessing information, and connecting course content to student interests and world experiences

B.1.1.2 Community guidelines

When discussing ARDEI in a classroom setting, we need to prepare students, TAs, and instructors to engage in that conversation in a safe and productive way. Setting up ground rules or communal guidelines

around discussion and collaboration helps ensure that in both full group discussions and small group/partnered work without the instructor present that there are ways for students to communicate respectfully with one another. Additionally, these communal guidelines help to prevent the reinforcing inequities and hierarchies that can exist among students. These ground rules can be developed by the instructor, or preferably as a discussion between the instructor and the students together, and can become part of the syllabus, thus setting the tone of empathy, understanding, and listening. We provide an example of community guidelines below; this list specifically was used during the Contextualizing Your Research Workshop hosted in Summer 2020.

Sample Community Guidelines

1. **Avoid Assumptions**: Avoid assumptions about any member of the class or generalizations about social groups. Do not ask individuals to speak for their (perceived) social group.
2. **Use "I" Language**: Understand that others will come to these discussions with different experiences from yours. Be careful about assumptions and generalizations you make based only on your own experience. When speaking about your own experiences, use "I" statements to clarify for whom you are speaking for--yourself.
3. **Treat Others How They Ask to Be Treated**: Speak with care. If you learn that something you've said was experienced as disrespectful or marginalizing, listen carefully and try to understand that perspective. Learn how you can do better in the future.
4. **Be Curious and Ask Respectfully**: Don't interrupt, turn to technology, or engage in private conversations while others are speaking. Use attentive, courteous body language. Comments that you make (whether asking for clarification, sharing critiques, or expanding on a point) should reflect that you have paid attention to the previous speakers' comments.
5. **Listen Actively**: Listen actively and with an ear to understanding others' views. (Don't just think about what you are going to say while someone else is talking.)
6. **Ideas, Not Individuals**: Speak to an individual's ideas, not their entire person.

7. **Encourage Learning**: Be open to changing your perspectives based on what you learn from others. Try to explore new ideas and possibilities. Think critically about the factors that have shaped your perspectives. Seriously consider points-of-view that differ from your current thinking.
8. **Acknowledge and Apologize for Mistakes**: Understand that we are bound to make mistakes in this space, as anyone does when approaching complex tasks or learning new skills. Strive to see your mistakes and others' as valuable elements of the learning process. If you make a mistake, just acknowledge it, apologize for it, and learn from it.
9. **Make Space for Everyone to Speak**: Share responsibility for including all voices in the conversation. If you tend to have a lot to say, make sure you leave sufficient space to hear from others. In this case, consider the "you-then-two" rule: let at least two other people speak after you before you speak again. This prevents any one person from dominating the conversation and gives everybody a chance to be heard and to listen. If you tend to stay quiet in group discussions, challenge yourself to contribute so others can learn from you.

B.1.1.3 Leaving space for discomfort and reflection

It is important to acknowledge that some students and instructors will not be comfortable interrogating inequitable practices, particularly if they think they do not need to, or worse, if they think that doing so will displace their own power and positionality. We need to help those students and instructors to sit in their discomfort, and frame this reflective process as a crucial aspect of their humanity (i.e. what does it mean to be human if you allow others to be dehumanized).

Developing the community guidelines is the first place to start in this process. During a class discussion, don't stop the discussion to move to the next topic simply because the discussion becomes uncomfortable (which we note is different than harmful, as harm needs to be directly addressed). Let the discussion push through the discomfort and come to a conclusion. Additionally, it is important to encourage student reflection. Consider giving students a minute or two to think, and maybe even have them jot down some of their thoughts, before answering a question or participating in a discussion. Another way to encourage reflection is to explicitly ask self-reflection questions on homework assignments. However, instructors may

want to consider grading these only for completion rather than content, and potentially even abstain from reading them should there be potential for students to not be as open if instructors are reading their responses to deeply personal questions.

B.1.1.4 Workshop reflection

How might you approach the idea of creating community guidelines for safe, productive discussion in your class?

B.1.2 Reading: incorporating ARDEI into Class Homework and Examples

B.1.2.1 Reading assignment

Northwestern's Chemical and Biological Engineering Department are not the first or only department tackling these important topics through the use of homework questions. Please read the Hirshfield and Mayes paper titled "Incorporating Inclusivity and Ethical Awareness into Chemical Reaction Engineering" (provided here on Canvas and linked below), published in AIChE's Chemical Engineering Education in Fall 2019, to see some examples of problems for a Kinetics class that addresses similar issues. The article also describes how providing example problems with a variety of contexts that are of interest students as well as those with contexts directly related to real-world problems and social justice can help create inclusive classroom that openly discusses and addresses engineering ethics. Our goal is to take this a step further and explicitly include anti-racism as well as social justice, but this article provides some good introductory context, rationale, and examples for what we are trying to achieve.

B.1.2.2 During and post-reading questions

As you read the paper, please think about the following questions:

- How does incorporating real-world, and specifically ARDEI, topics into course content and example problems contribute to an inclusive teaching environment?
- What is the potential impact of incorporating real-world, and specifically ARDEI, topics into course content and example problems on student engineering ethics?

- With what frequency do you think you need to implement these problems within a course to see the impact on students and course climate?
- Did this paper give you any ideas for ARDEI topics you could use as the context for your own course problems?

B.1.2.3 References

Hirshfield, L. J., & Mayes, H. B. (Fall 2019). Incorporating Inclusivity and Ethical Awareness into Chemical Reaction Engineering. Chemical Engineering Education, 53(4), 215-219.

B.1.3 Example problem from separations

B.1.3.1 Introduction

Here we will highlight example ARDEI questions we have written, some of which were written from scratch and some of which were adapted from context-less textbook problems, to give you some inspiration and example for how you can incorporate ARDEI contexts into your own course. Below is a video explanation of Lauren Simitz walking through the Separations ARDEI problem she wrote (**Supplementary Document B.2.1.3**). Further down we linked additional ARDEI example problems written for Fluids (by Ayinoluwa Abegunde) and Kinetics (by Alex Prybutok). If you choose to use these problems in future courses directly, please cite those who created the problem. But most importantly we encourage you to go through the process of writing problems for yourself as not only will you learn something in the process about the ARDEI topic the problem is contextualized in, but you will gain practice and become more comfortable with this over time.

Additionally, it is important to note the difference in type of problem you might write for a lower vs upper-level course. Students will build skills in analyzing these types of questions over time if all courses incorporate them. So students in lower division courses might be provided and asked to use resources, but students may be asked to find these resources in upper division courses. However, students at all level should be asked to engage with and reflect on this material.

B.1.3.2 Other example problems

B.1.3.2.1 Example kinetics problem

This problem (**Supplementary Document B.2.1.2**) focuses on how SIR (susceptible, infected, recovered) ordinary differential equation models are used to understand the spread of disease. The problem walks through the kinetic equations describing the basic SIR model, and subsequently asks students to interrogate how population dynamics change as a function of changing transmission and recovery rates. Finally, to incorporate the ARDEI component, students are asked to think about these models in the context of the COVID-19 pandemic, where disease spread and treatment were not equitably distributed among populations, and factors such as socioeconomic status, race, environmental conditions, access to health care, and underlying health conditions caused differences in disease dynamics, often most negatively impacting marginalized groups.

B.1.3.2.2 Example fluid dynamics problem

This problem (**Supplementary Document B.2.1.1**) focuses on how simple fluid dynamics concepts can be used to estimate the speed of a river current. The question is modified to incorporate ARDEI concepts by asking students to estimate the speed of the current of a contaminated river, specifically in Navajo rivers facilitated by uranium mining on Navajo Nation and Lakota Nation lands. Then, students are asked to think about the negative effects of Uranium mining on the Navajo community as well as what safeguards could have been implemented to prevent such impact on communities. This should help students think beyond the financial benefit of chemical engineering projects and consider the social impact of their decisions.

B.1.3.3 Assessing your ARDEI-focused problem

Additionally, you will find a ARDEI Post-Question Review Sheet (**Supplementary Document B.2.2.1**) with questions to ask yourself about the problem you've written as a filtering mechanism to prevent harm. Below, is a video walk through of the review sheet. Additionally, we have an example worksheet that has been filled out for the separations example problem you saw before (**Supplementary Document B.2.2.2**). You

will eventually also be using this same worksheet to assess problems written by your fellow colleagues during the in-person workshop.

B.1.4 Understanding and preventing harm

B.1.4.1 Introduction

The purpose of this section is to introduce the concept of positionality, bias, and harm, specifically how we can prevent harm upfront and address it should it occur. Please watch the video and read the information below for a more detailed description.

B.1.4.2 Understanding positionality and bias

Understanding your positionality and unconscious bias is important when discussing ARDEI topics, as these influence your perspective, personal experiences, and actions. It is important to learn to be empathetic to the experiences of those with differing identity regardless of your own. The first step to this is to reflect on your identities and how these identities have impacted your own experiences and perspectives. You might consider participating in the Social Identity Wheel activity yourself (linked) to undergo this reflection process.

It is also important to understand the power dynamics between faculty, TAs, and students and how that can make TAs and students hesitant to speak up if they witness or experience inequity, microaggressions, harassment, or even harm. It may benefit instructors to address this directly in class and invite students and TAs to speak up should any harm occur.

B.1.4.3 Understanding and preventing harm

While we want to address ARDEI topics in course, we want to ensure we do so in such a way that does not cause harm to students, TAs, instructors, or others. The first step to preventing harm is understanding the types of harm that can be caused. Dr. Susanna Calkins at the Searle Center explains that there are two types of harm:

- Some students in the classroom may hold marginalized identities and/or for some of whom these type of problems/discussions/cases studies may not be just an academic exercise—this may be a part of their lived experience, identities or backgrounds. These exercises may be triggering.
- There is significant harm caused when oppressive systems and systemic inequities are not interrogated and explored, but are allowed to remain in place, sustaining systematic oppressive thinking and activities. This larger harm can happen when assumptions and biases are allowed to remain unchecked, and in place.

Ideally, we are addressing the second type of harm by going through this exercise, writing these homework problems, and discussing these topics in the classroom. Those discussions must still be done with care, which the community guidelines ideally facilitate.

By asking instructors to first understand their positionality and bias before writing problems, rely on resources and research to write the problems, and asking a series of questions about the problem afterward, we are ideally addressing the first type of harm. Please take care when writing your problems to consider which community's voice and position is being uplifted and what information is strictly necessary to explain the problem without digging up excessive trauma. Consider running your example problem by a colleague or a few colleagues; other pairs of eyes may help catch potential harm before it happens. You can use the checklist we developed for the purpose of this workshop (which you will be expected to complete for your own problem, and complete when reviewing others' problems during the course of the workshop) for all future problems you develop!

Harm may still occur despite best attempts. If it happens, be honest with students that, like them, you continue to learn. Apologize and seek to understand how this harm arose, and consequently how to avoid such harm in the future. As you may not be aware you instigated harm when it happens, we encourage faculty to create an environment where students feel comfortable bringing forward harm if felt so an open-minded discussion can be had.

B.1.5 Inclusive teaching

B.1.5.1 Introduction

The purpose of this section is to learn about the definition and importance of inclusive teaching. We will discuss each of these, as well as some example practices, in the video and literature readings below.

B.1.5.2 Inclusive teaching: definition, scholarship, and practices

As stated before, inclusive teaching broadly involves teaching in such a way that all students are able to succeed and learn; this is often accomplished by including active learning, diverse ways of communicating and assessing information, and connecting course content to student interests and world experiences. By adapting questions that address inequities and force developing engineers to tackle these challenges while considering affected communities, we are taking steps towards this goal (Hirshfield, 2019).

We must also acknowledge that teaching is not neutral (hooks, 1994). The knowledge and work that is taught today is a function of whose voices and experiments were and are valued in the past. We must work to elevate the science and contributions of marginalized voices and communities. This can be done in course discussion or homework assignments. This practice can help work towards an inclusive classroom.

Other strategies for developing inclusive classes involve stating class/assignment expectations explicitly, establishing a welcoming space, humanizing yourself and asking students to do the same, promoting thoughtful participation, and embracing an asset-based approach such that all students are viewed as bringing strengths to the table (Johnson, 2019). We have uploaded a variety of materials on Canvas that discuss strategies for fostering inclusive classrooms. We hope you will look into them and implement these strategies in your courses.

B.1.5.3 Reading and activity

If you have the time, please look into the readings referenced above (linked below) and answer the following questions:

- What are the benefits of inclusive teaching on student learning and success?

- Are you already implementing some inclusive teaching practices into your courses? If so, which and why those? If not, why not?
- What are three specific inclusive teaching practices you haven't yet but could implement the next time you teach a course and why is each example you choose useful/how does it promote inclusive teaching?

B.1.5.4 References

Hirshfield, L. J., & Mayes, H. B. (Fall 2019). Incorporating Inclusivity and Ethical Awareness into Chemical Reaction Engineering. Chemical Engineering Education, 53(4), 215-219.

The goal of this article was to provide concrete examples of In Class Problems (ICPs) to be used in the undergraduate chemical engineering Chemical Reaction Engineering course that incorporated engineering ethics, such as social and environmental considerations, and/or real-world applications to provide students with contexts for the material they learn in class. Incorporating diverse topics, especially those related to showing how chemical engineering can be used to solve issues of equity and human healthy and safety, helps increase student participation via active learning as well as inclusivity by instilling the importance of considering ethics and helping marginalized communities, which may be of direct relevance/interest to some in the course.

hooks, b. (1994). Chapter 3: Embracing Change: Teaching in a Multicultural World. In Teaching to Transgress: Education as the Practice of Freedom (pp. 35-44). New York: Routlege.

In this chapter, hooks (her name is intentionally lowercase) discusses how education is inherently not neutral, and how we must work to embrace students of all backgrounds and discusses the challenges of multicultural education.

Johnson, K. M. S. (2019). Implementing inclusive practices in an active learning STEM classroom. Adv Physiol Educ, 43(2), 207-210. doi:10.1152/advan.00045.2019

This article lays out recommendations for instructors to make their classes more inclusive and asks the reader to reflect on their practices and perspectives through writing prompts. Some of the

inclusive practices suggested in this article include stating expectations clearly, establishing a welcome space, humanizing yourself and asking students to do the same, embracing an asset-based approach, and promoting thoughtful participation.

B.1.5.5 Additional reading and resources on inclusive teaching

Chavez, A. F., & Longerbeam, S. D. (2016). Chapter 5: Strengths-Based Teaching in Cultural Context. In Teaching Across Cultural Strengths: A Guide to Balancing Integrated and Individuated Cultural Frameworks in College Teaching (1st ed.). Serling, VA: Sylus Publishing

In this chapter, Chavez and Longerbeam discuss how student cultural backgrounds, learning processes, and personalities influence their experience in the classroom. Thus, they stress the importance of developing a course that spans many cultural frameworks, such as having both individual and collective activities, theory and examples, problem solving and critical thinking, silent reflection and classroom discussion, and mixed modes of taking in information such as lectures, case studies, imagery, and others. Designing courses in this way and adopting associated teaching pedagogies ensures that all students can benefit and learn in the classroom.

Killpack, T. L., & Melon, L. C. (Fall 2016). Toward Inclusive STEM Classrooms: What Personal Role Do Faculty Play? CBE Life Sci Educ, 15(es3), 1-9. doi:10.1187/cbe.16-01-0020

Taken from the abstract: "In this essay, we present a set of social science concepts that we can extend to our STEM courses to inform our efforts at inclusive excellence. We have recommended strategies for meaningful reflection and professional development with respect to diversity and inclusion, and aim to empower faculty to be change agents in their classrooms as a means to broadening participation in STEM fields."

Inclusive Teaching at Northwestern

This link provides information on the Northwestern Principles of Inclusive Teaching as well as information on the Inclusive Teaching Practicum.

Information about the Northwestern Principles of Inclusive Teaching is linked below.

> Published in summer 2021, Northwestern Principles of Inclusive Teaching represents the University's ongoing commitment to excellence and equity in teaching its students. The resource provides broad strategies that instructors can use to implement the eight key principles in their course preparation and teaching, and examples of how each principle can be applied in class. It also includes references to scholarly publications, a glossary and a list of helpful University resources.

This resource was developed for Northwestern instructors by partners in the Searle Center for Advancing Learning and Teaching, the Office of Institutional Diversity and Inclusion, the Office of Equity and the Office of the Provost.

View the Principles.

B.1.6 Additional resources

B.1.6.1 Additional resources

Here we link a series of additional resources on topics related to incorporating ARDEI and social justice into your courses. Some of these resources involve on campus resources (such as exhibits at the Block Museum, ChBE ARDEI website, Searle NU Resources handout) or other education resources. Some of these resources pertain to where you could find content or inspiration for future ARDEI questions, where you could find resources to support students or groups your students might be interested (and feel free to advertise these groups and their work in your course, especially if you use their content for your questions or reach out to them to collaborate with them on this content), and where you can find other ways to implement anti-racism in your course. We encourage that if you collaborate with student groups on campus, you cite them and their work in your course! But these groups could be good sources of information and generally good work being done on campus in the area of ARDEI, social justice, advocacy, and supporting students.

B.1.6.2 ChBE department and NU resources

The Use of Visual Art in Teaching Engineering

This document (**Supplementary Document B.2.3.1**) that Ayinoluwa compiled discusses how to use visual art to further communicate the gravity or impact of a situation or context. There is information on related Block Museum exhibits and collections by the artist exhibited. Specifically, the example shown could be directly linked to the Fluid Dynamics example question.

ChBE Anti-Racism, Diversity, Equity, and Inclusion Committee Website

This website also includes a list of information on student groups, including those doing social justice and advocacy work, who could be good sources of information or who might be of interest to students in your class.

NU Resources for Supporting Students Handout

Searle compiled a list of on campus resources for supporting students. Resources fall in the category of the following:

- General University Resources
- Academic Support Resources
- Pedagogical Support
- Support and Resources for Under-Represented Minority (URM) Students
- Wellness Resources
- Financial & Material Resources
- Resources for Student Organizations & Participants in Student Orgs

B.1.6.3 General STEM education resources

Social Justice Content in Math Courses

Kettering University in Michigan is creating new math courses combining math with writing exploring topics of racial justice, climate change, elections and voting, and human trafficking.

Toward an Anti-Racist Engineering Classroom for 2020 and Beyond: A Starter Kit

This *Advances in Engineering Education* article lists 20 action items to implement in your classroom and within your role as a faculty in the areas of culture, pedagogy, curriculum, and personnel to practice anti-racism. The link above links to the cite. The pdf of the article itself can be found on the webpage linked, but can also be found directly here.

Imagining the Future of Undergraduate STEM Education Symposium Summary and Materials

The National Academies Conference was held in November 2020. A summary of their conference, pulled from this site, and two papers they produced, are copied below. They also link video playlists from the conference on the site linked above. We directly linked the PDFs to the two papers below.

With sponsorship from the National Science Foundation, the National Academies of Sciences, Engineering, and Medicine is exploring ambitions for the future of undergraduate STEM education, including how we can transform undergraduate STEM education to meet the needs of students, science, and society.

The symposium brought together innovators from a diverse range of colleges and universities together with policy makers, funders, and representatives from associations and industry. Participants were able to share their own ideas about the future of undergraduate STEM education. You can read some of the stories they wrote about 2040 in the attachments below. Two commissioned papers prepared in advance of the symposium are also available here.

- *Transformation in the U.S. Higher Education System: Implications for Racial Equity* by Lindsey Malcom-Piqueux

- *Current Innovations in STEM Education and Equity Needs for the Future* by Sanjay Sarma and Aikaterini Bagiati

A proceedings of the symposium will be published in 2021 and will be available for free download from National Academies Press.

B.2 Supplementary Workshop Documents

B.2.1 Example ARDEI-context questions

B.2.1.1 Example fluid dynamics question

This question was a textbook problem adapted by Ayinoluwa Abegunde.

B.2.1.1.1 Original textbook problem

A 0.30m diameter cork ball (SG=0.21) is tied to an object on the bottom of a river as shown below. Estimate the speed of the river current. Neglect the weight of the cable, and the drag on it.

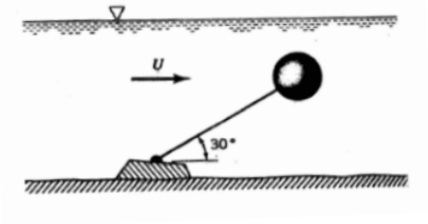

Source: Fundamentals of Fluid Mechanics, 7th edition. Munson, Okiishi, Huebsch & Rothmayer Wiley, 2013 (Used in problem for Week 5 Discussion Section – Fluid Dynamics Fall 2020).

B.2.1.1.2 Modified problem containing ARDEI-context

Uranium mining under the U.S military's Manhattan Project began on Navajo Nation and Lakota Nation lands. A few years late, widespread uranium mining began on Navajo and Lakota lands in a nuclear arms race with the Soviet Union during the Cold War, with little to no environmental regulation. The mining

endangered thousands of Navajo workers, as well as producing contamination that has persisted in adversely affecting air and water quality, and contamination Navajo lands.

If one wanted to measure the level of contamination in Navajo rivers, an experiment could be conducted. A 0.50m diameter cork ball (Density = 210 kg/m^3), is tied to an object on the bottom of the Puerco River as shown below. The dimensions of the river can be approximated to be 50m X 25m X 3m and an estimated average minimum of 20 µg/L of uranium was found in the river. Estimate the speed of the river current. Neglect the weight of the cable, and the drag on it.

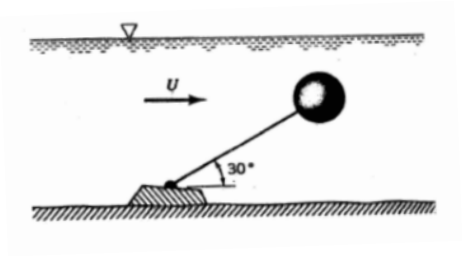

a. Estimate the speed of the river current.
b. The average speed of rivers in New Mexico before uranium mining began was 6 m/s. Compare this value to that which you calculated in part a. What might have caused this change? [Hint: Church Rock Uranium Mill Spill]
c. Uranium not only contaminated the water bodies but also affected the health of uranium miners which included members of the Navajo community. Studies were conducted to evaluate the health conditions of uranium miners. What are the adverse health effects that were found among them?
d. As chemical engineers, the irreparable damage caused by uranium mining and government negligence teaches us how our decisions can have significantly negative effects on different communities. Consider what safeguards could have been put in place to avoid what occurred in this case.

CITATIONS

1. https://www.who.int/water_sanitation_health/dwq/chemicals/uranium290605.pdf

2. https://www.npr.org/sections/health-shots/2016/04/10/473547227/for-the-navajo-nation-uranium-minings-deadly-legacy-lingers
3. https://en.wikipedia.org/wiki/Uranium_mining_and_the_Navajo_people
4. https://www.epa.gov/navajo-nation-uranium-cleanup/abandoned-mines-cleanup

B.2.1.2 Example kinetics question

This is an original homework question written by Alexis Prybutok.

QUESTION. Modeling disease spread over time.

The concepts of kinetics can be used in many fields, often modeling, including epidemiology. A common model, called the S-I-R model, is used to model the spread of disease.[1] This simplified model tracks three disease states, as if they were species—susceptible (S), infectious (I), and removed (R). The most common forms of these models state the following:

- Transmission of disease, and thus transition from a susceptible (S) to an infectious state (I), happens when those who are susceptible come into contact with those who are infectious. Thus, the rate of transition from a susceptible state to an infectious state is proportional to the product of the number of people in each state and a transmission rate constant (β).
- The rate at which infectious (I) individuals transition into the removed state (R) is dependent on how long the disease state lasts and is equal to the recovery rate constant (γ) times the number of infected individuals.
- The ratio of the transition rates characterizes the overall spread of the disease.

When converted into equations, these take the following forms:

$$\frac{dS}{dt} = -\beta\frac{SI}{N} \qquad \frac{dI}{dt} = \beta\frac{SI}{N} - \gamma I \qquad \frac{dR}{dt} = \gamma I$$

Where N is the total number of individuals. The ratio that characterizes the disease spread is equal to:

$$G = \frac{\beta}{\gamma}$$

When G = 0 the disease does not spread. When G < 1, on average one infected person infects less than one susceptible person and the disease is in decline. When G = 1, on average one infected person infects one susceptible person and the disease is stable. When G > 1, on average one infected person infects more than one susceptible person and the disease is spreading.

Models like this can be used to analyze the spread of disease and severity pandemics, such COVID-19 crisis we are amidst today. Imagine that we have parameters for the transition rates for COVID, starting with one infected person in a population of 100,000 total:

$\beta = 5$

$\gamma = 0.2$ (corresponds to an infection period of 5 days)

$S_0 = 99{,}999$

$I_0 = 1$

$R_0 = 0$

a. If S, I, and R are each in units of number of people, what are the units on β and γ?
b. Prove using the symbols and equations provided that the total number of people N is not changing over time.
c. Plot S, I, and R with the parameters given.
d. Apply a treatment to the base case model in part c—this will effectively increase γ to 0.5 such that individuals recover in 2 days instead of 5. Plot S, I, and R. Describe some differences between these plots and those in part c.
e. Apply a preventative measure, such as social distancing and masking, to the base case model in part c—this will effectively lower β to 1 such that individuals are infected at a slower rate. Plot S, I, and R. Describe some differences between these plots and those in part c.

f. Apply both the measures in parts d and e to the base case model. Plot S, I, and R. Describe some differences between these plots and those in part c.

g. If you were to apply both the measures in parts d and e, how would the disease spread G change compared to the base case model in part c?

h. If you were to treat individuals with a vaccination, how might this affect parameters β and/or γ? Please explain your reasoning.

i. Note, this model goes straight from susceptible individuals to actively infected individuals, but skips over those who are carriers of the latent virus prior to infection. How would you incorporate those individuals into the model?

j. The model also assumes that once you are recovered, you are no longer susceptible and cannot get re-infected. How would the model change if you could become re-infected?

k. In world-wide pandemics, such as the COVID-19 pandemic, systemic inequities related to access to healthcare, occupation, discrimination, environmental conditions, housing, and educational, income, and wealth gaps can cause dramatic downstream impacts on disease spread and ultimately human health and survival.[2] Even pre-existing conditions can be related to external inequities such as environmental injustice. These factors can also make access to interventions, such as vaccines, highly inequitable. During the global COVID-19 pandemic, marginalized groups, such as racial and ethnic minorities, faced increased risk of COVID-related disease contraction, hospitalization, and death as a result of the compounded systemic inequalities listed above. When developing disease interventions, preventions, and treatments, it is important to consider those most vulnerable in a population. The rate at which marginalized communities contracted COVID differed from that of more privileged groups. Thus, understanding spread and treatment in a community might not be as simple as modeling disease spread in a single population that assumes all individuals are equally susceptible. Please write out how you might approach modeling multiple but interacting populations that contract the disease at different rates and may also not have equal access to treatment and thus recovery. Please also list what factors you might need to consider when modeling these multiple populations. You do not need to write out or solve equations, just

describe a potential approach and important factors. You may look up examples in literature and reference their approach, citing sources you find.

CITATIONS

a. https://en.wikipedia.org/wiki/Compartmental_models_in_epidemiology#The_SIR_model
b. https://www.cdc.gov/coronavirus/2019-ncov/community/health-equity/race-ethnicity.html
c. https://towardsdatascience.com/extending-the-basic-sir-model-b6b32b833d76

B.2.1.3 Example phase equilibrium and separations question

This question was a textbook problem adapted by Lauren Simitz.

B.2.1.3.1 Original textbook problem

You are creating a process to remove hydrogen sulfide (H_2S) from a feed gas. To safely remove the H_2S, you will absorb it into water at 15 degrees C. The water entering for absorption is pure (e.g. mole fraction H_2O = 1) and is at a flow rate of 2,000 kmol/hr. The feed gas being cleaned initially contains 0.12 mol% H_2S and has a flow rate of 10.0 kmol/hr. You can assume both the gas and liquid flow rates remain constant throughout absorption. The total pressure is 2.5 atm. Your goal is to recover 97% of the H_2S in the water.

a. Calculate the outlet gas and liquid mole fractions of H_2S.
b. Calculate the number of equilibrium stages needed using a McCabe Thiele Diagram.

Source: Wankat 12.D2

B.2.1.3.2 Modified problem containing ARDEI-context

QUESTION. Hydrogen Sulfide (H2S) Separation

Parts a and b are modified from Wankat 12.D2. with additional context on H_2S.

You are creating a process to remove hydrogen sulfide (H_2S) from a feed gas. H_2S is a gas commonly found during the drilling and production of crude oil and natural gas, as well as in wastewater treatment and utility facilities and sewers [1].

Not only is H_2S considered a pollutant, lowering the value of the product stream, but is hazardous to human health; it is classified by OSHA as both "an irritant and chemical asphyxiant with effects on both oxygen utilization and the central nervous system" [1]. Dosages above 100 ppm can kill a person within a few breaths [1]. For these reasons, the Bureau of Labor Statistics (BLS) cites it as the leading cause of workplace gas inhalation deaths in the United States [2].

To safely remove the H_2S, you will absorb it into water at 15 degrees C. The water entering for absorption is pure (e.g. mole fraction H_2O = 1) and is at a flow rate of 2,000 kmol/hr. The feed gas being cleaned initially contains 0.12 mol% H_2S and has a flow rate of 10.0 kmol/hr. You can assume both the gas and liquid flow rates remain constant throughout absorption. The total pressure is 2.5 atm. Your goal is to recover 97% of the H_2S in the water.

c. Calculate the outlet gas and liquid mole fractions of H_2S.
d. Calculate the number of equilibrium stages needed using a McCabe Thiele Diagram.

Parts c, d, and e will require you to research using outside sources and explore demographic data on Social Explorer. You can access content on Social Explorer by creating a free (e.g. Northwestern-sponsored account) using your Northwestern email.

e. Based on the mole fraction of H2S now in the feed gas, if this stream leaked into the environment, would you be in violation of the Clean Air Act? What limits, if any, exist for H_2S release into ambient air? This review paper, specifically "H_2S Regulation in the US" may be helpful [3].
f. Read about what has been happening regarding hydrogen sulfide exposure in Mon Valley, PA. Briefly describe (one paragraph of 3-5 sentences) what you learned. Consider including:
    i. What is happening with hydrogen sulfide there?
    ii. Where is the H2S coming from?
    iii. What steps have been taken so far in response?
g. Now that you know the context for Mon Valley, let's look more specifically at the demographics of the area. To do this, we will use an interactive mapping software linked to census data called Social

Explorer. Once logged in to your free account, click “Explore” under the United States map. In the search bar at the top, type in “Clairton, PA” to put you inside the Mon Valley area.

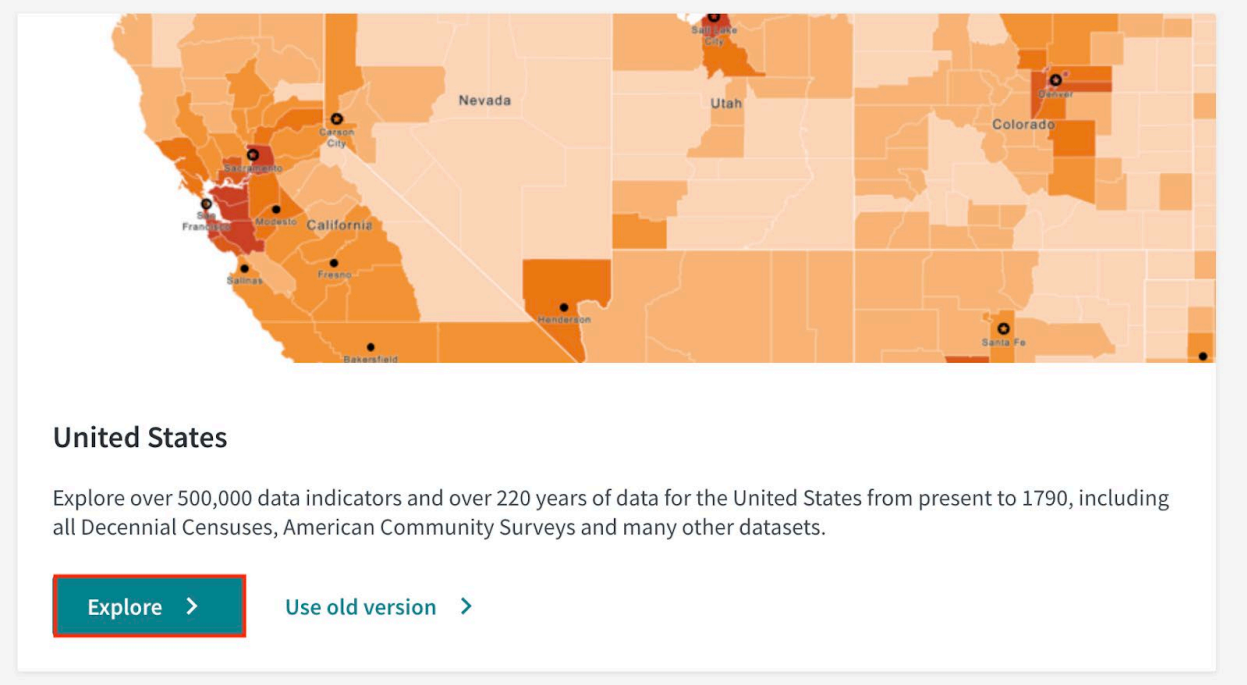

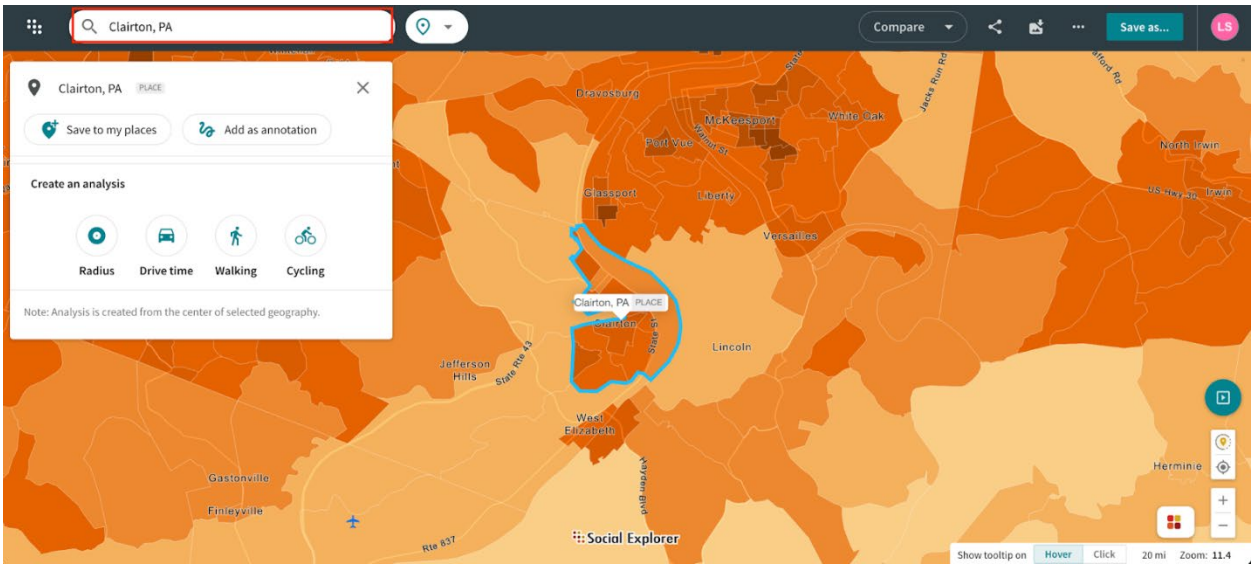

Rather than look at population density (the default), we want to change the data to look at race and income. Note that there are dozens of other datasets, and by no means are race and income comprehensive

demographics of an area with complex communities and identities present. For the sake of our analysis, these areas will provide additional insight.

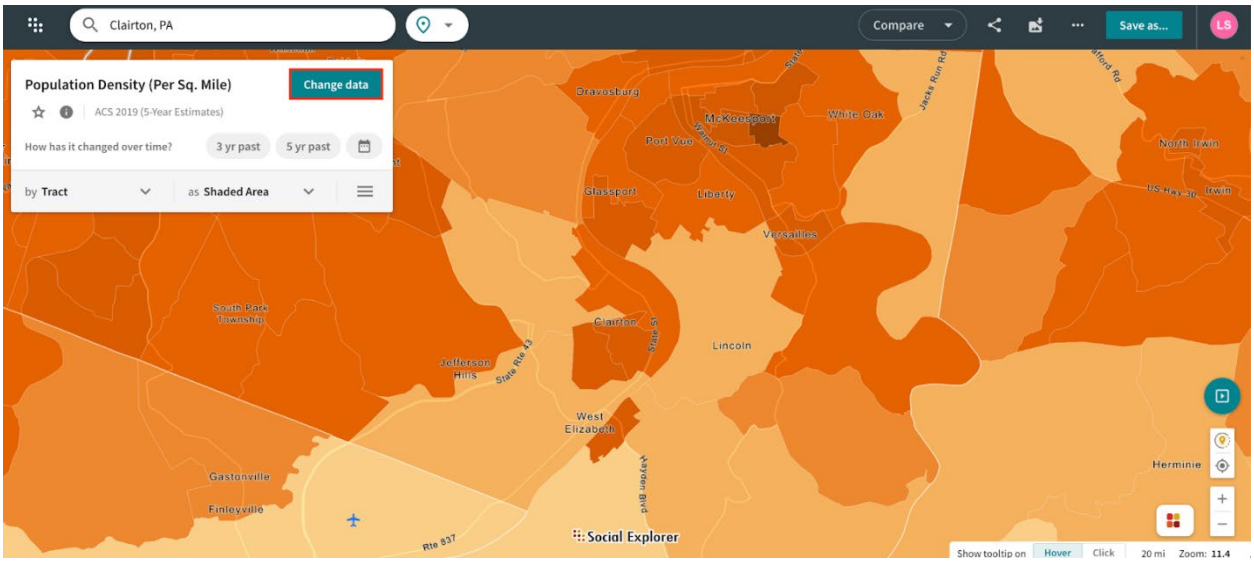

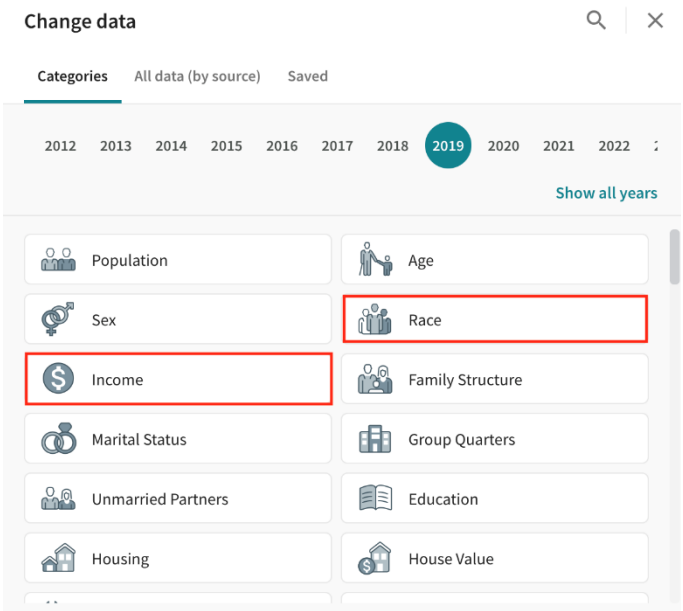

Explore Mon Valley using the Race and Income data for 2019. Compare the racial and economic status of Clairton, PA (Allegheny County, Census Tract 4927, 4928, 4929) where the US Steel Mill is versus West Mifflin, PA (Allegheny County, Census Tract 3102, 4883, 4885) upwind. What may this indicate about the relationship between chemical plants, pollution, and marginalized communities more broadly?

h. What process may you recommend to a company that is producing H_2S that is over the threshold, rather than emitting or burning it? (Hint: What process produces the most elemental sulfur?)

CITATIONS

1. *Hydrogen Sulfide - Overview. Occupational Safety and Health Administration* (OSHA). (n.d.). https://www.osha.gov/hydrogen-sulfide.
2. U.S. Bureau of Labor Statistics. (2020, December 22). *Census of Fatal Occupational Injuries (CFOI) - Current and Revised Data*. U.S. Bureau of Labor Statistics. https://www.bls.gov/iif/oshcfoi1.htm.
3. Malone Rubright, S. L., Pearce, L. L., & Peterson, J. (2017). Environmental Toxicology of Hydrogen Sulfide. *Nitric Oxide: Biology and Chemistry*, 71, 1–13. https://doi.org/10.1016/j.niox.2017.09.011.
4. Group Against Smog and Pollution. (2021, April 21). *Another Weekend, Another H2S Air Quality Exceedance for Mon Valley*. pgh.org. https://gasp-pgh.org/2021/04/19/another-weekend-another-h2s-air-quality-exceedance-for-mon-valley/?utm_source=rss&utm_medium=rss&utm_campaign=another-weekend-another-h2s-air-quality-exceedance-for-mon-valley.
5. Pennsylvania Income Eligibility. *PA Department of Community & Economic Development*. (2021, February 23). https://dced.pa.gov/housing-and-development/weatherization/income-eligibility/.
6. Department of Energy (DOE). (n.d.). *The Claus Process*. netl.doe.gov. https://netl.doe.gov/research/coal/energy-systems/gasification/gasifipedia/claus-process.

B.2.2 ARDEI-question post-question review list

B.2.2.1 Template review list

GENERAL TOPIC/CONTENT

1. What is the technical content of the question?
2. What is the ARDEI content of the question?
3. What are students being asked to do?

4. Are the students being asked to do something related to the ARDEI content, or is the ARDEI content simply providing context/background but not related to answering the question?

RESOURCES

1. What technical resources is this question based on?
    a. Are those resources cited?
    b. Do students have easy and free access to those resources if needed?
2. What ARDEI resources is this question based on?
    a. What did you need to learn about or find to create this question?
    b. Where did you find those resources/what or who created that content?
        i. Are the resources from those are affected by the issue being described?
        ii. Or are the resources from those who study and publish on the issue being described?
    c. Are those resources cited?
    d. Do students have easy and free access to those resources if they were curious, wanted more information, or if needed for the question?
3. What technical resources do students need to answer the question?
    a. Are those resources explicitly stated or do students need to find them themselves?
    b. Do students have easy and free access to those resources?
4. What ARDEI resources do students need to answer the question?
    a. Are those resources explicitly stated or do students need to find them themselves?
    b. Do students have easy and free access to those resources?

ARDEI POSITIONALITY AND PREVENTING HARM

1. Whose (as in what community's) position is being explained/uplifted?
2. How does your identity relate to those of the community in question?
3. What is the potential of this question to cause harm to students reading it?

4. What is the potential of this question to cause harm to students (to themselves, instructor, or other students) through answering it?
5. What is the purpose of the question/discussion/exercise?
6. Are you confirming (or pushing back against) stereotypical attitudes and beliefs?
7. Are there places for students to confront their own assumptions and biases prior to working with others?
8. Does the choice of problem/exercise and related reading materials and resources uphold, affirm, sustain (or reject) systemic inequities?
9. Does the choice of technology for solving/working on the exercise uphold, affirm, sustain (or reject) systemic inequities?
10. Does the assessment of the work uphold, affirm, sustain (or reject) systemic inequities?

B.2.2.2 Example review list completed for example separations question

This example review sheet was completed by Chloé Archuleta. Responses are listed below the question and colored in blue.

GENERAL TOPIC/CONTENT

1. What is the technical content of the question?

   The technical content provided to the student includes information on H_2S, technical OSHA requirements, and mass balance and VLE data.

2. What is the ARDEI content of the question?

   The student will be provided content about the worker hazards, environmental and health impacts, and regulations of H_2S and demographic data for chemical plant locations.

3. What are students being asked to do?

   The student will perform separations calculations and analyze how the relationship between chemical plant locations and demographics disproportionately affects surrounding marginalized communities.

4. Are the students being asked to do something related to the ARDEI content, or is the ARDEI content simply providing context/background but not related to answering the question?

   The student is explicitly being asked to analyze the relationship between their solved technical data (H_2S removal) to current demographic data.

RESOURCES

1. What technical resources is this question based on?

   This problem is modified from Wankat 12.D2., with references from OSHA and Bureau of Labor Statistic

   a. Are those resources cited?

      Yes

   b. Do students have easy and free access to those resources if needed?

      Yes – this is a required textbook and copies are available in the library, and the other links are free

2. What ARDEI resources is this question based on?

   Review on H2S regulation and census data (Social Explorer)

   a. What did you need to learn about or find to create this question?

      Required a review article, news article, census data, and chemical plant locations

   b. Where did you find those resources/what or who created that content?

      Websites and journal articles based on national and local data

      i. Are the resources from those are affected by the issue being described?

         Yes – the review article and Social Explorer link are included, and instructions to use the census data tool

      ii. Or are the resources from those who study and publish on the issue being described?

   c. Are those resources cited?

      Yes

   d. Do students have easy and free access to those resources if they were curious, wanted more information, or if needed for the question?

      Yes

3. What technical resources do students need to answer the question?

   Students require mass balance equations, vapor-liquid equilibrium data and regulation statistics.

   a. Are those resources explicitly stated or do students need to find them themselves?

      The McCabe-Thiele Diagram is provided, equations will be found in the textbook or class notes, and relevant statistics are given.

   b. Do students have easy and free access to those resources?

      Yes, the resources are given and the links are free

4. What ARDEI resources do students need to answer the question?

   Review article and Social Explorer

   a. Are those resources explicitly stated or do students need to find them themselves?

      Yes, the review article and census data are linked

   b. Do students have easy and free access to those resources?

      Yes, Northwestern provides access to both resources

ARDEI POSITIONALITY AND PREVENTING HARM

1. Whose (as in what community's) position is being explained/uplifted?

   Marginalized communities affected by chemical plant environmental consequences – specifically for Black, Indigenous, People of Color and LatinX.

2. How does your identity relate to those of the community in quesion?

   As a personal exercise, it is important understand your positionality and bias when writing these problems and what systemic inequities you may be reinforcing as a result. If your background is not that of the POC affected by the issue, this is a good opportunity when with the class to acknowledge your positionality and explain that these problems are an effort to encourage ARDEI discussion in context of their work, as you are with your own.

3. What is the potential of this question to cause harm to students reading it?

Aspects of this problem (locations, consequences) may be triggering for a student based on individual experiences, so this problem provides only information that is strictly necessary to explain the problem. The problem does not include information related to violent or personal experiences that may become triggering.

4. What is the potential of this question to cause harm to students (to themselves, instructor, or other students) through answering it?

   Students are mostly asked specific questions about technical data and processes not likely to cause harm, however, the context of part (e) can be a potential source of harm to the student answering. For example, answering this problem could be a reminder for a family member who has had negative health consequences as a result of chemical plant emission violations and may find the exercise triggering. While you cannot predict your students' personal experiences, you can encourage an understanding culture for students that may have difficulty completing this problem, such as with a rubric adapted for these potential situations.

   Additionally, this question could also prompt discussion that leads to harm of a student studying with peers. In this situation, an open communication line can be helpful to address these situations confidentially in a safe environment for the student.

   The open-ended nature of part (e) can also be an opportunity of harm to the instructors and TAs grading the work. For example, a student may perpetuate stereotypes of community members living near chemical plants. Should this situation arise in a written assignment such as this, you should check with your TAs that may have been harmed as a result of reading the response. It is also recommended to address the situation with the student by going over community guidelines and explaining the potential for harm. To prevent additional harm, instructors and TAs should never share homework grades or answers between students, per FERPA regulations.

5. What is the purpose of the question/discussion/exercise?

   The purpose of this problem is to use chemical engineering fundamentals to solve an environmentally relevant separations problem and to contextualize hazardous wastes with surrounding demographics.

6. Are you confirming (or pushing back against) stereotypical attitudes and beliefs?

This problem pushes back against the stereotypical belief that chemical engineering education must be only technical without understanding the impacts of hazardous waste on the surrounding demographics. This problem as written does not introduce or reinforce any stereotypes about community members of the surrounding chemical plant.

7. Are there places for students to confront their own assumptions and biases prior to working with others?

   This problem does not require any group work, but it is important to be mindful that these discussions may be brought up in peer study groups. Creating a classroom culture following ARDEI community guidelines includes making space for student self-reflection prior to assigning these problems.

8. Does the choice of problem/exercise and related reading materials and resources uphold, affirm, sustain (or reject) systemic inequities?

   The choice of problem and related materials rejects systemic inequities by amplifying experiences from marginalized communities.

9. Does the choice of technology for solving/working on the exercise uphold, affirm, sustain (or reject) systemic inequities?

   The chosen technologies reject systemic inequities through independent correlation between racial and economic demographics and chemical plant geographical locations.

10. Does the assessment of the work uphold, affirm, sustain (or reject) systemic inequities?

    The assessment of the work rejects systemic inequities by accommodating various acceptable answers for open-ended questions.

B.2.3 Additional supplementary documents

B.2.3.1 The use of visual art in teaching engineering

This resource was compiled by Ayinoluwa Abegunde.

The Use of Visual Art in Teaching Chemical Engineering

Visual stimuli can be very impactful in communicating the gravity of the situation. Below are works of Will Willson which could be used in conjunction with the *fluid dynamics example problem.* The first, a drone picture of Church Rock Uranium Mill Spill referred to in this modified problem and the second showing the impact of the toxic environment he inhabits as a Najavo man due to the environmental damage.

The Block Museum at Northwestern is extremely open to collaboration for using art in teaching (see more after images below).

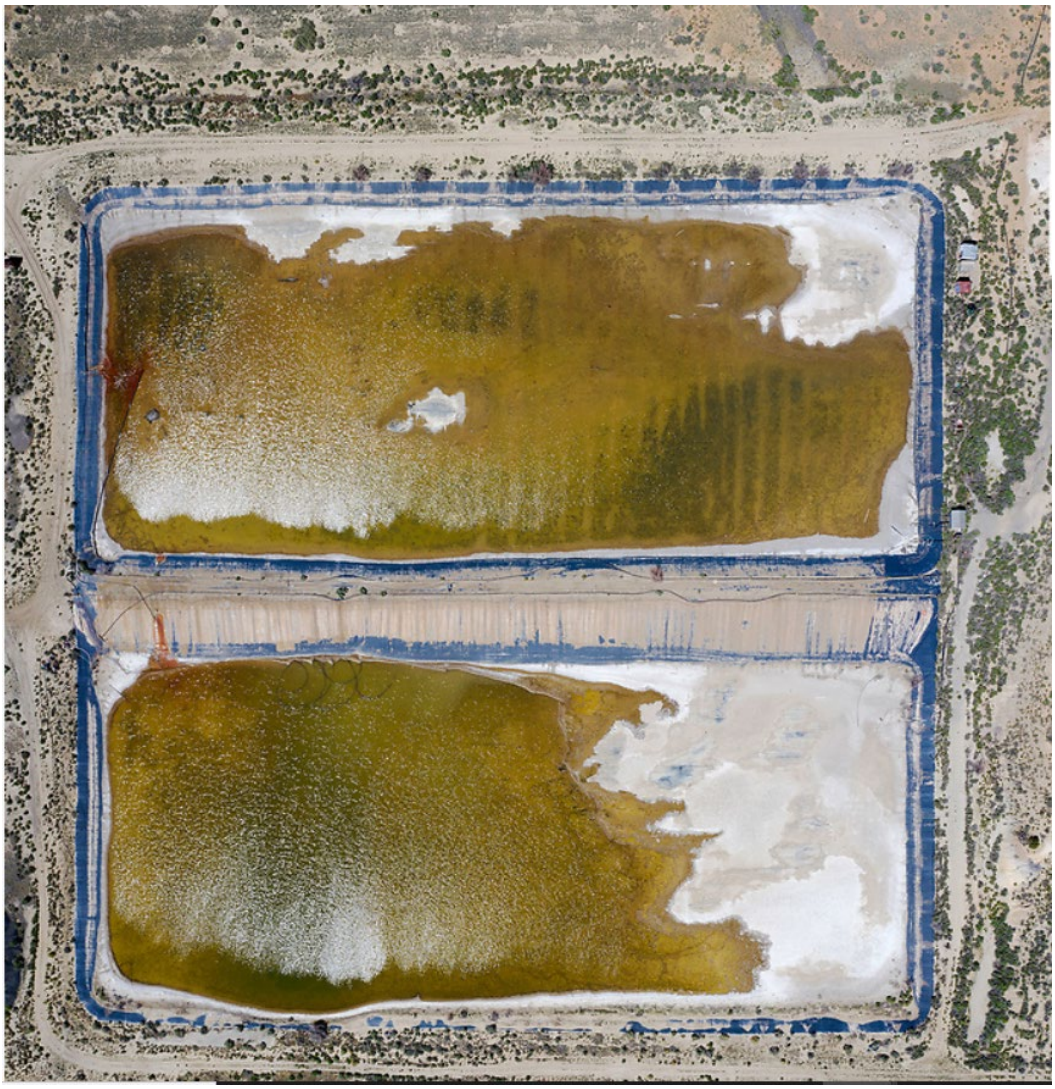

Church Rock Uranium Mill Spill Drone: https://willwilson.photoshelter.com/gallery-image/Connecting-the-Dots/G0000_E93oSBnsNk/I0000zslKJJFRNi0 [Series: Connecting the Dots by Will Wilson]

Will Wilson Auto Immune Response (AIR) series. Wilson describes the series' subject as "the quixotic relationship between a post-apocalyptic Diné (Navajo) man and the devastatingly beautiful, but toxic environment he inhabits."

Browse Wilson's collection:

https://www.extractionart.org/mocna

https://willwilson.photoshelter.com/gallery/Connecting-the-Dots/G0000_E93oSBnsNk

Collaboration with the Block Museum at Northwestern

"The Block supports teaching with visual art across Northwestern campuses. Through our work with exhibitions, collections, and programming we aspire to connect with every department and school at Northwestern and to make The Block meaningful to your work and to your students. Faculty who have worked with The Block come from departments as diverse as Anthropology, Art History, English, and Music, and Schools as diverse as Engineering, Law, and Journalism. Connect with us to develop projects and

exchange ideas on how to incorporate museum experiences into teaching and research. “ - The Block Museum

Link to Block Museum: https://www.blockmuseum.northwestern.edu/teaching-learning/index.html

References

1. Jackson HJ, Rafiq S, Brentjens RJ: **Driving CAR T-cells forward**. *Nat Rev Clin Oncol* 2016, **13**:370-383.

2. Barrett DM, Singh N, Porter DL, Grupp SA, June CH: **Chimeric antigen receptor therapy for cancer**. *Annu Rev Med* 2014, **65**:333-347.

3. Gilham DE, Debets R, Pule M, Hawkins RE, Abken H: **CAR-T cells and solid tumors: tuning T cells to challenge an inveterate foe**. *Trends Mol Med* 2012, **18**:377-384.

4. Lim WA, June CH: **The Principles of Engineering Immune Cells to Treat Cancer**. *Cell* 2017, **168**:724-740.

5. Savoldo B, Ramos CA, Liu E, Mims MP, Keating MJ, Carrum G, Kamble RT, Bollard CM, Gee AP, Mei Z, et al.: **CD28 costimulation improves expansion and persistence of chimeric antigen receptor-modified T cells in lymphoma patients**. *J Clin Invest* 2011, **121**:1822-1826.

6. Finney HM, Lawson AD, Bebbington CR, Weir AN: **Chimeric receptors providing both primary and costimulatory signaling in T cells from a single gene product**. *J Immunol* 1998, **161**:2791-2797.

7. Castellarin M, Watanabe K, June CH, Kloss CC, Posey AD, Jr.: **Driving cars to the clinic for solid tumors**. *Gene Ther* 2018, **25**:165-175.

8. Yanez-Munoz RJ, Grupp SA: **CAR-T in the clinic: drive with care**. *Gene Ther* 2018, **25**:157-161.

9. NCI: **CAR T Cells: Engineering Patients' Immune Cells to Treat Their Cancers**. 2022.

10. Kalos M, Kalos M, Levine BL, Porter DL, Katz S, Grupp SA, Bagg A, June CH: **T Cells with Chimeric Antigen Receptors Have Potent Antitumor Effects and Can Establish Memory in Patients with Advanced Leukemia**. *Sci Transl Med* 2011, **3**:1-11.

11. Rosenbaum L: **Tragedy, Perseverance, and Chance - The Story of CAR-T Therapy**. *N Engl J Med* 2017, **377**:1313-1315.

12. Kakarla S, Gottschalk S: **CAR T cells for solid tumors: armed and ready to go?** *Cancer J* 2014, **20**:151-155.

13. **The Nobel Prize in Physiology or Medicine 2018**. In *The Nobel Prize*. Nobel Media AB; 2018.

14. Galluzzi L, Chan TA, Kroemer G, Wolchok JD, Lopez-Soto A: **The hallmarks of successful anticancer immunotherapy**. *Sci Transl Med* 2018, **10**:1-14.

15. Whiteside TL: **The tumor microenvironment and its role in promoting tumor growth**. *Oncogene* 2008, **27**:5904-5912.

16. Maus MV, June CH: **Making Better Chimeric Antigen Receptors for Adoptive T-cell Therapy**. *Clin Cancer Res* 2016, **22**:1875-1884.

17. Huang Y, Li D, Qin DY, Gou HF, Wei W, Wang YS, Wei YQ, Wang W: **Interleukin-armed chimeric antigen receptor-modified T cells for cancer immunotherapy**. *Gene Ther* 2018, **25**:192-197.

18. Rafiq S, Yeku OO, Jackson HJ, Purdon TJ, van Leeuwen DG, Drakes DJ, Song M, Miele MM, Li Z, Wang P, et al.: **Targeted delivery of a PD-1-blocking scFv by CAR-T cells enhances anti-tumor efficacy in vivo**. *Nat Biotechnol* 2018, **36**:847-856.

19. Liu X, Ranganathan R, Jiang S, Fang C, Sun J, Kim S, Newick K, Lo A, June CH, Zhao Y, et al.: **A Chimeric Switch-Receptor Targeting PD1 Augments the Efficacy of Second-Generation CAR T Cells in Advanced Solid Tumors**. *Cancer Res* 2016, **76**:1578-1590.

20. Cherkassky L, Morello A, Villena-Vargas J, Feng Y, Dimitrov DS, Jones DR, Sadelain M, Adusumilli PS: **Human CAR T cells with cell-intrinsic PD-1 checkpoint blockade resist tumor-mediated inhibition**. *J Clin Invest* 2016, **126**:3130-3144.

21. Bonifant CL, Jackson HJ, Brentjens RJ, Curran KJ: **Toxicity and management in CAR T-cell therapy**. *Mol Ther Oncolytics* 2016, **3**:16011.

22. Caruso HG, Hurton LV, Najjar A, Rushworth D, Ang S, Olivares S, Mi T, Switzer K, Singh H, Huls H, et al.: **Tuning Sensitivity of CAR to EGFR Density Limits Recognition of Normal Tissue While Maintaining Potent Antitumor Activity**. *Cancer Res* 2015, **75**:3505-3518.

23. Johnson LA, Scholler J, Ohkuri T, Kosaka A, Patel PR, McGettigan SE, Nace AK, Dentchev T, Thekkat P, Loew A, et al.: **Rational development and characterization of humanized anti-EGFR variant III chimeric antigen receptor T cells for glioblastoma**. *Sci Transl Med* 2015, **7**:275ra222.

24. Liu X, Jiang S, Fang C, Yang S, Olalere D, Pequignot EC, Cogdill AP, Li N, Ramones M, Granda B, et al.: **Affinity-Tuned ErbB2 or EGFR Chimeric Antigen Receptor T Cells Exhibit an Increased Therapeutic Index against Tumors in Mice**. *Cancer Res* 2015, **75**:3596-3607.

25. Hegde M, Corder A, Chow KK, Mukherjee M, Ashoori A, Kew Y, Zhang YJ, Baskin DS, Merchant FA, Brawley VS, et al.: **Combinational targeting offsets antigen escape and enhances effector functions of adoptively transferred T cells in glioblastoma**. *Mol Ther* 2013, **21**:2087-2101.

26. Hegde M, Mukherjee M, Grada Z, Pignata A, Landi D, Navai SA, Wakefield A, Fousek K, Bielamowicz K, Chow KK, et al.: **Tandem CAR T cells targeting HER2 and IL13Ralpha2 mitigate tumor antigen escape**. *J Clin Invest* 2016, **126**:3036-3052.

27. Cho JH, Collins JJ, Wong WW: **Universal Chimeric Antigen Receptors for Multiplexed and Logical Control of T Cell Responses**. *Cell* 2018, **173**:1426-1438 e1411.

28. Lanitis E, Poussin M, Klattenhoff AW, Song D, Sandaltzopoulos R, June CH, Powell DJ, Jr.: **Chimeric antigen receptor T Cells with dissociated signaling domains exhibit focused antitumor activity with reduced potential for toxicity in vivo**. *Cancer Immunol Res* 2013, **1**:43-53.

29. Wilkie S, van Schalkwyk MC, Hobbs S, Davies DM, van der Stegen SJ, Pereira AC, Burbridge SE, Box C, Eccles SA, Maher J: **Dual targeting of ErbB2 and MUC1 in breast cancer using chimeric antigen receptors engineered to provide complementary signaling**. *J Clin Immunol* 2012, **32**:1059-1070.

30. Wu CY, Roybal KT, Puchner EM, Onuffer J, Lim WA: **Remote control of therapeutic T cells through a small molecule-gated chimeric receptor**. *Science* 2015, **350**:aab4077.

31. Sommermeyer D, Hudecek M, Kosasih PL, Gogishvili T, Maloney DG, Turtle CJ, Riddell SR: **Chimeric antigen receptor-modified T cells derived from defined CD8+ and CD4+ subsets confer superior antitumor reactivity in vivo**. *Leukemia* 2016, **30**:492-500.

32. Turtle CJ, Hanafi LA, Berger C, Gooley TA, Cherian S, Hudecek M, Sommermeyer D, Melville K, Pender B, Budiarto TM, et al.: **CD19 CAR-T cells of defined CD4+:CD8+ composition in adult B cell ALL patients**. *J Clin Invest* 2016, **126**:2123-2138.

33. Guedan S, Posey AD, Jr., Shaw C, Wing A, Da T, Patel PR, McGettigan SE, Casado-Medrano V, Kawalekar OU, Uribe-Herranz M, et al.: **Enhancing CAR T cell persistence through ICOS and 4-1BB costimulation**. *JCI Insight* 2018, **3**.

34. Kawalekar OU, O'Connor RS, Fraietta JA, Guo L, McGettigan SE, Posey AD, Jr., Patel PR, Guedan S, Scholler J, Keith B, et al.: **Distinct Signaling of Coreceptors Regulates Specific Metabolism Pathways and Impacts Memory Development in CAR T Cells**. *Immunity* 2016, **44**:380-390.

35. Zhao Z, Condomines M, van der Stegen SJC, Perna F, Kloss CC, Gunset G, Plotkin J, Sadelain M: **Structural Design of Engineered Costimulation Determines Tumor Rejection Kinetics and Persistence of CAR T Cells**. *Cancer Cell* 2015, **28**:415-428.

36. Mehta MM, Weinberg SE, Chandel NS: **Mitochondrial control of immunity: beyond ATP**. *Nat Rev Immunol* 2017, **17**:608-620.

37. Buck MD, O'Sullivan D, Pearce EL: **T cell metabolism drives immunity**. *J Exp Med* 2015, **212**:1345-1360.

38. Pearce EL: **Metabolism in T cell activation and differentiation**. *Curr Opin Immunol* 2010, **22**:314-320.

39. Gerriets VA, Rathmell JC: **Metabolic pathways in T cell fate and function**. *Trends Immunol* 2012, **33**:168-173.

40. Chang CH, Pearce EL: **Emerging concepts of T cell metabolism as a target of immunotherapy**. *Nat Immunol* 2016, **17**:364-368.

41. Prybutok AN, Cain JY, Leonard JN, Bagheri N: **Fighting fire with fire: deploying complexity in computational modeling to effectively characterize complex biological systems**. *Curr Opin Biotechnol* 2022, **75**:102704.

42. Chavali AK, Gianchandani EP, Tung KS, Lawrence MB, Peirce SM, Papin JA: **Characterizing emergent properties of immunological systems with multi-cellular rule-based computational modeling**. *Trends Immunol* 2008, **29**:589-599.

43. Yu JS, Bagheri N: **Multi-class and multi-scale models of complex biological phenomena**. *Curr Opin Biotechnol* 2016, **39**:167-173.

44. Hwang M, Garbey M, Berceli SA, Tran-Son-Tay R: **Rule-Based Simulation of Multi-Cellular Biological Systems-A Review of Modeling Techniques**. *Cell Mol Bioeng* 2009, **2**:285-294.

45. Anderson AR, Weaver AM, Cummings PT, Quaranta V: **Tumor morphology and phenotypic evolution driven by selective pressure from the microenvironment**. *Cell* 2006, **127**:905-915.

46. Waclaw B, Bozic I, Pittman ME, Hruban RH, Vogelstein B, Nowak MA: **A spatial model predicts that dispersal and cell turnover limit intratumour heterogeneity**. *Nature* 2015, **525**:261-264.

47. Wells DK, Chuang Y, Knapp LM, Brockmann D, Kath WL, Leonard JN: **Spatial and functional heterogeneities shape collective behavior of tumor-immune networks**. *PLoS Comput Biol* 2015, **11**:e1004181.

48. Jafari Nivlouei S, Soltani M, Carvalho J, Travasso R, Salimpour MR, Shirani E: **Multiscale modeling of tumor growth and angiogenesis: Evaluation of tumor-targeted therapy**. *PLoS Comput Biol* 2021, **17**:e1009081.

49. Yu JS, Bagheri N: **Modular microenvironment components reproduce vascular dynamics *de novo* in a multi-scale agent-based model**. *Cell Syst* 2021, **12**:795-809 e799.

50. Gong C, Milberg O, Wang B, Vicini P, Narwal R, Roskos L, Popel AS: **A computational multiscale agent-based model for simulating spatio-temporal tumour immune response to PD1 and PDL1 inhibition**. *J R Soc Interface* 2017, **14**.

51. Leschiera E, Lorenzi T, Shen S, Almeida L, Audebert C: **A mathematical model to study the impact of intra-tumor heterogeneity on anti-tumor CD8+ T cell immune response**. *Journal of Theoretical Biology* 2022:111028.

52. Narang V, Decraene J, Wong SY, Aiswarya BS, Wasem AR, Leong SR, Gouaillard A: **Systems immunology: a survey of modeling formalisms, applications and simulation tools**. *Immunol Res* 2012, **53**:251-265.

53. Vodovotz Y, Xia A, Read EL, Bassaganya-Riera J, Hafler DA, Sontag E, Wang J, Tsang JS, Day JD, Kleinstein SH, et al.: **Solving Immunology?** *Trends Immunol* 2017, **38**:116-127.

54. Zhang L, Wang Z, Sagotsky JA, Deisboeck TS: **Multiscale agent-based cancer modeling**. *J Math Biol* 2009, **58**:545-559.

55. Norton KA, Wallace T, Pandey NB, Popel AS: **An agent-based model of triple-negative breast cancer: the interplay between chemokine receptor CCR5 expression, cancer stem cells, and hypoxia**. *BMC Syst Biol* 2017, **11**:68.

56. Yu JS, Bagheri N: **Agent-Based Models Predict Emergent Behavior of Heterogeneous Cell Populations in Dynamic Microenvironments**. *Front Bioeng Biotechnol* 2020, **8**:249.

57. Folcik VA, An GC, Orosz CG: **The Basic Immune Simulator: an agent-based model to study the interactions between innate and adaptive immunity**. *Theor Biol Med Model* 2007, **4**:39.

58. Cess CG, Finley SD: **Multi-scale modeling of macrophage-T cell interactions within the tumor microenvironment**. *PLoS Comput Biol* 2020, **16**:e1008519.

59. Farrell S, Godwin A, Riley DM: **A Sociocultural Learning Framework for Inclusive Pedagogy in Engineering**. *Chemical Engineering Education* 2021, **55**:192-204.

60. Godwin A, Verdín D, Kirn A, Satterfield D: **The intersection of gender and race: Exploring chemical engineering students' attitudes**. *Chemical Engineering Education* 2018, **52**:89-97.

61. Patrick AD, Prybutok AN, Borrego M: **Predicting persistence in engineering through an engineering identity scale**. *International journal of engineering education* 2018, **34**.

62. ASEE: **Profiles of Enginering and Engineering Technology: Engineering & Engineering Technology By the Numbers 2020**. 2021.

63. Long III L, Mejia JA: **Conversations about diversity: Institutional barriers for underrepresented engineering students**. *Journal of Engineering* 2016, **105**:211.

64. Malcom-Piqueux L: **Transformation in the US Higher Education System: Implications for Racial Equity**. 2020.

65. Hickey W: **College rankings have made school less affordable, less equitable, and more miserable for students. The pandemic exposed just how broken the system is.**; 2021.

66. Patrick A, Borrego M: **A Review of the Literature Relevant to Engineering Identity**. In *American Society for Engineering Education Annual Conference*; 2016.

67. Godwin A, Lee WC: **A cross-sectional study of engineering identity during undergraduate education**. *School of Engineering Education Faculty Publications* 2017, **Paper 13**.

68. Prybutok AN, Patrick AD, Borrego M, Seepersad CC, Kirisits M: **Cross-sectional survey study of undergraduate engineering identity**. In *American Society for Engineering Education Annual Conference*; 2016.

69. Johnson KM: **Implementing inclusive practices in an active learning STEM classroom**. American Physiological Society Bethesda, MD; 2019:207-210.

70. Sanger CS: **Inclusive pedagogy and universal design approaches for diverse learning environments**. In *Diversity and inclusion in global higher education*. Palgrave Macmillan, Singapore; 2020:31-71.

71. Tanner KD: **Structure matters: twenty-one teaching strategies to promote student engagement and cultivate classroom equity**. *CBE Life Sci Educ* 2013, **12**:322-331.

72. Matters ME, Brightman AO, Buzzanell PM, Zoltowski CB: **Inclusive Teaching in Isolating Situations: Impact of COVID-19 on Efforts Toward Increasing Diversity in BME**. *Biomed Eng Educ* 2021, **1**:73-77.

73. Hirshfield LJ, Mayes HB: **Incorporating Inclusivity and Ethical Awareness Into Chemical Reaction Engineering**. *Chemical Engineering Education* 2019, **53**:215-219.

74. Minerick AR, Koretsky MD: **Diversity, Equity, and Inclusion: Language, Concepts, and Intent Mapped Through History**. *Chemical Engineering Education* 2021, **55**:190-191.

75. Cech EA: **Culture of disengagement in engineering education?** *Science, Technology, & Human Values* 2014, **39**:42-72.

76. Leydens JA, Johnson KE, Moskal BM: **Engineering student perceptions of social justice in a feedback control systems course**. *Journal of Engineering Education* 2021, **110**:718-749.

77. Long III LL: **Toward an Anti-Racist Engineering Classroom for 2020 and Beyond: A Starter Kit**. *Advances in Engineering Education* 2021.

78. Buolamwini J, Gebru T: **Gender Shades: Intersectional Accuracy Disparities in Commercial Gender Classification**. In *Proceedings of the 1st Conference on Fairness, Accountability and Transparency*. Edited by Sorelle AF, Christo W. PMLR; 2018:77--91.

79. ACLU: **Man wrongfully arrested because face recognition can't tell black people apart**. 2020.

80. Sunter DA, Castellanos S, Kammen DM: **Disparities in rooftop photovoltaics deployment in the United States by race and ethnicity**. *Nature Sustainability* 2019, **2**:71-76.

81. Reynante B: **Learning to design for social justice in community-engaged engineering**. *Journal of Engineering Education* 2021, **111**:338-356.

82. Riley D: **Pedagogies of liberation in an engineering thermodynamics class**. In *2003 Annual Conference*; 2003:8.918. 911-918.918. 916.

83. Riley D: **Engineering thermodynamics and 21st century energy problems: A textbook companion for student engagement**. *Synthesis Lectures on Engineering* 2011, **6**:1-97.

84. Riley DM: **Pushing the boundaries of mass and energy: Sustainability and social justice integration in core engineering science courses**. In *2015 ASEE Annual Conference & Exposition*; 2015:26.1286. 1281-1226.1286. 1212.

85. Catalano G, Baillie C, Riley D, Nieusma D, Byrne C, Bailey M, Haralampides K: **Integrating social justice ideas into a numerical methods course in bioengineering**. In *2010 Annual Conference & Exposition*; 2010:15.772. 771-715.772. 777.

86. Hoople GD, Chen DA, Lord SM, Gelles LA, Bilow F, Mejia JA: **An integrated approach to energy education in engineering**. *Sustainability* 2020, **12**:9145.

87. LaChance AM, Pascal J, Gan D, Welsh JJP, Pauly TJ, Paul P: **Teaching Environmental Justice Principles to Chemical Engineering Seniors: An Antiracist, Collaborative Approach**. In *2021 ASEE Virtual Annual Conference Content Access*; 2021.

88. AIChE: **Equity, Diversity and Inclusion Certificate Program**.

89. Riley D, Rivera-Jiménez SM: **Liberating Learning: Social Justice in The Chemical Engineering Curriculum**. 2021.

90. Prybutok AN, Yu JS, Leonard JN, Bagheri N: **Mapping CAR T-cell design space using agent-based models**. *bioRxiv* 2022:2022.2004.2007.487561.

91. Hou B, Tang Y, Li W, Zeng Q, Chang D: **Efficiency of CAR-T Therapy for Treatment of Solid Tumor in Clinical Trials: A Meta-Analysis**. *Dis Markers* 2019, **2019**:3425291.

92. Rohrs JA, Zheng D, Graham NA, Wang P, Finley SD: **Computational Model of Chimeric Antigen Receptors Explains Site-Specific Phosphorylation Kinetics**. *Biophys J* 2018, **115**:1116-1129.

93. Cess CG, Finley SD: **Data-driven analysis of a mechanistic model of CAR T cell signaling predicts effects of cell-to-cell heterogeneity**. *J Theor Biol* 2020, **489**:110125.

94. Rohrs JA, Siegler EL, Wang P, Finley SD: **ERK Activation in CAR T Cells Is Amplified by CD28-Mediated Increase in CD3zeta Phosphorylation**. *iScience* 2020, **23**:101023.

95. Owens K, Bozic I: **Modeling CAR T-Cell Therapy with Patient Preconditioning**. *Bull Math Biol* 2021, **83**:42.

96. Liadi I, Singh H, Romain G, Rey-Villamizar N, Merouane A, Adolacion JR, Kebriaei P, Huls H, Qiu P, Roysam B, et al.: **Individual Motile CD4(+) T Cells Can Participate in Efficient Multikilling through Conjugation to Multiple Tumor Cells**. *Cancer Immunol Res* 2015, **3**:473-482.

97. Golubovskaya V, Wu L: **Different Subsets of T Cells, Memory, Effector Functions, and CAR-T Immunotherapy**. *Cancers (Basel)* 2016, **8**.

98. Kuse R, Schuster S, Schubbe H, Dix S, Hausmann K: **Blood lymphocyte volumes and diameters in patients with chronic lymphocytic leukemia and normal controls**. *Blut* 1985, **50**:243-248.

99. Lauffenburger DA, Linderman JJ: *Receptors: Models for Binding, Trafficking, and Signaling*. Oxford University Press; 1993.

100. Robertson KW, Reeves JR, Smith G, Keith WN, Ozanne BW, Cooke TG, Stanton PD: **Quantitative estimation of epidermal growth factor receptor and c-erbB-2 in human breast cancer**. *Cancer Res* 1996, **56**:3823-3830.

101. Frauwirth KA, Riley JL, Harris MH, Parry RV, Rathmell JC, Plas DR, Elstrom RL, June CH, Thompson CB: **The CD28 Signaling Pathway Regualtes Glucose Metabolism**. *Immunity* 2002, **16**:769-777.

102. De Boer RJ, Homann D, Perelson AS: **Different dynamics of CD4+ and CD8+ T cell responses during and after acute lymphocytic choriomeningitis virus infection**. *J Immunol* 2003, **171**:3928-3935.

103. Deenick EK, Gett AV, Hodgkin PD: **Stochastic model of T cell proliferation: a calculus revealing IL-2 regulation of precursor frequencies, cell cycle time, and survival**. *J Immunol* 2003, **170**:4963-4972.

104. Iwashima M: **Kinetic perspectives of T cell antigen receptor signaling. A two-tier model for T cell full activation**. *Immunol Rev* 2003, **191**:196-210.

105. Jacobs SR, Herman CE, Maciver NJ, Wofford JA, Wieman HL, Hammen JJ, Rathmell JC: **Glucose uptake is limiting in T cell activation and requires CD28-mediated Akt-dependent and independent pathways**. *J Immunol* 2008, **180**:4476-4486.

106. Busse D, de la Rosa M, Hobiger K, Thurley K, Flossdorf M, Scheffold A, Hofer T: **Competing feedback loops shape IL-2 signaling between helper and regulatory T lymphocytes in cellular microenvironments**. *Proc Natl Acad Sci U S A* 2010, **107**:3058-3063.

107. Yoon H, Kim TS, Braciale TJ: **The cell cycle time of CD8+ T cells responding in vivo is controlled by the type of antigenic stimulus**. *PLoS One* 2010, **5**:e15423.

108. Wang R, Dillon CP, Shi LZ, Milasta S, Carter R, Finkelstein D, McCormick LL, Fitzgerald P, Chi H, Munger J, et al.: **The transcription factor Myc controls metabolic reprogramming upon T lymphocyte activation**. *Immunity* 2011, **35**:871-882.

109. Altman BJ, Dang CV: **Normal and cancer cell metabolism: lymphocytes and lymphoma**. *FEBS J* 2012, **279**:2598-2609.

110. Robertson-Tessi M, El-Kareh A, Goriely A: **A mathematical model of tumor-immune interactions**. *J Theor Biol* 2012, **294**:56-73.

111. Stone JD, Aggen DH, Schietinger A, Schreiber H, Kranz DM: **A sensitivity scale for targeting T cells with chimeric antigen receptors (CARs) and bispecific T-cell Engagers (BiTEs)**. *Oncoimmunology* 2012, **1**:863-873.

112. Cheng X, Veverka V, Radhakrishnan A, Waters LC, Muskett FW, Morgan SH, Huo J, Yu C, Evans EJ, Leslie AJ, et al.: **Structure and interactions of the human programmed cell death 1 receptor**. *J Biol Chem* 2013, **288**:11771-11785.

113. Heskamp S, Hobo W, Molkenboer-Kuenen JD, Olive D, Oyen WJ, Dolstra H, Boerman OC: **Noninvasive Imaging of Tumor PD-L1 Expression Using Radiolabeled Anti-PD-L1 Antibodies**. *Cancer Res* 2015, **75**:2928-2936.

114. Kinjyo I, Qin J, Tan SY, Wellard CJ, Mrass P, Ritchie W, Doi A, Cavanagh LL, Tomura M, Sakaue-Sawano A, et al.: **Real-time tracking of cell cycle progression during CD8+ effector and memory T-cell differentiation**. *Nat Commun* 2015, **6**:6301.

115. Obst R: **The Timing of T Cell Priming and Cycling**. *Front Immunol* 2015, **6**:563.

116. Harris DT, Kranz DM: **Adoptive T Cell Therapies: A Comparison of T Cell Receptors and Chimeric Antigen Receptors**. *Trends Pharmacol Sci* 2016, **37**:220-230.

117. Arcangeli S, Rotiroti MC, Bardelli M, Simonelli L, Magnani CF, Biondi A, Biagi E, Tettamanti S, Varani L: **Balance of Anti-CD123 Chimeric Antigen Receptor Binding Affinity and Density for the Targeting of Acute Myeloid Leukemia**. *Mol Ther* 2017, **25**:1933-1945.

118. Borghans J, Ribeiro RM: **The maths of memory**. *eLife* 2017, **6**.

119. Gherbi K, Briddon SJ, Charlton SJ: **Micro-pharmacokinetics: Quantifying local drug concentration at live cell membranes**. *Sci Rep* 2018, **8**:3479.

120. Salter AI, Ivey RG, Kennedy JJ, Voillet V, Rajan A, Alderman EJ, Voytovich UJ, Lin C, Sommermeyer D, Liu L, et al.: **Phosphoproteomic analysis of chimeric antigen receptor signaling reveals kinetic and quantitative differences that affect cell function**. *Science Signaling* 2018, **11**.

121. Jones RG, Thompson CB: **Revving the engine: signal transduction fuels T cell activation**. *Immunity* 2007, **27**:173-178.

122. MacIver NJ, Michalek RD, Rathmell JC: **Metabolic regulation of T lymphocytes**. *Annu Rev Immunol* 2013, **31**:259-283.

123. Malek TR, Castro I: **Interleukin-2 receptor signaling: at the interface between tolerance and immunity**. *Immunity* 2010, **33**:153-165.

124. Liao W, Lin JX, Leonard WJ: **Interleukin-2 at the crossroads of effector responses, tolerance, and immunotherapy**. *Immunity* 2013, **38**:13-25.

125. Rosenberg SA: **IL-2: the first effective immunotherapy for human cancer**. *J Immunol* 2014, **192**:5451-5458.

126. Ross SH, Cantrell DA: **Signaling and Function of Interleukin-2 in T Lymphocytes**. *Annu Rev Immunol* 2018, **36**:411-433.

127. Sampson JH, Choi BD, Sanchez-Perez L, Suryadevara CM, Snyder DJ, Flores CT, Schmittling RJ, Nair SK, Reap EA, Norberg PK, et al.: **EGFRvIII mCAR-modified T-cell therapy cures mice with established intracerebral glioma and generates host immunity against tumor-antigen loss**. *Clin Cancer Res* 2014, **20**:972-984.

128. Chmielewski M, Hombach A, Heuser C, Adams GP, Abken H: **T cell activation by antibody-like immunoreceptors: increase in affinity of the single-chain fragment domain above threshold does not increase T cell activation against antigen-positive target cells but decreases selectivity**. *J Immunol* 2004, **173**:7647-7653.

129. Hudecek M, Lupo-Stanghellini MT, Kosasih PL, Sommermeyer D, Jensen MC, Rader C, Riddell SR: **Receptor affinity and extracellular domain modifications affect tumor recognition by ROR1-specific chimeric antigen receptor T cells**. *Clin Cancer Res* 2013, **19**:3153-3164.

130. Ghorashian S, Kramer AM, Onuoha S, Wright G, Bartram J, Richardson R, Albon SJ, Casanovas-Company J, Castro F, Popova B, et al.: **Enhanced CAR T cell expansion and prolonged persistence in pediatric patients with ALL treated with a low-affinity CD19 CAR**. *Nat Med* 2019, **25**:1408-1414.

131. Watanabe K, Terakura S, Martens AC, van Meerten T, Uchiyama S, Imai M, Sakemura R, Goto T, Hanajiri R, Imahashi N, et al.: **Target antigen density governs the efficacy of anti-CD20-CD28-CD3 zeta chimeric antigen receptor-modified effector CD8+ T cells**. *J Immunol* 2015, **194**:911-920.

132. Majzner RG, Rietberg SP, Sotillo E, Dong R, Vachharajani VT, Labanieh L, Myklebust JH, Kadapakkam M, Weber EW, Tousley AM, et al.: **Tuning the Antigen Density Requirement for CAR T-cell Activity**. *Cancer Discov* 2020, **10**:702-723.

133. Hamieh M, Dobrin A, Cabriolu A, van der Stegen SJC, Giavridis T, Mansilla-Soto J, Eyquem J, Zhao Z, Whitlock BM, Miele MM, et al.: **CAR T cell trogocytosis and cooperative killing regulate tumour antigen escape**. *Nature* 2019, **568**:112-116.

134. Fu W, Lei C, Liu S, Cui Y, Wang C, Qian K, Li T, Shen Y, Fan X, Lin F: **CAR exosomes derived from effector CAR-T cells have potent antitumour effects and low toxicity**. *Nature communications* 2019, **10**:1-12.

135. Hernandez-Lopez RA, Yu W, Cabral KA, Creasey OA, del Pilar Lopez Pazmino M, Tonai Y, Guzman AD, Makela A, Saksela K, Gartner ZJ, et al.: **T cell circuits that sense antigen density with an ultrasensitive threshold**. *Science* 2021, **1855**.

136. van Stipdonk MJ, Hardenberg G, Bijker MS, Lemmens EE, Droin NM, Green DR, Schoenberger SP: **Dynamic programming of CD8+ T lymphocyte responses**. *Nat Immunol* 2003, **4**:361-365.

137. Akbar AN, Henson SM: **Are senescence and exhaustion intertwined or unrelated processes that compromise immunity?** *Nat Rev Immunol* 2011, **11**:289-295.

138. Crespo J, Sun H, Welling TH, Tian Z, Zou W: **T cell anergy, exhaustion, senescence, and stemness in the tumor microenvironment**. *Curr Opin Immunol* 2013, **25**:214-221.

139. Janas ML, Groves P, Kienzle N, Kelso A: **IL-2 regulates perforin and granzyme gene expression in CD8+ T cells independently of its effects on survival and proliferation**. *J Immunol* 2005, **175**:8003-8010.

140. Kasakovski D, Xu L, Li Y: **T cell senescence and CAR-T cell exhaustion in hematological malignancies**. *J Hematol Oncol* 2018, **11**:91.

141. Long AH, Haso WM, Shern JF, Wanhainen KM, Murgai M, Ingaramo M, Smith JP, Walker AJ, Kohler ME, Venkateshwara VR, et al.: **4-1BB costimulation ameliorates T cell exhaustion induced by tonic signaling of chimeric antigen receptors**. *Nat Med* 2015, **21**:581-590.

142. Macian F, Im SH, Garcia-Cozar FJ, Rao A: **T-cell anergy**. *Curr Opin Immunol* 2004, **16**:209-216.

143. Schwartz RH: **Models of T Cell Anergy: Is There a Common Molecular Mechanism?** *J Exp Med* 1996, **184**:1-8.

144. Schwartz RH: **T cell anergy**. *Annu Rev Immunol* 2003, **21**:305-334.

145. Verbist KC, Guy CS, Milasta S, Liedmann S, Kaminski MM, Wang R, Green DR: **Metabolic maintenance of cell asymmetry following division in activated T lymphocytes**. *Nature* 2016, **532**:389-393.

146. Watanabe K, Kuramitsu S, Posey AD, Jr., June CH: **Expanding the Therapeutic Window for CAR T Cell Therapy in Solid Tumors: The Knowns and Unknowns of CAR T Cell Biology**. *Front Immunol* 2018, **9**:2486.

147. Wherry EJ: **T cell exhaustion**. *Nat Immunol* 2011, **12**:492-499.

148. Wherry EJ, Kurachi M: **Molecular and cellular insights into T cell exhaustion**. *Nat Rev Immunol* 2015, **15**:486-499.

149. Yost KE, Satpathy AT, Wells DK, Qi Y, Wang C, Kageyama R, McNamara KL, Granja JM, Sarin KY, Brown RA, et al.: **Clonal replacement of tumor-specific T cells following PD-1 blockade**. *Nat Med* 2019, **25**:1251-1259.

150. University of Michigan College of Literature S, and the Arts: **Social Identity Wheel**.

151. hooks b: **Chapter 3: Embracing Change: Teaching in a Multicultural World**. In *Teaching to transgress: Education as the practice of freedom*; 1994:35-44.

152. Johnson KMS: **Implementing inclusive practices in an active learning STEM classroom**. *Adv Physiol Educ* 2019, **43**:207-210.

153. Chavez AF, Longerbeam SD: **Chapter 5: Strengths-Based Teaching in Cultural Context**. In *Teaching Across Cultural Strengths: A Guide to Balancing Integrated and Individuated Cultural Frameworks in College Teaching*, edn 1st. Sylus Publishing LLC; 2016.

154. Killpack TL, Melon LC: **Toward Inclusive STEM Classrooms: What Personal Role Do Faculty Play?** *CBE Life Sci Educ* 2016, **15**:es3.

155. Northwestern University Department of Chemical and Biological Engineering Anti-Racism D, Equity, and Inclusion Committee: **ChBE Anti-Racism, Diversity, Equity, and Inclusion Committee**.

156. Redden E: **Math for Social Justice**. Inside Higher Ed; 2021.

157. The National Academies of Science E, and Medicine: **Imagining the Future of Undergraduate STEM Education Symposium**. The National Academies of Science, Engineering, and Medicine.

158. **Social Explorer**.

159. ABET: **ABET Criteria Available for Public Review and Comment**. 2022.

160. Maude SL, Frey N, Shaw PA, Aplenc R, Barrett DM, Bunin NJ, Chew A, Gonzalez VE, Zheng Z, Lacey SF, et al.: **Chimeric antigen receptor T cells for sustained remissions in leukemia**. *N Engl J Med* 2014, **371**:1507-1517.

161. Donahue PS, Draut JW, Muldoon JJ, Edelstein HI, Bagheri N, Leonard JN: **The COMET toolkit for composing customizable genetic programs in mammalian cells**. *Nat Commun* 2020, **11**:779.

162. Dolberg TB, Meger AT, Boucher JD, Corcoran WK, Schauer EE, Prybutok AN, Raman S, Leonard JN: **Computation-guided optimization of split protein systems**. *Nat Chem Biol* 2021, **17**:531-539.

163. Manhas J, Edelstein HI, Leonard JN, Morsut L: **The evolution of synthetic receptor systems**. *Nat Chem Biol* 2022, **18**:244-255.

164. Edelstein HI, Donahue PS, Muldoon JJ, Kang AK, Dolberg TB, Battaglia LM, Allchin ER, Hong M, Leonard JN: **Elucidation and refinement of synthetic receptor mechanisms**. *Synth Biol (Oxf)* 2020, **5**:ysaa017.

165. Muldoon JJ, Kandula V, Hong M, Donahue PS, Boucher JD, Bagheri N, Leonard JN: **Model-guided design of mammalian genetic programs**. *Sci Adv* 2021, **7**:eabe9375.

166. Hartfield RM, Schwarz KA, Muldoon JJ, Bagheri N, Leonard JN: **Multiplexing Engineered Receptors for Multiparametric Evaluation of Environmental Ligands**. *ACS Synth Biol* 2017, **6**:2042-2055.

167. Martinez M, Moon EK: **CAR T Cells for Solid Tumors: New Strategies for Finding, Infiltrating, and Surviving in the Tumor Microenvironment**. *Front Immunol* 2019, **10**:128.

168. Xu X, Gnanaprakasam JNR, Sherman J, Wang R: **A Metabolism Toolbox for CAR T Therapy**. *Front Oncol* 2019, **9**:322.